



Universiteit
Leiden
The Netherlands

Osteoarthritis in the knee. Cartilage MR imaging

Kornaat, P.R.

Citation

Kornaat, P. R. (2006, November 7). *Osteoarthritis in the knee. Cartilage MR imaging*. Retrieved from <https://hdl.handle.net/1887/8767>

Version: Corrected Publisher's Version

License: [Licence agreement concerning inclusion of doctoral thesis in the Institutional Repository of the University of Leiden](#)

Downloaded from: <https://hdl.handle.net/1887/8767>

Note: To cite this publication please use the final published version (if applicable).

Osteoarthritis in the knee

Cartilage MR imaging

Osteoarthritis in the knee

Cartilage MR imaging

PROEFSCHRIFT

ter verkrijging van
de graad van Doctor aan de Universiteit Leiden,
op gezag van de Rector Magnificus Dr. D.D. Breimer,
hoogleraar in de faculteit der Wiskunde en
Natuurwetenschappen en die der Geneeskunde,
volgens besluit van het College voor
Promoties te verdedigen op woensdag
15 november 2006 klokke 13.45 uur

door

Peter Ronald Kornaat
geboren te Eindhoven
in 1976

Promotiecommissie

Promotor:	Prof. Dr. J.L. Bloem
Copromotores:	Dr. I. Watt Dr. G. Kloppenburg
Referent:	Prof. Dr. P. Slagboom
Lid:	Prof. Dr. R.G.H.H. Nelissen

© P.R. Kornaat, Leiden, The Netherlands. All rights preserved. No parts of this publication may be reproduced or transmitted in any form or by any means, electronic or mechanical, including photocopy, recording, or any information storage and retrieval system, without prior written permission of the author.

Cover design by Caroline Ellerbeck
Printed by Lecturis, Eindhoven, 2006

ISBN-10: 90-9021149-7
ISBN-13: 978-90-9021149-7

Publication of this thesis was financially supported by Pfizer bv, Foundation Imago, Philips, Dutch Arthritis Association and Guerbet Nederland.

Contents

Chapter 1:	General introduction	7
Chapter 2:	Knee Osteoarthritis Scoring System (KOSS): inter-observer and intra-observer reproducibility of a compartment-based scoring system Skeletal Radiology February 2005	11
Chapter 3:	Magnetic resonance imaging of knee cartilage using a water selective balanced steady-state free precession sequence Journal of Magnetic Resonance Imaging November 2004	27
Chapter 4:	MR Imaging of Articular Cartilage at 1.5T and 3.0T: Comparison of SPGR and SSFP sequences Osteoarthritis and Cartilage April 2005	41
Chapter 5:	Comparison of quantitative cartilage measurements acquired on two 3.0T MR imaging systems from different manufacturers Journal of Magnetic Resonance Imaging March 2006	55
Chapter 6:	Central Osteophytes in the Knee: Prevalence and Association with Cartilage Defects on MR Imaging American Journal of Roentgenology February 2001	65
Chapter 7:	The relationship between the MRI features of mild osteoarthritis in the patellofemoral and tibiofemoral compartment of the knee European Radiology August 2005	79
Chapter 8:	Magnetic resonance imaging in knees of patients with osteoarthritis at multiple sites: association with clinical findings Radiology June 2006	93
Chapter 9:	Bone marrow edema lesions change in volume in the majority of patients with osteoarthritis; association with clinical features Submitted Radiology	109
Chapter 10:	Summary and general conclusion Samenvatting en algemene conclusie Curriculum Vitae	121



Chapter 1

Introduction

Osteoarthritis (OA) of the knee increases in prevalence with age and is more common in women than in man. Risk factors include obesity, knee injury, previous knee surgery, and occupational knee bending and lifting. OA of the knee can be part of a generalized diathesis, including OA of the hand, which may be inherited. The natural history of OA of the knee is highly variable, with the disease improving in some patients, remaining stable in others, and gradually worsening in others. OA is a leading cause of impaired mobility in the elderly. Many persons with knee pain have limitations in function that prevent them from engaging in their usual activities (1). OA is suspected when patients have pain in the commonly involved joints. According to the American College of Rheumatology (ACR) criteria, symptomatic knee OA is defined as pain or stiffness on most days in the month in combination with osteophytes on radiographs.

Although radiographs remain the usual means of assessing osteoarthritic changes in the knee (by joint space narrowing and the presence of osteophytes), the association between osteoarthritic findings on radiographs and clinical features is poor (2). Fortunately a new imaging modality, magnetic resonance (MR) imaging, allows another perspective of the structural abnormalities associated with OA. MR imaging, with its excellent soft-tissue contrast, is the best non-invasive technique currently available for the assessment of cartilage injury and other internal dearrangements of the knee (3,4).

The impact and consequences of OA in the aging population of the industrialized world are motivating the medical and pharmaceutical communities to develop disease-modifying drugs to prevent or delay the development of disability. Disease markers need to be identified in order to predict and quantify progression. MR imaging has potential in this process of identifying markers because of its

ability to assess joint pathology and depict lesions that are frequently associated with OA (3,4). Possible markers in OA are cartilage, osteophytes, cysts, bone marrow edema, joint effusion, synovitis and ligamentous and cartilaginous defects. Recently, the National Institutes of Health (NIH) advised the use of 3.0T MR scanners for this purpose, and several international longitudinal studies have been initiated. Most of the data presented in this thesis is based on a 1.5T longitudinal MR study called the "Genetica, Artrose & Progressie" (GARP) study.

The first purpose of this thesis is to develop "tools" to facilitate the assessment of MR imaging characteristics in order to associate these MR imaging characteristics with clinical findings in patients with OA. One of these tools is a MR scoring system which, at the start of the study, was not yet described in literature. Another tool is a MR imaging sequence specifically optimized and validated for cartilage imaging. As higher field systems, typically 3.0 Tesla (T), have become more prevalent in the clinical setting and longitudinal MR imaging studies are performed on both a 1.5T and 3.0T scanners, both field strengths were studied for this purpose.

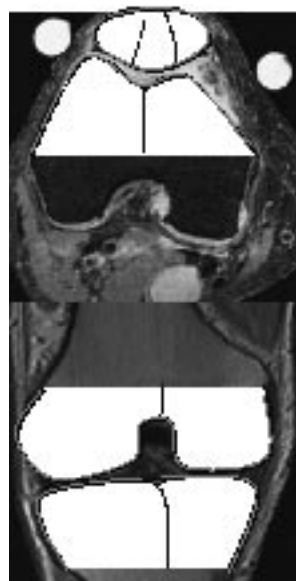
Secondly, as the correlation between radiographic osteoarthritic findings and clinical features is poor the author would like to find an answer on the following question: does MR imaging of the knee tell us more about the relation between osteoarthritic structural findings (cartilage defects, bone marrow edema, etc.) and clinical features of OA (pain and stiffness)? Are MR imaging characteristics specific for the presence of OA or specific for clinical features of OA? Also, can MR imaging be used to detect changes in early OA stages, and more specific, earlier than radiographs do? And whether changes in MR specific characteristics of OA correlate with progression of OA, expressed as progression of clinical features (pain and stiffness)?

Therefore, in Chapter 2 a scoring system for quantifying OA changes of the knee as identified by MR imaging, including its inter- and intra-observer reproducibility, which can be used to monitor medical therapy in research studies is described. In Chapter 3 an optimized water selective balanced steady-state free precession sequence (WS-bSSFP) with conventional MR sequences in imaging cartilage of OA knees are compared. In Chapter 4 three-dimensional spoiled gradient recalled echo (3D SPGR) and two 3D steady-state free precession (SSFP) sequences for MR imaging of articular cartilage at 1.5T and 3.0T are compared. In Chapter 5 the comparability of two OA surrogate endpoints, average cartilage thickness and cartilage volume, acquired from healthy volunteers on two 3.0T MR imaging systems from different manufacturers are investigated. In Chapter 6 the prevalence and location of central osteophytes in patients referred for MR imaging of the knee and the relationship of central osteophytes with other derangements of the knee as seen on MR imaging are investigated. In Chapter 7 the relationship between OA changes seen on MR images of the patellofemoral (PF) or tibiofemoral

(TF) compartments in patients with mild OA of the knee are demonstrated. In Chapter 8 the association between clinical features and structural abnormalities found at MR imaging of their knees are described prospectively in patients with OA. In Chapter 9 changes of bone marrow edema (BME) over a time period of two years, as well as its association with clinical features, are described.

References

1. Felson DT. Clinical practice. Osteoarthritis of the knee. *N Engl J Med* 2006; 354(8):841-848
2. Lawrence JS, Bremner JM, Bier F. Osteo-arthritis. Prevalence in the population and relationship between symptoms and x-ray changes. *Ann.Rheum.Dis.* 1966;25(1):1-24.
3. Vincken PW, ter Braak BP, van Erkel AR, et al. Effectiveness of MR imaging in selection of patients for arthroscopy of the knee. *Radiology* 2002; 223:739–746.
4. Peterfy CG. Scratching the surface: articular cartilage disorders in the knee. *Magn Reson Imaging Clin North Am* 2000; 8:409–430.



2

Chapter 2

Knee Osteoarthritis Scoring System (KOSS): inter-observer and intra-observer reproducibility of a compartment-based scoring system

Peter R Kornaat
Ruth YT Ceulemans
Herman M Kroon
Naghmeh Riyazi
Margreet Kloppenburg
Wayne O Carter
Thasia G Woodworth
Johan L Bloem

Abstract

Objective

To develop a scoring system for quantifying osteoarthritic changes of the knee as identified by magnetic resonance (MR) imaging, and to determine its inter- and intra-observer reproducibility, in order to monitor medical therapy in research studies.

Design and patients

Two independent observers evaluated 25 consecutive MR examinations of the knee in patients with previously defined clinical symptoms and radiological signs of osteoarthritis. We acquired on a 1.5 T system: coronal and sagittal proton density- and T2-weighted dual spin echo (SE) images, sagittal three-dimensional T1-weighted gradient echo (GE) images with fat suppression, and axial dual turbo SE images with fat suppression. Images were scored for the presence of cartilaginous lesions, osteophytes, subchondral cysts, bone marrow edema, and for meniscal abnormalities. Presence and size of effusion, synovitis and Baker's cyst were recorded. All parameters were ranked on a previously defined, semiquantitative scale, reflecting increasing severity of findings. Kappa, weighted kappa and intraclass correlation coefficient (ICC) were used to determine inter and intra-observer variability.

Results

Inter-observer reproducibility was good (ICC value 0.77). Inter and intra-observer reproducibility for individual parameters was good to very good (inter-observer ICC value 0.63–0.91; intra-observer ICC value 0.76–0.96).

Conclusion

The presented comprehensive MR scoring system for osteoarthritic changes of the knee has a good to very good inter-observer and intra-observer reproducibility. Thus the score form with its definitions can be used for standardized assessment of osteoarthritic changes to monitor medical therapy in research studies.

Introduction

The impact of osteoarthritis on the aging population in the industrialized world is illustrated by the fact that osteoarthritis is the major cause of disability in those over the age of 65 years [1]. This motivates the medical and pharmaceutical community to develop disease-modifying drugs to prevent or slow down the course of disability. The current interest in development of new therapies for osteoarthritis of the knee requires reliable techniques for evaluation of the

disease allowing accurate definition and detection of osteoarthritic changes. Magnetic resonance (MR) imaging is a non-invasive, multiplanar high-contrast tomographic method that has successfully been used to visualize osteoarthritic changes [2, 3, 4, 5]. MR imaging can visualize osteophytes in locations that are not easily exhibited by conventional radiography [6]. It is highly sensitive to bone marrow edema and uniquely able to allow detection and quantification of joint effusion and synovitis [7, 8]. For evaluation of internal derangements, MR imaging has established itself as the imaging method of choice [9]. Although semiquantitative scoring methods based on the work by Shahriaree [10] and Outerbridge [11] have been developed to allow MR grading of cartilaginous defects [6, 12, 13, 14, 15, 16, 17, 18], no semiquantitative scoring method has been accepted as a standard for clinical research [19]. Neither has, in the literature, a comprehensive scoring method for cartilage injury and other imaging findings in osteoarthritis been standardized and evaluated for reproducibility. The purpose of the present study was to develop a comprehensive MR Knee Osteoarthritis Scoring System (KOSS) that quantifies osteoarthritic changes of compartments in the knee, in patients with known osteoarthritis, and to determine its inter- and intra-observer reproducibility, in order to monitor medical therapy in research studies.

Patients and methods

Patients

As part of a longitudinal natural history study of familial generalized osteoarthritis, knees of 25 consecutive patients were imaged using MR imaging. Patients with familial generalized osteoarthritis were recruited from outpatient clinics of rheumatology or orthopedic surgery or by general practitioners in our region. Patients included were diagnosed with clinical and radiographic characteristics of familial generalized osteoarthritis. Generalized osteoarthritis was defined as involvement of at least two joints of four anatomical regions (hand, spine, knee and hip). Patients with secondary osteoarthritis or a knee joint in the radiographic end-stage of osteoarthritic disease (Kellgren grade 4) were excluded [20]. The 25 patients included in this report ranged from 50 to 75 years in age (median age 63 years). Written informed consent was obtained from the patient prior to the study. The study was approved by our institution's medical ethics review board.

MR acquisition

Knees were imaged using a dedicated knee coil in a 1.5T superconducting magnet (Philips Medical Systems, Best, The Netherlands). Each examination consisted of: coronal proton density- and T2-weighted dual spin echo (SE) images (with repetition time (TR) of 2,200; echo time (TE) of 20/80; 5 mm slice thickness; 0.5 mm intersection gap; 16 cm field of view; 256 x 256 acquisition matrix); sagittal proton density- and T2-weighted dual SE images (TR 2,200; TE 20/80; 4 mm slice

thickness; 0.4 mm intersection gap; 16 cm field of view; 256 x 256 acquisition matrix); sagittal three-dimensional (3D) T1-weighted spoiled gradient echo (GE) frequency selective fat-suppressed images (TR 46; TE 2.5; flip angle 40°; 1.5 mm slice thickness; no gap; 18 cm field of view; 256 x 512 acquisition matrix); and axial proton density- and T2- weighted turbo spin echo (TSE) fat-suppressed images (TR 2,500; TE 7.1/40; echo train length 6; 2 mm slice thickness; no gap; 18 cm field of view; 256 x 256 acquisition matrix). Total acquisition time (including the initial survey sequence) was 30 min.

MR interpretation

Two observers, one of whom is an experienced musculoskeletal radiologist (observer 1) and the other a research fellow (observer 2), independently evaluated the MR examinations on a workstation in cine loop fashion. Both observers were masked to the patients' biometrical data, and were trained in using the scoring form. During the training both observers scored 50 patients together in 20 sessions over a period of 3 months. Intra-observer reproducibility was assessed using at least a 2 week interval between the randomized readings. Findings were recorded on a radiological record form (RRF), consisting of nine osteoarthritic parameters. Cartilaginous and osteochondral defects, osteophytes, subchondral cysts and bone marrow edema were assigned to the following anatomical locations: the patellar crest (*crista patellae*), medial or lateral patellar facet, the medial or lateral trochlear articular facet, the medial or lateral femoral condyle (excluding the trochlear groove), the medial or lateral tibial plateau. The medial and lateral meniscus were reviewed for the presence of meniscal tears, subluxation, intrasubstance degeneration or absence of a meniscal portion. A meniscal abnormality was assigned to the body, the anterior or posterior horn. Joint effusion, synovitis and Baker's cysts were noted.

Cartilaginous defects were graded as diffuse, or focal defects or osteochondral defects. Both coronal and sagittal SE images and sagittal GE images were used to assess the femorotibial cartilage. Axial TSE images and sagittal GE and SE images were used to assess the patellofemoral cartilage. The depth of diffuse and focal cartilage loss was qualitatively rated in relation to the height of the adjacent intact cartilage or the expected, normal cartilage contour. Because readers were masked to the age of the patient, the average cartilage contour of a healthy 30-year-old person was used as the expected normal cartilage contour. The depth (D) of a cartilaginous defect was graded using a modification of the Yulish classification [21]: grade 0, absent (no abnormality in signal intensity or morphology); grade 1, less than 50% reduction of cartilage thickness; grade 2, 50% or greater reduction of cartilage thickness; grade 3, full-thickness or near-full-thickness cartilage defect (Fig. 1). The depth (D) of the osseous component of the osteochondral defect was scored by estimating the distance between the actual osteochondral defect and the extrapolated subchondral cortex, and was graded as follows: grade 0, absent; grade 1, minimal (<2 mm); grade 2, moderate (2–5 mm); grade 3, severe (>5 mm).

The surface extent (S) of a diffuse, focal or osteochondral cartilage defect was estimated by its maximal diameter and graded as follows: grade 0, absent; grade 1, minimal (<5 mm); grade 2, moderate (5–10 mm); grade 3, severe (>10 mm). A cartilaginous defect was called focal in the case of an abrupt transition (acute angle) between the cartilage defect and the surrounding cartilage, resembling a crater. It was called diffuse in the case of a smooth and gradual transition zone (obtuse angle) between normal and thinned cartilage. When a focal chondral or osteochondral defect was superimposed on diffuse cartilage loss, both defects were scored.

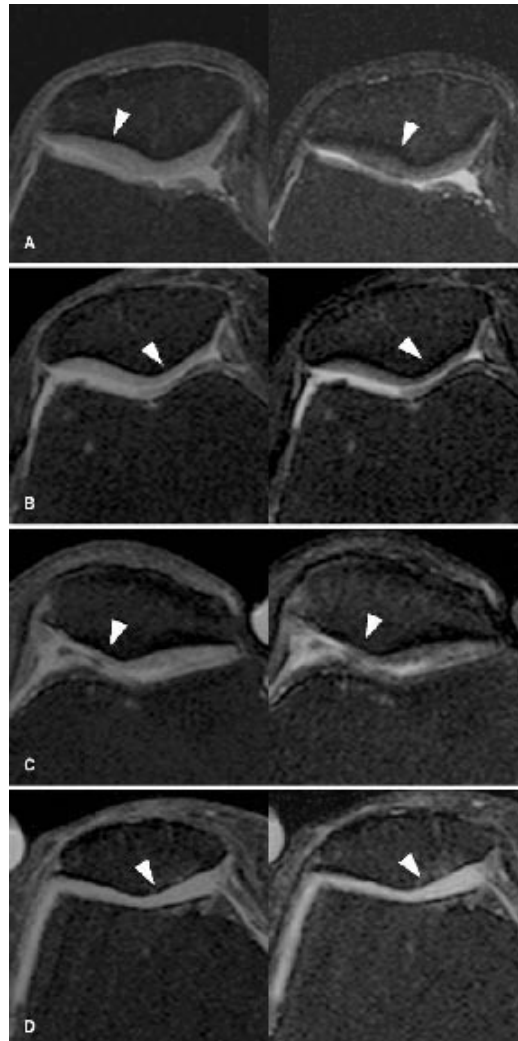


Figure 1. Axial dual turbo spin echo MR images of different grades of cartilage thinning at the patella (arrowheads demonstrate the example area): A grade 0 (normal cartilage); B grade 1; C grade 2; D grade 3 (full thickness)

Osteophytes were defined as focal bony excrescences, seen on axial, sagittal or coronal images, extending from a cortical surface. Osteophytes were further specified as being marginal, intercondylar or central (Fig. 2). A marginal osteophyte arises from the peripheral edge of the hyaline-covered articular surface, an intercondylar osteophyte at the central edge of the hyaline-covered articular surface, e.g., when located at the medial articular margin of the lateral femoral condyle or the lateral articular margin of the medial femoral condyle. A central osteophyte arises from the subchondral bone plate and is surrounded, but not necessarily covered, by articular cartilage. Osteophytes were assessed using the following scale: grade 0, absent; grade 1, minimal (<3 mm); grade 2, moderate (3–5 mm); grade 3, severe (>5 mm). Size was measured from the base to the tip of the osteophyte [6].

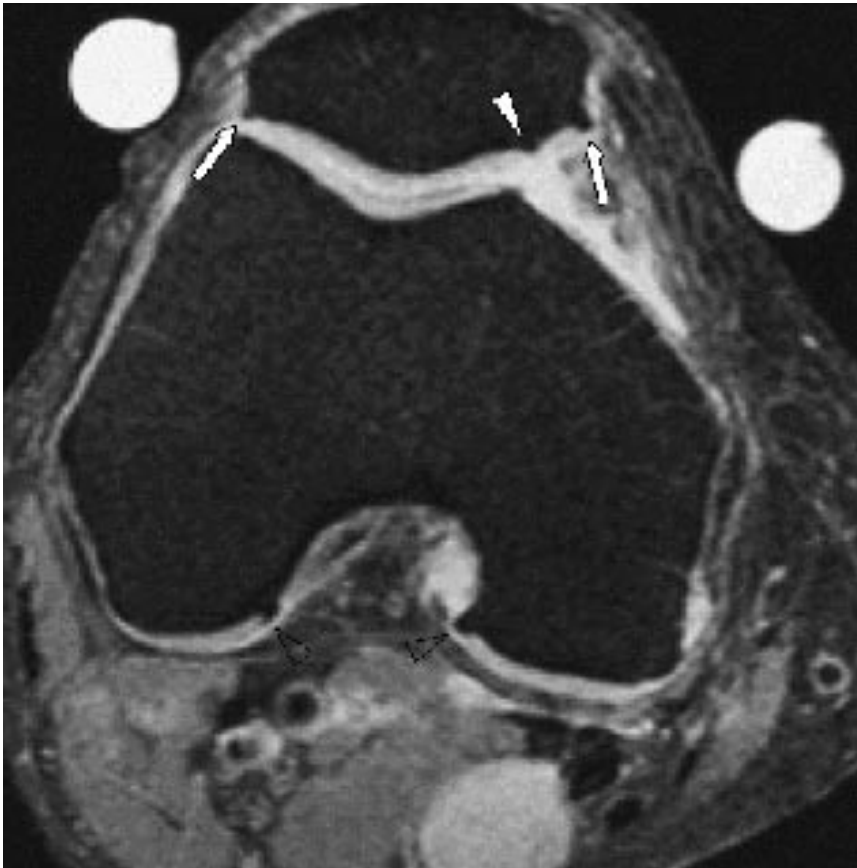


Figure 2. Axial turbo spin echo MR image. All three types of osteophytes are appreciated on this image: marginal osteophytes (arrows), intercondylar osteophytes (open arrowhead) and a central osteophyte (filled arrowhead)

Subchondral cysts were defined as well-defined foci of high signal intensity on T2-weighted images, in the cancellous bone underlying the joint cartilage. Their greatest dimension was measured and they were graded as follows: grade 0, absent; grade 1, minimal (<3 mm); grade 2, moderate (3–5 mm); grade 3, severe (>5 mm).

Bone marrow edema was assessed as an ill-defined area of increased signal intensity on T2 weighted images in the subchondral cancellous bone, extending away from the articular surface over a variable distance [22]. The lesions were graded as follows (Fig. 3): grade 0, absent; grade 1, minimal (diameter <5 mm); grade 2, moderate (diameter 5 mm to 2 cm); grade 3, severe (diameter >2 cm).

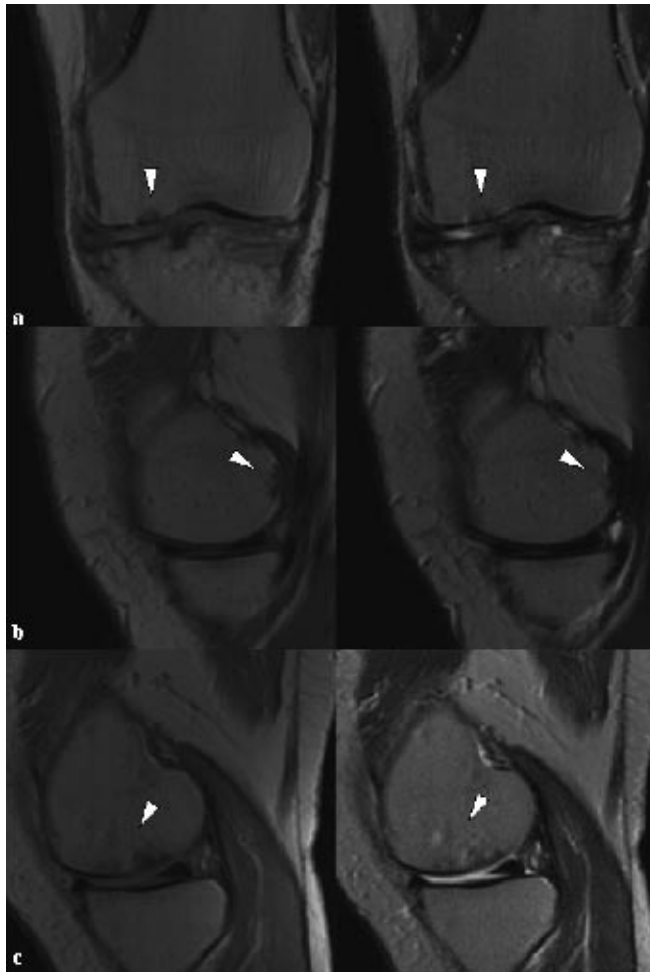


Figure 3. Coronal or sagittal dual spin echo MR images of different grades of bone marrow edema (arrowheads): A grade 1; B grade 2; C grade 3

A meniscal tear was defined as a region of intermediate signal intensity on proton density-weighted images within the meniscus, communicating with its superior or inferior surface or inner margin [23]. Meniscal tears were classified according to their shape as: 1, horizontal; 2, vertical; 3, radial; 4, complex; and 5, bucket-handle [24].

Meniscal subluxation was defined as protrusion, usually of the body of the meniscus, over the edge of the tibial plateau on coronal proton density-weighted images and was graded as follows: grade 0, absent; grade 1, minimal ($<1/3$ width of the meniscus bulging); grade 2, moderate ($1/3-2/3$ meniscal width involved); grade 3, severe ($>2/3$ meniscal width involved).

Meniscal intrasubstance degeneration was scored on proton density-weighted images as: grade 0, absent; grade 1, when a small, central focus of intermediate signal intensity on proton density-weighted images was noticed in the meniscus; grade 2, when the intrameniscal focus of intermediate signal intensity on proton density-weighted images was surrounded by a broad, hypointense peripheral rim; grade 3, when only a thin, hypointense peripheral rim outlined the intermediate signal intensity meniscal center.

Presence of a knee joint effusion was evaluated on T2-weighted coronal, sagittal and axial sequences. The GE sequences with fat suppression were used to differentiate effusion from synovitis. No joint effusion was assumed to be present when a small, physiological sliver of synovial fluid was observed. A small effusion was present when a small amount of fluid distended one or two of the joint recesses (suprapatellar pouch, medial or lateral patellar recess, dorsal femorotibial joint space, popliteal tendon sheath, recesses surrounding the cruciate ligaments, meniscosynovial recesses), moderate effusion when more than two joint recesses were partially distended, and massive effusion when there was full, marked distention of all the joint recesses.

Synovitis reflected by thickening and/or irregularity of the normally pencil-thin rim of high signal intensity synovium, was evaluated on sagittal T1-weighted GE images. Synovial thickening was classified as present or absent.

A Baker's cyst, or a distended gastrocnemial-semimembranosal bursa, was diagnosed when a circumscribed mass with intermediate signal intensity on proton density-weighted and high signal intensity on T2-weighted dual SE sequences was observed, originating from the dorsomedial femorotibial joint space, extending between the tendons of the medial head of the gastrocnemius and the semimembranosus and dissecting either caudally, cranially or both. Bursal distention was classified as minimal, moderate or severe.

Statistical analysis

Kappa (κ) statistics were used to assess inter- and intra-observer agreement in grading cartilaginous defects, osteophytes, subchondral cysts, bone marrow edema, meniscal tears, effusion, synovitis and Baker's cysts. A weighted kappa was used when the degree of disagreement was taken into account, as opposed to kappa when disagreements were treated equally [25]. If the grade scores agreed, the weighting was 1.00 (maximal agreement). If the scores differed by one grade, the weighting was 0.66; if they differed by two, the weighting was 0.33; if they differed by three, the weighting was 0.00 (no better than chance agreement). Values between 0 and 1 are interpreted according to modified [25] published guidelines [26]: a value of 1.00–0.81 is considered very good agreement, 0.80–0.61 good, 0.60–0.41 moderate, 0.40–0.21 fair, and 0.20–0.00 poor agreement. We calculated single measured interclass correlation coefficients (ICCs), which are a measure of the quadrated difference among the values on an ordinal scale [27]. ICCs were calculated using the entire grading scale (0=absent; 1=minimal; 2=moderate; 3=severe), and because inter- and intra-observer reproducibility may be biased by an overemphasis on patients with grade 0 findings, ICC values were also calculated with the exclusion of grade 0 findings. To calculate a combined ICC for the complete score form, all assessments of each individual osteoarthritic parameter were summed and equally weighted.

Results

The frequency distribution of abnormalities found on MR imaging in our 25 patients is listed in Table 1. Data on inter- and intra-observer reproducibility are given in Table 2. Intra-observer reproducibility measured by weighted kappas ranged from 0.56 to 0.91. Intra-observer reproducibility measured by ICCs ranged from a minimal value of 0.78 for cartilaginous defects to a maximal value of 0.96 for Baker's cysts. The median ICC for all 10 parameters is 0.82. Inter-observer reproducibility measured by weighted kappas ranged from 0.57 to 0.88. ICCs for inter-observer reproducibility ranged from 0.63 for osteochondral defects to 0.91 for bone marrow edema. The median ICC for all 10 parameters is 0.74. The ICC value for intra-observer reproducibility of the complete score form was 0.83 (CI: 0.81–0.84) and inter-observer reproducibility of the complete score form was 0.77 (CI: 0.75–0.79). Intra-observer reproducibility with the exclusion of grade 0 findings, measured by ICCs, ranged from a minimal value of 0.59 for subluxation of the meniscus to a maximal value of 1.00. ICCs for inter-observer reproducibility with the exclusion of grade 0 findings ranged from 0.51 for cartilaginous defects to 1.00.

Table 1. Frequency distribution of abnormalities in 25 patients scored by the two observers

	Observer 1			Observer 2		
	N	Median	(Range)	N	Median	(Range)
Cartilaginous defects	104	4	(0-9)	104	5	(0-9)
Osteochondral defects	21	0	(0-3)	24	0	(0-4)
Osteophytes	115	4	(0-11)	136	6	(0-9)
Subchondral cysts	28	1	(0-5)	33	1	(0-4)
Bone marrow edema	23	0	(0-3)	23	0	(0-4)
Meniscal tears	17	2	(0-6)	15	2	(0-5)
Effusion & Synovitis	14	1	(0-1)	14	0	(0-1)
Baker's Cyst	12	0	(0-1)	11	0	(0-1)

Table 1 Frequency distribution of abnormalities in 25 patients scored by the two observers (n number of abnormalities found in the entire population, Median median number of defects per patient)

Table 2. Inter- and intra-observer reproducibility of MR findings in 25 patients

	Inter-observer reproducibility				Intra-observer reproducibility			
	ICC (95% CI)	ICC Ex 0	w-kappa		ICC (95% CI)	ICC Ex 0	w-kappa	
Cartilaginous defects	0,64 (0,58-0,69)	0,51	0,57		0,78 (0,74-0,81)	0,81	0,67	
Osteochondral defects	0,63 (0,55-0,70)	1,00	0,66		0,87 (0,83-0,90)	1,00	0,87	
Osteophytes	0,71 (0,67-0,76)	0,73	0,67		0,76 (0,72-0,80)	0,78	0,79	
Subchondral cysts	0,87 (0,83-0,89)	0,75	0,83		0,90 (0,87-0,92)	0,80	0,87	
Bone marrow edema	0,91 (0,88-0,93)	0,76	0,88		0,93 (0,91-0,94)	0,92	0,91	
Meniscal tears*	0,70 (0,61-0,77)		0,70		0,78 (0,70-0,83)		0,78	
I.S. Degeneration	0,78 (0,68-0,85)	0,71	0,66		0,76 (0,66-0,83)	0,71	0,56	
Sub luxation	0,67 (0,57-0,75)	0,57	0,65		0,82 (0,75-0,86)	0,59	0,82	
Effusion & Synovitis	0,74 (0,58-0,85)	1,00	0,69		0,81 (0,69-0,89)	1,00	0,77	
Baker Cyst	0,89 (0,76-0,95)	0,85	0,80		0,96 (0,90-0,98)	0,93	0,91	
All Parameters	0,77 (0,75-0,79)				0,83 (0,81-0,84)			

Table 2 Inter- and intra-observer reproducibility of the MR imaging findings in 25 patients (Ex0:intraclass correlation coefficient calculated without grade 0 findings (see text for explanation), ICC intraclass correlation coefficient, w-kappa weighted kappa)

* Kappa statistics were used instead of ICC (tear/no tear)

Discussion

Our comprehensive MR Knee Osteoarthritis Scoring System (KOSS) for osteoarthritic changes in the knee has an overall good to very good inter- and

intra-observer reproducibility (Table 2). Several communications reporting on inter- and intra-observer variability of various anatomical structures exist, but an outline of a similar comprehensive MR scoring system for osteoarthritis in the knee has, to the best of our knowledge, been presented only in an abstract by Wildy et al. [28]. Boegard et al. [14] reported an inter-observer agreement of 0.39–1.00 and an intra-observer agreement of 0.61–1.00 in the assessment of cartilage, subchondral bone and menisci in patients with osteoarthritis. Interobserver variability among three observers, using three grades of cartilage assessment (normal, partial-thickness, and full-thickness cartilage defects), was reported to be within the same range (0.54) as ours [29]. The kappa coefficient increased to 0.63 when the three grades were reduced to two (positive or negative for disease). In contrast, inter-observer agreement substantially lower than ours (k 0.0 – 0.4) has also been reported [15]. Although agreement appears to increase when structures other than cartilage are evaluated, the reported agreements still vary to a large extent. Inter-observer reproducibility, expressed by means of ICCs, of 0.58 for synovitis, 0.62 for bone erosions and 0.30 for joint space narrowing were reported in a study addressing rheumatoid arthritis in the hand using MR imaging. This study, conducted in five centers without intergroup calibration, suggests the need for better standardization [30]. A whole-organ MR imaging scoring method for knee osteoarthritis has been developed (WORMS), and has been presented as a poster and abstract. This scoring method also demonstrates high reliability (ICC 0.59–0.93) among well-trained readers. Compared with this study our ICC values are somewhat higher for bone marrow edema and subchondral cysts, similar for the scoring of meniscal tears, and lower for cartilage defects and osteophytes [28]. Our ICC values are in general somewhat higher than those published before. This might be explained by the fact that our study is a single-center study where both observers spend time in using the scoring system and its definitions in a uniform way. However, good inter- and intra-observer reproducibility was difficult to obtain for cartilaginous and osteochondral defects. These defects are easily overlooked because the small, focal type of defect is only visible on a single image, and because some lesions may be visualized to a lesser extent or not at all by either the SE or SPGR imaging techniques, their conspicuity and hence detection decreasing. As already stated by McCauley et al., incorporating both imaging techniques into the clinical imaging protocol might prove helpful in increasing sensitivity for focal cartilage defects [31]. The required assignment of a focal chondral defect to an anatomical compartment potentially decreases ICCs. When a defect is located at the junction of two adjacent compartments, the observer has to decide in which compartment the defect is scored. However, when we corrected for disparity in anatomical location, the ICC value for focal chondral lesions improved by only 0.04. The main difficulty in the scoring of osteophytes was distinguishing between their absence and presence. Most of the discrepancies between observers (86%) occurred between grade 0 (no osteophyte) and grade 1 (minimal osteophyte). Once both observers detected an osteophyte, it was graded identically in the

majority of cases (91%). The main limitation of our study is the lack of a reference standard such as arthroscopy. However, we wanted to avoid population bias and the MR sequences have been successfully used to evaluate cartilage and non-cartilaginous joint structures [2, 3, 4, 5, 32] with accuracies of more than 90% [12, 13, 17, 33]. It needs to be emphasized, however, that the present study was purely an evaluation by two observers of a scoring system as opposed to an evaluation of a scoring system against a secondary gold standard. Another limitation is that we did not evaluate signal intensity changes within cartilage. We feel that with current clinically available equipment and pulse sequences, consistent reproducible diagnosis of signal intensity changes within otherwise normal cartilage is not yet robust enough to use in longitudinal studies. Because our objective was to present a scoring system for all grades of osteoarthritis, and not specifically early osteoarthritis, that can be used in longitudinal studies allowing monitoring of change over time, we decided not to incorporate these signal intensity changes. Neither did we grade signal intensity changes within bone marrow edema. A major disadvantage of our scoring system is the time required for analysis. Depending on the amount of focal chondral and osteochondral defects, each MR examination requires approximately 30 min of careful evaluation. In contrast, another MRI-based study required only 15 – 30 min of evaluation [14]. In that study, however, only focal cartilage defects, osteochondral defects and meniscal tears were assessed and graded. The time required to use KOSS is in our opinion commensurate with the advantage of having a reproducible, comprehensive compartment-based scoring system available for monitoring medical therapy in research studies. However, our scoring system takes too much time to be useful in daily clinical practice. It may seem a disadvantage that most abnormalities of the different osteoarthritic characteristics fall within grade 0 and 1 (Table 2). The reason for this is that we graded nine different anatomical locations in each patient. When a grade 3 abnormality was present in one of these anatomical locations the eight other anatomical locations usually did not show severe abnormalities. Our analysis excluding grade 0 shows that inter- and intra-observer agreement remains the same. A comprehensive scoring system with acceptable inter- and intra-observer agreement creates the opportunity for weighting of the various osteoarthritis characteristics. Further studies will be needed to determine these weighting factors. Once weighting factors have been determined an overall score would be of value, both for longitudinal studies and clinical correlation. The ultimate aim is to calculate a prognostic value for the development and progression of osteoarthritis, which in turn would improve patient selection for and monitoring of therapy. A reliable scoring system will also improve our ability to evaluate the relationship, if any, between clinical symptoms and imaging characteristics. In conclusion, we present a comprehensive MR scoring system, using detailed definitions, for osteoarthritic changes of the knee with good to very good inter-observer and intra-observer reproducibility. Thus the score form with its definitions can be used for standardized assessment of osteoarthritic changes to monitor medical therapy in research studies.

Acknowledgements

Pfizer Inc., Groton, Conn., USA provided generous support for this work. The authors would also like to acknowledge support of the cooperating hospitals and referring rheumatologists, orthopaedic surgeons and general practitioners in our region. We also wish to thank Annette van den Berg-Huysmans for her statistical assistance.

References

1. Felson DT, Naimark A, Anderson J, Kazis L, Castelli W, Meenan RF. The prevalence of knee osteoarthritis in the elderly. The Framingham Osteoarthritis Study. *Arthritis Rheum* 1987; 30:914–918.
2. Recht M, Bobic V, Burstein D, et al. Magnetic resonance imaging of articular cartilage. *Clin Orthop* 2001; 391 (Suppl):S379–S396.
3. Peterfy CG, Genant HK. Emerging applications of magnetic resonance imaging in the evaluation of articular cartilage. *Radiol Clin North Am* 1996; 34:195–213, ix.
4. Eckstein F, Reiser M, Englmeier KH, Putz R. In vivo morphometry and functional analysis of human articular cartilage with quantitative magnetic resonance imaging: from image to data, from data to theory. *Anat Embryol (Berl)* 2001; 203:147–173.
5. Peterfy CG. Scratching the surface: articular cartilage disorders in the knee. *Magn Reson Imaging Clin North Am* 2000; 8:409–430.
6. McCauley TR, Kornaat PR, Jee WH. Central osteophytes in the knee: prevalence and association with cartilage defects on MR imaging. *AJR Am J Roentgenol* 2001; 176:359–364.
7. Ostergaard M, Stoltzenberg M, Henriksen O, Lorenzen I. The accuracy of MRI-determined synovial membrane and joint effusion volumes in arthritis. A comparison of pre- and post-aspiration volumes. *Scand J Rheumatol* 1995; 24:305–311.
8. Ostergaard M, Stoltzenberg M, Lovgreen- Nielsen P, Volck B, Jensen CH, Lorenzen I. Magnetic resonance imaging-determined synovial membrane and joint effusion volumes in rheumatoid arthritis and osteoarthritis: comparison with the macroscopic and microscopic appearance of the synovium. *Arthritis Rheum* 1997; 40:1856–1867.
9. Vincken PW, ter Braak BP, van Erkel AR, et al. Effectiveness of MR imaging in selection of patients for arthroscopy of the knee. *Radiology* 2002; 223:739–746.
10. Shahriaree H. Chondromalacia. *Contemp Orthop* 1985; 11:27–39.
11. Outerbridge RE. The etiology of chondromalacia patellae. *Clin Orthop* 2001; 389:5–8.
12. Disler DG, McCauley TR, Kelman CG, et al. Fat-suppressed three-dimensional spoiled gradient-echo MR imaging of hyaline cartilage defects in the knee: comparison with standard MR imaging and arthroscopy. *AJR Am J Roentgenol* 1996; 167:127–132.
13. Potter HG, Linklater JM, Allen AA, Hannafin JA, Haas SB. Magnetic resonance imaging of articular cartilage in the knee. An evaluation with use of fast-spin-echo imaging. *J Bone Joint Surg Am* 1998; 80:1276–1284.
14. Boegard TL, Rudling O, Petersson IF, Jonsson K. Magnetic resonance imaging of the knee in chronic knee pain. A 2-year follow-up. *Osteoarthritis Cartilage* 2001; 9:473–480.
15. McNicholas MJ, Brooksbank AJ, Walker CM. Observer agreement analysis of MRI grading of knee osteoarthritis. *J R Coll Surg Edinb* 1999; 44:31–33.
16. Biswal S, Hastie T, Andriacchi TP, Bergman GA, Dillingham MF, Lang P. Risk factors for progressive cartilage loss in the knee: a longitudinal magnetic resonance imaging study in fortythree patients. *Arthritis Rheum* 2002; 46:2884–2892.
17. Bredella MA, Tirman PF, Peterfy CG, et al. Accuracy of T2-weighted fast spin-echo MR imaging with fat saturation in detecting cartilage defects in the knee: comparison with arthroscopy in 130 patients. *AJR Am J Roentgenol* 1999; 172:1073–1080.
18. Link TM, Steinbach LS, Ghosh S, et al. Osteoarthritis: MR imaging findings in different stages of disease and correlation with clinical findings. *Radiology* 2003; 226:373–381.
19. Peterfy CG. Imaging of the disease process. *Curr Opin Rheumatol* 2002; 14:590–596.
20. Kellgren JH, Lawrence RC. Radiographic assessment of osteoarthritis. *Ann Rheum Dis* 1957; 16:494–502.

21. Yulish BS, Montanez J, Goodfellow DB, Bryan PJ, Mulopulos GP, Modic MT. Chondromalacia patellae: assessment with MR imaging. *Radiology* 1987; 164:763–766.
22. Mink JH, Deutsch AL. Occult cartilage and bone injuries of the knee: detection, classification, and assessment with MR imaging. *Radiology* 1989; 170:823–829.
23. Stoller DW, Martin C, Crues JV, III, Kaplan L, Mink JH. Meniscal tears: pathologic correlation with MR imaging. *Radiology* 1987; 163:731–735.
24. Lewandrowski KU, Muller J, Schollmeier G. Concomitant meniscal and articular cartilage lesions in the femorotibial joint. *Am J Sports Med* 1997; 25:486–494.
25. Altman DG. *Practical statistics for medical research*. London: Chapman & Hall, 1991.
26. Landis JR, Koch GG. The measurement of observer agreement for categorical data. *Biometrics* 1977; 33:159–174.
27. Armitage P, Berry G. *Statistical methods in medical research*, 3rd edn. Oxford: Blackwell Science, 1994.
28. Wildy KS, Zaim S, Peterfy CG, Newman AB, Kritchevsky S, Nevitt M. Reliability of the Whole-Organ MRI Scoring (WORMS) Method for knee OA in a multi-center study. *Arthritis Rheum* 2001; 44 (Suppl 9):S155.
29. Sonin AH, Pensy RA, Mulligan ME, Hatem S. Grading articular cartilage of the knee using fast spin-echo proton density-weighted MR imaging without fat suppression. *AJR Am J Roentgenol* 2002; 179:1159–1166.
30. Ostergaard M, Klarlund M, Lassere M, et al. Interreader agreement in the assessment of magnetic resonance images of rheumatoid arthritis wrist and finger joints: an international multicenter study. *J Rheumatol* 2001; 28:1143–1150.
31. McCauley TR, Recht MP, Disler DG. Clinical imaging of articular cartilage in the knee. *Semin Musculoskelet Radiol* 2001; 5:293–304.
32. Recht MP, Resnick D. MR imaging of articular cartilage: current status and future directions. *AJR Am J Roentgenol* 1994; 163:283–290.
33. Recht MP, Piraino DW, Paletta GA, Schils JP, Belhobek GH. Accuracy of fat-suppressed three-dimensional spoiled gradient-echo FLASH MR imaging in the detection of patellofemoral articular cartilage abnormalities. *Radiology* 1996; 198:209–212.



3

Chapter 3

Magnetic resonance imaging of knee cartilage using a water selective balanced steady-state free precession sequence

Peter R Kornaat
Joost Doornbos
Aart J van der Molen
Margreet Kloppenburg
Rob G Nelissen
Pancras CW Hogendoorn
Johan L Bloem

Abstract

Purpose

To compare an optimized water selective balanced steady-state free precession sequence (WS-bSSFP) with conventional magnetic resonance (MR) sequences in imaging cartilage of osteoarthritic knees.

Materials and Methods

Flip angles of sagittal and axial WS-bSSFP sequences were optimized in three volunteers. Subsequently, the knees of 10 patients with generalized osteoarthritis were imaged using sagittal and axial WS-bSSFP and conventional MR imaging techniques. We calculated contrast-to-noise ratios (CNR) between cartilage and its surrounding tissues to quantitatively analyze the various sequences. Using dedicated software we compared, in two other patients, the accuracy of cartilage volume measurements with anatomic sections of the tibial plateau.

Results

CNR_{total eff} (CNR efficiency between cartilage and its surrounding tissue) using WS-bSSFP was maximal with a 20–25° flip angle. CNR_{total eff} was higher in WS-bSSFP than in conventional images: 6.1 times higher compared to T1-weighted gradient echo (GE) images, 5.1 compared to proton-density (PD) fast spin echo (FSE) images, and 4.8 compared to T2-weighted FSE images. The mean difference of cartilage volume measurement on WS-bSSFP and anatomic sections was 0.06 mL compared to 0.24 mL for T1-GE and anatomic sections.

Conclusion

A WS-bSSFP sequence is superior to conventional MR imaging sequences in imaging cartilage of the knee in patients with osteoarthritis.

Introduction

Magnetic resonance (MR) imaging has been used successfully to visualize cartilage (1). Currently, the techniques most widely used for imaging cartilage are fat suppressed proton-density weighted fast spin-echo (PD-FSE), fat suppressed T2-weighted fast spin-echo (T2-FSE), and fat suppressed T1-weighted gradient echo (T1-GE) sequences (2,3). Recently, several other MR imaging pulse sequences have attracted attention with regard to their optimal visualization of cartilage (4,5). These sequences include steady-state free precession (SSFP) techniques such as fluctuating equilibrium MR (FEMR) (6), fat suppressed steady-state free precession (FS-SSFP) (7), linear combination steady state free precession (LC-SSFP) (8), Dixon SSFP imaging (9), and dual-echo steady-state (DESS) (10). Other imaging

techniques successfully used for cartilage imaging are driven equilibrium Fourier transform (DEFT) (11), three-dimensional fat-suppressed echo planar imaging (EPI) (12,13), magnetization-transfer contrast (MTC) (14), and selective water excitation (15–18). Our purpose was to optimize a three-dimensional balanced SSFP imaging sequence in combination with water excitation for MR imaging of articular cartilage of the knee, and to compare this sequence with conventional MR imaging sequences in patients with osteoarthritis. The other sequences included were T1-GE, PD-FSE, and T2-FSE, all in combination with fat-suppression.

Materials and methods

Patients

The study was approved by our institution's medical ethical review board. Written informed consent was obtained from the patients before the study and permission was given by the patients, who underwent total knee arthroplasty, to use the tibial plateau for the purpose of this study. Twelve patients and three normal volunteers were included in this study. Images of the three volunteers were used to optimize MR image contrast. Subsequently, knees of 10 patients with radiographic characteristics of osteoarthritis were imaged using the optimized sequences. Osteoarthritis of the knee was defined as a Kellgren and Lawrence score on conventional radiographs of the knee of more than 1 (19). The 10 patients aged between 54 to 74 years (median 61 years). Anatomic sections of the tibial plateau were obtained in two patients (64 and 70 years old) who underwent total knee arthroplasty because of severe osteoarthritis. Optimization in Three Volunteers The flip angle of the WS-bSSFP sequence was optimized in three volunteers. Each volunteer was scanned 11 times using the WS-bSSFP sequence, with stepwise increase of the flip angle. Flip angles used were 5, 10, 15, 20, 25, 30, 40, 50, 60, 70, and 80°. The optimal flip angle for articular cartilage imaging was defined as the maximal contrast-to-noise ratio (CNR) between cartilage and its surrounding tissues. This was performed both in the sagittal and axial orientated WS-bSSFP images.

MR Acquisition

All MR images were acquired with a 1.5-T superconducting MRI-system (Gyrosan Intera, Philips Medical Systems, Best, The Netherlands) using a dedicated knee coil. Each examination consisted of the following sequences: sagittal three-dimensional fat suppressed T1-GE sequence (repetition time [TR] 46 msec; echo time [TE] 2.5 msec; flip angle 40°; 3.0-mm slice thickness; slice overlap 1.5 mm; 180 mm field of view [FOV]; 205 x 256 acquisition matrix; voxel size 0.70 x 0.88 x 3.00 mm; bandwidth/pixel: 628.7; acquisition time 7 minutes 55 seconds), axial fat-suppressed proton density- and T2-weighted dual FSE (PD/T2-FSE) sequence (TR 2500 msec; TE 7.1/40 msec; echo train length 6; 2-mm slice thickness; no gap; 170 mm FOV; 205 x 256 acquisition matrix; voxel size 0.66 x 0.83 x 2.00 mm;

bandwidth/pixel: 200.3; acquisition time eight minutes and five seconds), and a sagittal and axial WS-bSSFP sequence (Fig. 1) (TR 16 msec [shortest]; TE 8 msec [shortest]; 2.0-mm slice thickness; slice overlap 1 mm; 75 slices; 140 mm FOV; 272 x 272 acquisition matrix; voxel size 0.51 x 0.51 x 2.00 mm; flip angle: 25°; automatic shim; 1:1 water excitation [Proset: a frequency selective and spatially selective binomial shaped water excitation pulse with a pulse duration of 3.41 msec]; bandwidth/pixel: 98.6; acquisition time five minutes and five seconds). Total acquisition time of the four sequences (including the initial survey sequence) was 27 minutes.

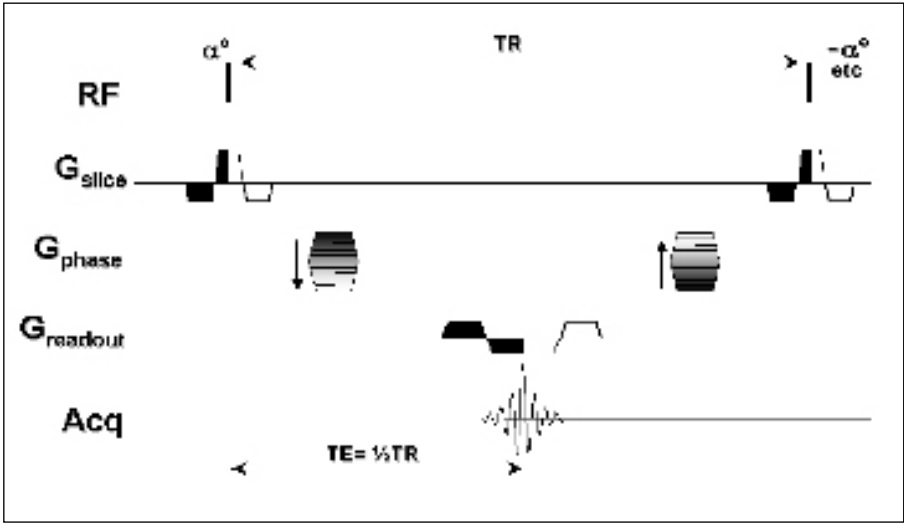


Figure 1. Schematic display of a WS-bSSFP sequence. RF: radio frequency pulse; G: gradient; Acq: signal acquisition.

Quantitative Analysis

For quantitative analyses, not only signal intensities (SI) of cartilage and synovial fluid, but also other surrounding tissues including bone, menisci, muscles, and fat, were measured on axial and sagittal WSbSSFP, T1-GE, and PD/T2-FSE images. The regions of interest (ROI) used to measure SI were placed at identical positions on matching sections in each patient. We selected a single slice displaying all above mentioned tissue types in each patient (Fig. 2). The mean SI over the ROIs was used to represent the tissue's signal. The minimal surface area of a ROI was 15 mm², and the mean surface area of a ROI was 163 mm². We calculated CNR between cartilage (ca) and fluid using the following formula:

$$CNR_{ca-fluid} = |SI_{cartilage} - SI_{fluid}| / SI_{noise}$$

Because cartilage is only in contact with synovial fluid for a small percentage of the total cartilage perimeter, we are also interested in a sequence with good

contrast between cartilage and other surrounding tissue. Therefore, we calculated CNR_{total} between cartilage and all of the cartilage surrounding tissues (n) using the formula:

$$CNR_{total} = (|SI_{cartilage} - SI_{tissue_n}| / SI_{noise}) \times (Tissue_n \text{ to cartilage interface (mm)} / \text{Total cartilage perimeter (mm)})$$

In this formula, tissue to cartilage interface is the length in millimeters where bone, fluid, menisci, fat, and muscle, respectively, are in direct contact with cartilage. Tissue-to- cartilage interface divided by the total cartilage perimeter represents the percentage of cartilage that is in direct contact with a specific tissue. For example, for bone this percentage is 50% because half of the cartilage (the nonarticular side) is always in direct contact with bone. When calculating CNR_{total} we used the same slice per sequence in each patient to keep the tissue-to-cartilage interface the same for all compared sequences. Additionally, we calculated CNR efficiencies for comparison. CNR efficiency is the ratio of CNR to the square root of total imaging time (4). In comparing sequences, the relative CNR efficiency numbers are used. All CNR efficiency calculations are normalized by voxel volume. Because SSFP techniques are sensitive to magnetic field inhomogeneity, we compared CNRs between bone and cartilage that were based on SI measurements of both the most medial and most lateral sections of the axially orientated WS-bSSFP image sequence.

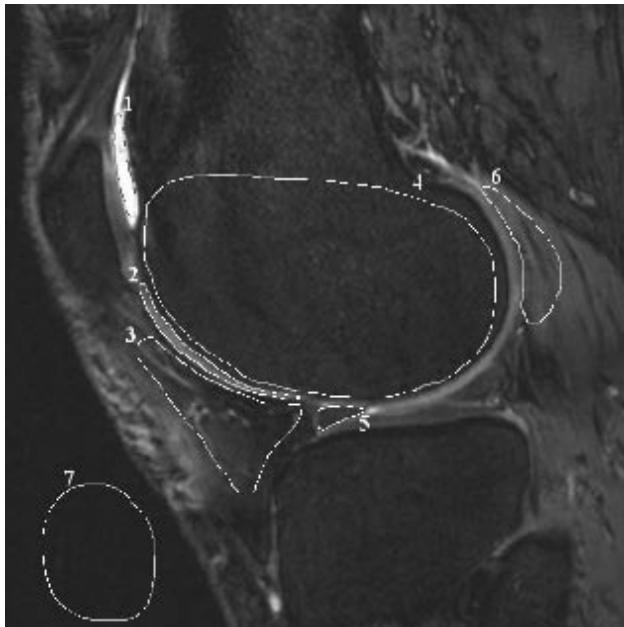


Figure 2. Example of placement of ROI on sagittal WS-bSSFP image. ROI 1 = fluid; ROI 2 = cartilage; ROI 3 = fat; ROI 4 = bone; ROI 5 = meniscus; ROI 6 = muscle; ROI 7 = noise.

Cartilage Volume Measurements

In two patients who underwent total knee arthroplasty, the preoperatively obtained MR images and the anatomic sections of the tibial plateau were used to determine and compare cartilage volume measurements. Immediately after total knee arthroplasty, sagittal anatomic sections of the tibia plateau were obtained with a thickness of 4 mm, using a diamond band saw (Exact Apparatebau, Norderstedt, Germany) that is capable of creating anatomic sections without damaging the cartilage. The anatomic sections were placed next to a ruler and were digitally photographed (Fig. 3). The sagittal WS-bSSFP and T1-GE sequences and the digital photographs were analyzed quantitatively on an IPC workstation (SUN Microsystems Inc., Mountain View, CA), by one observer, using the MASS software package (20). All cartilage contours were drawn manually. Cartilage volumes measured on the anatomic sections of the tibia plateau were compared with the cartilage volumes measured on the two MR sequences.

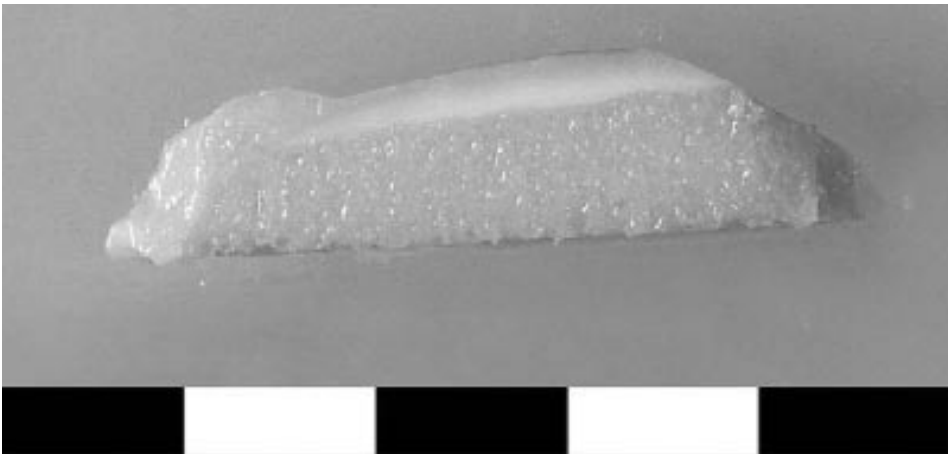


Figure 3. Digitally photographed anatomic section of tibia plateau, placed next to a centimeter ruler.

Results

Figure 4 shows the CNR between cartilage and fluid and CNR between cartilage and surrounding tissues as a Maximum CNR between cartilage and fluid and cartilage and surrounding tissues in a WS-bSSFP sequence is displayed at 20° for the axial orientated images and at 25° for the sagittal images. CNRs and acquisition times of the sequences are presented in Table 1. CNR efficiencies between cartilage and synovial fluid, and between cartilage and all its surrounding tissues, obtained with WS-bSSFP sequences are higher than those obtained with conventional sequences. Figure 5 shows an example of cartilage surface detail on WS-bSSFP images and on conventional images. Field inhomogeneity on the WS-bSSFP sequence is reflected by differences in SI obtained on medial and lateral sides on axial images. Over all 10 patients, the average SI of bone at the medial

side was 46.28 and 47.40 at the lateral side of the knee. The average difference of bone signal between medial and lateral side was 1.92 (3.2%). Table 2 shows the cartilage volume of the medial and lateral tibia plateau in the anatomic sections, WSbSSFP, and T1-GE images in two patients. The differences between cartilage volumes measured on anatomic sections and on MR images were smallest using WS-bSSFP images in three out of four regions. The mean difference between cartilage volume measurements on anatomic sections and WS-bSSFP images was 0.06 mL. The mean difference between anatomic sections and T1-GE images was 0.24 mL.

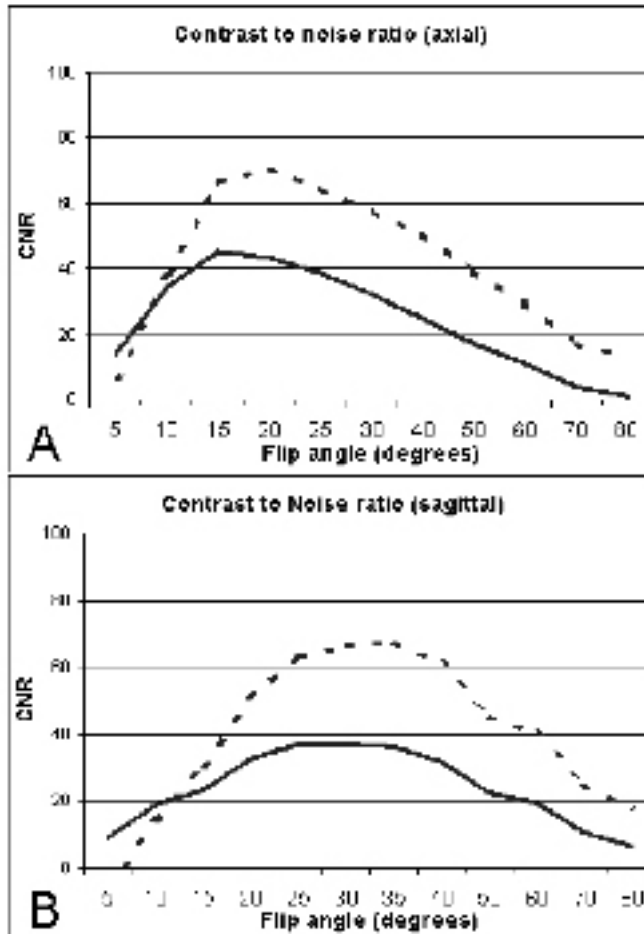


Figure 4. a: CNR of cartilage and fluid (dashed line) and cartilage and all of its surrounding tissue (bold line) in axial WS-bSSFP images. b: CNR of cartilage and fluid (dashed line) and cartilage and all of its surrounding tissue (bold line) in sagittal WS-bSSFP images.

Table 1 Average CNR Efficiencies Between Cartilage and Other Tissues (Interpatient Variation) Over 10 Patients

	WS-bSSFP	T1-GE ^a	PD-FSE ^a	T2-FSE ^a
CNRca-fluid eff	1	0.05 (0.03–0.12)	0.15 (0.06–0.57)	0.17 (0.09–0.38)
CNRca-bone eff	1	0.23 (0.16–0.48)	0.27 (0.17–0.41)	0.28 (0.14–1.12)
CNRca-meniscus eff	1	0.14 (0.08–0.79)	b	b
CNRca-muscle eff	1	0.18 (0.08–0.81)	b	b
CNRca-fat eff	1	0.19 (0.11–0.38)	b	b
CNRtotal eff	1	0.16 (0.11–0.35)	0.20 (0.12–0.28)	0.21 (0.15–0.32)
Tacq (min)	5.05	7.55	4.03	4.03

Table 1 Average CNR Efficiencies Between Cartilage and Other Tissues (Interpatient Variation) Over 10 Patients

^aAll CNR efficiencies and interpatient variation are relative to the WS-bSSFP sequence.
^bContrast between cartilage and meniscus, cartilage and muscle, and cartilage and fat was not calculated on axial PD-FSE and T2-FSE weighted images.
CNRca-fluid eff = contrast to noise ratio efficiency between cartilage and fluid, CNRtotal eff. = contrast to noise ratio efficiency between cartilage and all of its surrounding tissue, WS-bSSFP = balanced steady-state free precession with water excitation, T1-GE = T1 weighted gradient echo sequence with fat suppression, PD-FSE = proton-density weighted fast spin echo sequence with fat suppression, T2-FSE = T2 weighted fast spin echo sequence with fat suppression, Tacq = acquisition time.

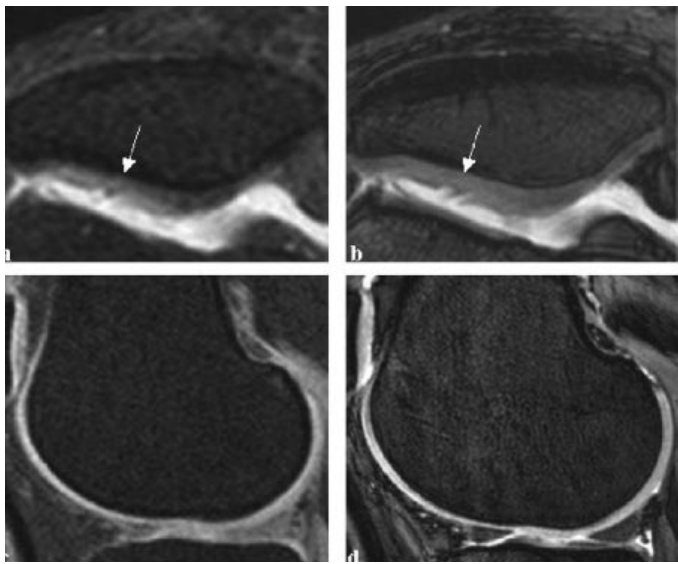


Figure 5. Axial fat suppressed T2-FSE image (a) compared to the axial WSbSSFP image (b) of patellar cartilage shows a clear delineation of the cartilage surface in the latter. Note that a small focal cartilage defect is appreciated better on the WS-bSSFP image than on the fat suppressed T2-FSE image (white arrow). Comparison of fat suppressed T1-GE image (c), and the WS-bSSFP image (d). The latter shows better cartilage surface detail and less blurring of cartilage. Note the difference in cartilage SI between the anterior and posterior part of the cartilage in d. This might be due to the sensitivity profile of the knee coil.

Table 2. Cartilage Volume in mL of Tibia Plateau in Two Patients Measured on Sagittal MR Images and Sagittal Anatomical Sections

		Anatomical sections	WS-bSSFP	T1-GE
Patient 1	Medial	0.86	0.90	0.60
Patient 1	Lateral	1.62	1.63	1.88
Patient 2	Medial	0.96	0.84	0.92
Patient 2	Lateral	1.84	1.76	2.22

Table 2 Cartilage Volume in mL of Tibia Plateau in Two Patients Measured on Sagittal MR Images and Sagittal Anatomical Sections Anatomical sections
mL = milliliters, WS-bSSFP = balanced steady-state free precession with water excitation, T1-GE = T1 weighted gradient echo with fat suppression.

Discussion

CNR between cartilage and the cartilage surrounding tissues on WS-bSSFP sequence is optimal with a flip angle of 20–25°. Our result is in accordance with theoretical SI curves derived from literature (4,9,21,22). Reeder et al (9) optimized flip angles for SSFP imaging of cartilage with a method that is similar in principle to the method used to optimize the flip angle for SPGR sequences using the Ernst angle. In that study the flip angle that maximized the cartilage signal of an SSFP image was 27°. CNR between cartilage and surrounding tissue in axial orientated images is somewhat higher than in the sagittal orientated images. The reason for this small difference in CNR is the difference in composition of the tissues surrounding cartilage in axial and sagittal images. In the sagittal images, the cartilage contacts also the menisci and muscle. However, on axial images, cartilage does not contact the menisci and muscle. CNR between cartilage and fluid is similar for the sagittal and axially orientated images. CNR between cartilage and synovial fluid is higher in WS-bSSFP images than in the T1-GE, PD-FSE, and T2-FSE images. More importantly, we found an increased CNR between cartilage and all of its surrounding tissue in WS-bSSFP images compared to conventional images. This is important because techniques for quantifying cartilage volume have been developed (16,23–26). These techniques require segmentation. Segmentation in its turn requires high contrast between cartilage and surrounding tissues combined with a high spatial resolution. Therefore, an optimal imaging technique for automatic or semi-automatic assessment of cartilage volume should have a high CNR between cartilage and all cartilage surrounding tissue, together with an optimal delineation of cartilage surface detail. These requirements make the WS-bSSFP imaging technique ideal for cartilage imaging. Another advantage of WS-bSSFP over the conventional imaging techniques is the excellent cartilage surface detail. Actual sharpness of the cartilage is not quantitated, but the observed sharpness is better because the voxel size used in the WS-bSSFP sequence is smaller than that of the conventional sequences. Decrease of voxel size in the WSbSSFP sequence was possible because CNRs in the WS-bSSFP sequence are high compared to conventional imaging techniques. This sharp delineation of the tissues (i.e., low blurring) is highly desirable because it makes

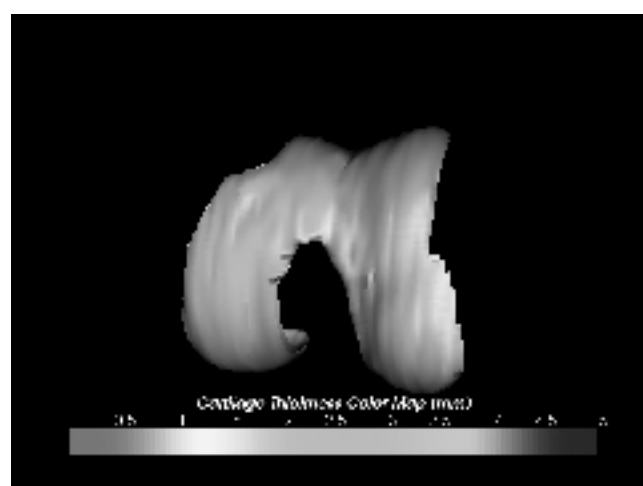
the process of cartilage segmentation much easier. These advantages can be obtained using clinically acceptable acquisition times. WS-BSSFP sequences have an acquisition time that is two-thirds of the fat suppressed T1-GE, and one minute longer than the PD-FSE and T2-FSE sequences used in this study. We found less difference between cartilage volumes measured on anatomic sections and WS-bSSFP images than between cartilage volumes measured on anatomic sections and T1-GE images. Because WS-bSSFP images show a more detailed cartilage contour and CNR between cartilage and surrounding tissues is higher, WS-bSSFP images allow a more unequivocal contour tracing of cartilage than T1-GE images because of superior CNR and sharpness. MR images of articular cartilage acquired with WSbSSFP sequences have several advantages over those with conventional fat suppressed T1-GE and PD/T2- FSE sequences. WS-bSSFP imaging technique uses water excitation instead of fat saturation techniques in the conventional cartilage imaging sequences. This provides a better fat suppression because the lipid signal is never excited (27). It has been shown that an increased CNR between cartilage and fluid is obtained using SSFP sequences alone (4), or with the use of selective water excitation (15–18) compared to conventional imaging techniques such as FSE and GE sequences. Although already described in 1958 by Carr (28), balanced steady-state free precession (commercially also known as True-FISP, FIESTA, or balanced FFE) has become feasible and popular in clinical practice during the past four years (22). The WS-bSSFP sequence, presented in this paper is characterized by time-balanced gradients for all gradient directions (X, Y, Z). Its contrast is related to T2/T1 ratio, independent of the repetition time. An alternating phase of excitation pulse ensures combined acquisition of echo and free induction decay (FID) signal. Balanced gradient echo sequences are flow compensated and show few flow artifacts. The WS-bSSFP sequence needs field shimming to improve field homogeneity because SSFP techniques are sensitive to magnetic field inhomogeneity. Shimming improves image quality especially in and near Hoffa's fat pad and subcutaneous fat near the coil. After shimming of the WS-bSSFP sequence, no influence of field inhomogeneity is measured as CNRs are similar at the lateral and medial side of the knee. We measured a difference of only 1.8%. In the current study we compared WS-bSSFP sequence to conventional SPGR and FSE sequences. Comparing WS-bSSFP sequence with other SSFP based sequences is difficult. In the present study we ran the WS-bSSFP sequence on a Philips 1.5-T system. Most of the other SSFP sequences described in the literature, such as FEMR, LC-SSFP, FS-SSFP, and Dixon SSFP sequences, run on a GE or Siemens 1.5-T system (6– 9,11). Therefore, we could not directly compare the WSbSSFP sequence to the other SSFP sequences in the same patients. In theory, the primary difference between WS-bSSFP and other SSFP sequences is the fat suppression technique. Most of the SSFP sequences described in literature use fat suppression as opposed to the water excitation of the WS-bSSFP technique. The contrast achieved, however, should be similar because the sequences all use a SSFP technique. The Dixon SSFP is even more similar to the WS-bSSFP sequence because it acquires water-weighted images. Main advantage of WS-bSSFP

above the other SSFP sequences is that it benefits from the homogeneous field of the Philips scanner. A disadvantage of WS-bSSFP compared to the other SSFP sequences is the slightly longer scan time. Other SSFP based techniques show acquisition times of three to four minutes, where WS-bSSFP lasts five minutes and five seconds. A limitations of this study is that the number of patients used for determining the accuracy of the WSbSSFP sequences to measure cartilage volume is relatively small. However, there is a clear trend in the results, showing that the WS-bSSFP sequence provides higher accuracy in the determination of cartilage volume. Another limitation of this study is that we compared our sequences with validated conventional T1-GE, PDFSE, and T2-FSE sequences by means of CNR. We did not correlate our findings with cadaver knees. However, although results of new sequences are correlated sometimes with cadaver knees (12), comparison between SNR and CNR of the sequences is the usual method. An advantage of this study is that it has been performed in patients with osteoarthritis. When articular cartilage is damaged, the structure of its collagen framework is disorganized leading to abnormal consistency of cartilage (29). Therefore, comparison of cartilage MR sequences developed to image damaged articular cartilage should be performed in patients with this different consistency of cartilage in contrast to control subjects with healthy cartilage. In conclusion, WS-bSSFP MR imaging sequence allows, relative to conventional MR imaging sequences, optimal imaging of cartilage in the osteoarthritic knee, with clinically acceptable acquisition times.

References

1. Peterfy CG. Scratching the surface: articular cartilage disorders in the knee. *Magn Reson Imaging Clin N Am* 2000;8:409–430.
2. Recht M, Bobic V, Burstein D, et al. Magnetic resonance imaging of articular cartilage. *Clin Orthop* 2001;(391 Suppl):S379–S396.
3. McCauley TR, Recht MP, Disler DG. Clinical imaging of articular cartilage in the knee. *Semin Musculoskelet Radiol* 2001;5:293–304.
4. Hargreaves BA, Gold GE, Beaulieu CF, Vasanawala SS, Nishimura DG, Pauly JM. Comparison of new sequences for high-resolution cartilage imaging. *Magn Reson Med* 2003;49:700–709.
5. Gold GE, McCauley TR, Gray ML, Disler DG. What's new in cartilage? *Radiographics* 2003;23:1227–1242.
6. Vasanawala SS, Pauly JM, Nishimura DG, Gold GE. MR imaging of knee cartilage with FEMR. *Skeletal Radiol* 2002;31:574–580.
7. Scheffler K, Heid O, Hennig J. Magnetization preparation during the steady state: fat-saturated 3D TrueFISP. *Magn Reson Med* 2001;45:1075–1080.
8. Vasanawala SS, Pauly JM, Nishimura DG. Linear combination steady-state free precession MRI. *Magn Reson Med* 2000;43:82–90.
9. Reeder SB, Pelc NJ, Alley MT, Gold GE. Rapid MR imaging of articular cartilage with steady-state free precession and multipoint fat-water separation. *AJR Am J Roentgenol* 2003;180:357–362.
10. Hardy PA, Recht MP, Piraino D, Thomasson D. Optimization of a dual echo in the steady state (DESS) free-precession sequence for imaging cartilage. *J Magn Reson Imaging* 1996;6:329–335.
11. Hargreaves BA, Gold GE, Lang PK, et al. MR imaging of articular cartilage using driven equilibrium. *Magn Reson Med* 1999;42:695–703.

12. Karantanas AH, Zibis AH, Kitsoulis P. Fat-suppressed 3D-T1-weighted-echo planar imaging: comparison with fat-suppressed 3D-T1-weighted-gradient echo in imaging the cartilage of the knee. *Comput Med Imaging Graph* 2002;26:159–165.
13. Trattinig S, Huber M, Breitenseher MJ, et al. Imaging articular cartilage defects with 3D fat-suppressed echo planar imaging: comparison with conventional 3D fat-suppressed gradient echo sequence and correlation with histology. *J Comput Assist Tomogr* 1998;22:8–14.
14. Wolff SD, Chesnick S, Frank JA, Lim KO, Balaban RS. Magnetization transfer contrast: MR imaging of the knee. *Radiology* 1991; 179:623–628.
15. Burgkart R, Glaser C, Hyhlik-Durr A, Englmeier KH, Reiser M, Eckstein F. Magnetic resonance imaging-based assessment of cartilage loss in severe osteoarthritis: accuracy, precision, and diagnostic value. *Arthritis Rheum* 2001;44:2072–2077.
16. Glaser C, Faber S, Eckstein F, et al. Optimization and validation of a rapid high-resolution T1-w 3D FLASH water excitation MRI sequence for the quantitative assessment of articular cartilage volume and thickness. *Magn Reson Imaging* 2001;19:177–185.
17. Hauger O, Dumont E, Chateil JF, Moinard M, Diard F. Water excitation as an alternative to fat saturation in MR imaging: preliminary results in musculoskeletal imaging. *Radiology* 2002;224: 657–663.
18. Yoshioka H, Alley M, Steines D, et al. Imaging of the articular cartilage in osteoarthritis of the knee joint: 3D spatial-spectral spoiled gradient-echo vs. fat-suppressed 3D spoiled gradient-echo MR imaging. *J Magn Reson Imaging* 2003;18:66–71. Cartilage Imaging Using WS-bSSFP 855
19. Kellgren JH, Lawrence RC. Radiographic assessment of osteoarthritis. *Ann Rheum Dis* 1957;16:494–502.
20. Pattynama PM, Lamb HJ, Van der Velde EA, van der Geest RJ, van der Wall EE, de Roos A. Reproducibility of MRI-derived measurements of right ventricular volumes and myocardial mass. *Magn Reson Imaging* 1995;13:53–63.
21. Vasawala SS, Pauly JM, Nishimura DG, Gold GE. MR imaging of knee cartilage with FEMR. *Skeletal Radiol* 2002;31:574–580.
22. Scheffler K, Lehnhardt S. Principles and applications of balanced SSFP techniques. *Eur Radiol* 2003;13:2409–2418.
23. Peterfy CG, van Dijke CF, Janzen DL, et al. Quantification of articular cartilage in the knee with pulsed saturation transfer subtraction and fat-suppressed MR imaging: optimization and validation. *Radiology* 1994;192:485–491.
24. Eckstein F, Winzheimer M, Hohe J, Englmeier KH, Reiser M. Interindividual variability and correlation among morphological parameters of knee joint cartilage plates: analysis with three-dimensional MR imaging. *Osteoarthritis Cartilage* 2001;9:101–111.
25. Cicuttini F, Forbes A, Asbeutah A, Morris K, Stuckey S. Comparison and reproducibility of fast and conventional spoiled gradient echo magnetic resonance sequences in the determination of knee cartilage volume. *J Orthop Res* 2000;18:580–584.
26. Cohen ZA, McCarthy DM, Kwak SD, et al. Knee cartilage topography, thickness, and contact areas from MRI: in-vitro calibration and in vivo measurements. *Osteoarthritis Cartilage* 1999;7:95–109.
27. Hardy PA, Recht MP, Piraino DW. Fat suppressed MRI of articular cartilage with a spatial-spectral excitation pulse. *J Magn Reson Imaging* 1998;8:1279–1287.
28. Carr HY. Steady-state free precession in nuclear magnetic resonance. *Phys Rev* 1958;112:1693–1701.
29. Buckwalter JA, Mankin HJ. Articular cartilage: degeneration and osteoarthritis, repair, regeneration, and transplantation. *Instr Course Lect* 1998;47:487–504.



4

Chapter 4

MR Imaging of Articular Cartilage at 1.5T and 3.0T: Comparison of SPGR and SSFP sequences

Peter R Kornaat
Scott B Reeder
Seungbum Koo
Jean H Brittain
Huanzhou Yu
Thomas P Andriacchi
Garry E Gold

Abstract

Objective

To compare articular cartilage signal-to-noise ratio (SNR), contrast-to-noise ratio (CNR), and thickness measurements on a 1.5 T and a 3.0 T magnetic resonance (MR) scanner using three-dimensional spoiled gradient recalled echo (3D-SPGR) and two 3D steady-state free precession (SSFP) sequences.

Methods

Both knees of five volunteers were scanned at 1.5 T and at 3.0 T using a transmit-receive quadrature extremity coil. Each examination consisted of a sagittal 3D-SPGR sequence, a sagittal fat suppressed 3D-SSFP (FS-SSFP) sequence, and a sagittal Dixon 3DSSFP sequence. For quantitative analysis, we compared cartilage SNR and CNR efficiencies, as well as average cartilage thickness measurements.

Results

For 3D-SPGR, cartilage SNR efficiencies at 3.0 T increased compared to those at 1.5 T by a factor of 1.83 (range: 1.40 -2.09). In comparison to 3D-SPGR, the SNR efficiency of FS-SSFP increased by a factor of 2.13 (range: 1.81-2.39) and for Dixon SSFP by a factor of 2.39 (range: 1.95 -2.99). For 3D-SPGR, CNR efficiencies between cartilage and its surrounding tissue increased compared to those at 1.5 T by a factor of 2.12 (range: 1.75 - 2.47), for FS-SSFP by a factor 2.11 (range: 1.58 - 2.80) and for Dixon SSFP by a factor 2.39 (range 2.09 - 2.83). Average cartilage thicknesses of load bearing regions were not different at both field strengths or between sequences ($P>0.05$). Mean average cartilage thickness measured in all knees was 2.28 mm.

Conclusion

Articular cartilage imaging of the knee on a 3.0 T MR scanner shows increased SNR and CNR efficiencies compared to a 1.5 T scanner, where SSFP-based techniques show the highest increase in SNR and CNR efficiency. There was no difference between average cartilage thickness measurements performed at the 1.5 T and 3.0 T scanners or between the three different sequences.

Introduction

The impact and consequences of osteoarthritis (OA) in the aging population of the industrialized world are very apparent in light of the recent declaration of the Bone and Joint Decade¹. The impact and prevalence of OA motivates the medical and pharmaceutical communities to develop disease-modifying drugs that

prevent or slow the course of disability. Accurate evaluation of articular cartilage is essential in the development of disease-modifying drugs, since cartilage volume, cartilage thickness and cartilage deformation are potentially valuable surrogate endpoint markers for OA (2,3). Magnetic resonance (MR) imaging has been successful in the visualization of articular cartilage (4) and the measurement of cartilage volumes (5,6). For this reason, various longitudinal MR imaging studies have been started to investigate the role of cartilage in OA. Most of these longitudinal MR imaging studies are performed on a 1.5 T scanner. Recently, higher field systems, typically 3.0 T, have become more prevalent in the clinical setting. There has been little clinical experience with optimal cartilage imaging at 3.0 T. Theoretically, longitudinal magnetization varies linearly with field strength, and as a result, imaging at 3.0 T should provide approximately twice the intrinsic signal-to-noise ratio (SNR) of imaging at 1.5 T, assuming other parameters, including RF coils are equivalent (7). However, field-dependent changes in tissue relaxation times and in the chemical shift difference between fat and water may limit the SNR benefit seen at 3.0 T (8). Although various longitudinal MR imaging studies have already been started, there still is a controversy about the optimal cartilage imaging sequence on 1.5 T and 3.0 T. Currently, the most widely used techniques for articular cartilage imaging on MR are fat suppressed proton-density weighted fast spin-echo, fat suppressed T2-weighted fast spin-echo, and fat suppressed spoiled gradient recalled echo (SPGR) sequences (9,10). SPGR sequences are often chosen for cartilage volume and thickness estimation because the three-dimensional (3D) acquisition, along with hyperintense cartilage signal provide robust visualization of cartilage, and detection of cartilage pathology. However, new MR imaging pulse sequences, specifically steady-state free precession (SSFP) (11-13) have recently attracted attention with regards to their optimal visualization of cartilage because of increased cartilage signal intensity (SI), increased cartilage SNR and contrast-to-noise ratio (CNR), and reduced imaging time compared to conventional pulse sequences (4,14). The purpose of this study was to compare articular cartilage SNR, CNR, and thickness measurements on a 1.5 T with those acquired on a 3.0 T MR scanner using 3D-SPGR and two SSFP sequences.

Methods

MR acquisition

Ten knees from five healthy volunteers included in the study (four males, one female, ages 26-38) were scanned at 1.5 T (GE Signa TwinSpeed) and at 3.0 T (GE Signa VH/i). The local institutional review board approved our protocol, and informed consent was obtained for each study. Each examination consisted of a sagittal fat suppressed 3D-SPGR (FS-3D-SPGR) sequence (1.5 T: TR/TE (Repetition Time/Echo Time): 14.8/1.2 ms; FA (Flip Angle): 12°; 3 NSA (Number of Signal Averages); 11:47 min; 3.0 T: TR/TE: 13.5/1.5 ms; FA: 10°; 3 NSA; 9:41 min), a sagittal

fat suppressed 3D-SSFP (FS-SSFP) sequence (1.5 T: TR/TE: 4.1/1.4 ms; FA: 30°; 1 NSA; 3:07 min; 3.0 T: TR/TE: 5.6/1.5 ms; FA: 30°; 1 NSA; 3:20 min), and a sagittal Dixon 3D-SSFP sequence (1.5 T: TR/TE: 6.1/1.4 ms; FA: 30°; 3 NSA; 4:53 min; 3.0 T: TR/TE: 5.1/1.3 ms; FA: 30°; 3 NSA; 3:40 min). All scans were acquired using a 256x256 matrix, 17 cm Field of View (FOV), 1.5 mm section thickness, 52 sections, a bandwidth of 62.5 kHz, and all scans offer 3D coverage. Both the 1.5 T and 3.0 T scans used a transmit-receive quadrature extremity coil (MRI Devices).

MR imaging methods

FS-3D-SPGR sequences yield hyperintense cartilage signal, with excellent depiction of cartilage morphology (14,11) [Fig. 1(a,d)]. 3D coverage with high SNR is achievable in reasonable scan times (around 5e6 min). These sequences are also advantageous for volume measurement; segmentation is simplified because cartilage has the highest signal in these images. Its primary disadvantage is that there is little contrast between cartilage and synovial fluid. The contrast produced with fat suppressed SSFP methods is favorable for cartilage imaging. It yields hyperintense signal of synovial fluid while preserving cartilage signal [Fig. 1(b,c,e,f)]. The overall SNR efficiency and speed of the SSFP-based techniques make them very attractive for routine morphologic cartilage imaging. The major disadvantage of SSFP techniques is sensitivity to off resonance artifacts (4). Synovial fluid appears very bright in SSFP images, which provides an arthrographic effect helping to depict cartilage contour defects. Unfortunately, this increases the complexity of segmentation algorithms that must use upper and lower threshold limits for cartilage segmentation.

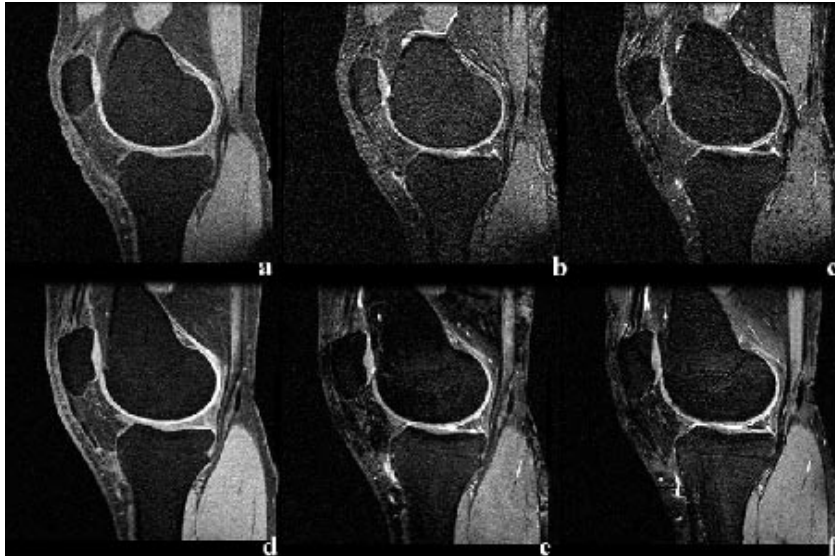


Figure 1. Different sequences on 1.5 T and 3.0 T scanners. a, 1.5 T 3D-SPGR sequence; b, 1.5 T FS-SSFP sequence; c, 1.5 T Dixon SSFP sequence; d, 3.0 T 3D-SPGR sequence; e, 3.0 T FS-SSFP sequence; f, 3.0 T Dixon SSFP sequence.

Optimizing sequences

Eq. (1) was used to optimize flip angles for SSFP imaging with a method that is similar in principle to the method used to optimize the flip angle for 3D-SPGR sequences using the Ernst angle (12). The flip angle (α) that maximizes the signal of an SSFP image for a material with a given T1, T2, and TR is given by the Eq. (1):

$$\alpha = \cos^{-1} ((e^{-TR/T1} - e^{-TR/T2}) / (1 - (e^{-TR/T1} e^{-TR/T2})))$$

where the phase of the subsequent radiofrequency pulses is alternated between 0° and 180°. Cartilage T1 and T2 relaxation times used in this equation were for 1.5 T: T1/T2 1060 ms/42 ms and for 3.0 T: T1/T2 1240 ms/37 ms (8).

Quantitative analyses

For quantitative analysis, we compared sequences based on maximal cartilage SNR, maximal CNR between cartilage and fluid, and maximal CNR between cartilage and its surrounding tissue. In order to measure SI of each tissue, regions of interest (ROIs) were placed on each different type of tissue using a custom software tool (ImageJ 1.31v, NIH, USA). ROIs were placed at identical positions on matching sections in each patient. ROIs were placed at the cartilage of the weight bearing and posterior area of the femoral condyles, patellofemoral joint fluid, medial gastrocnemius muscle, femoral bone marrow, medial subcutaneous fat, and posterior horn of the medial meniscus. ROIs in the fluid and cartilage were relatively small due to smaller volumes of tissue present. The minimal surface area of an ROI was 96 pixels, the mean surface area of an ROI was 3566 pixels. SNR was calculated by dividing the SI by the standard deviation of the noise, which was measured from an ROI outside the knee in a region free of artifact. SNR efficiency was calculated by dividing the SNR by the square root of the scan time. Finally, all SNR efficiencies were multiplied by 0.65, to calculate the SNR measured from these magnitude images in the presence of noise (13). Because cartilage is only in contact with synovial fluid for a small percentage of the total cartilage perimeter, we are also interested in contrast between cartilage and other surrounding tissue. Therefore, we calculated CNR_{total} between cartilage and all of the cartilage surrounding tissues (n) using the following formula:

$$CNR_{total} = (|SI_{cartilage} - SI_{tissue_n}| / SI_{noise}) \times (Tissue_n \text{ to cartilage interface (mm)} / \text{Total cartilage perimeter (mm)})$$

In this formula, tissue to cartilage interface is the length in millimeters where bone, fluid, menisci, fat and muscle, respectively, are in direct contact with cartilage. Tissue to cartilage interface divided by the total cartilage perimeter represents the percentage of cartilage that is in direct contact with a specific tissue. For example, with bone this percentage is 50% since half of the cartilage (the nonarticular side) is always in direct contact with bone. When calculating CNR_{total} we used the same slice per sequence in each patient to keep the tissue

to cartilage interface the same for all compared sequences. In addition to the measured cartilage SI of the weight bearing and posterior areas of the femoral condyles, cartilage SI was also measured at the anterior aspect of the femoral condyles, trochlea, tibial plateau, and patella. This was performed because cartilage SI may vary between the different parts of the cartilage.

Average cartilage thickness measurements

We used the B-spline Snakes method with manual initialization in the process of average cartilage thickness measurements of the medial and lateral femoral condyle, in order to detect the cartilage boundary on each MR image with high precision (15). The segmentation using B-spline Snakes is semi-automatic and requires manual correction, as MR images do not always have consistent brightness. This interactive tool allows segmentation in a minimal amount of time with reliable results. When the segmentation process was completed for all MR images, a 3D model was created from the segmented images using the Marching Cubes algorithm which is a surface rendering algorithm. The Marching Cubes algorithm divides the space that contains a stack of segmented images into regular cubical cells and calculates scalar values at each grid point to create surface patches of each cell. The 3D surface models were then made by connecting these surface patches. The Laplacian smoothing algorithm was used to regularize the surface points (16). On average the 3D model used 80,000 points for the cartilagebone and 80,000 points for the cartilagesoft tissue surface interface. In order to calculate the cartilage thickness in this 3D model, a closest point on the cartilagebone surface was found for each point at the cartilagesoft tissue surface interface. We divided the femoral cartilage into six regions to examine average cartilage thickness. These regions were divided into regions based on the load bearing areas of the knee during walking (Fig. 2). The neutral position is taken as the reference line, and then two new lines were drawn, at -30 degrees and 30 degrees from the neutral position about the center of the arc through the distal condyles. Another line was drawn at an angle of 30 degrees from the middle of the second (-30 degrees) line. The location of the measurement in the medial to lateral direction of the femoral cartilage was determined by using a fixed distance from the middle of the two femoral condyles to the intercondylar center (17,18). Comparison of the average cartilage thickness from images acquired at 1.5 T and 3.0 T MR images was performed. In order to ensure that the average cartilage thickness was measured at identical regions, the two cartilage models were aligned on each other using a Rapid- Form (Inus tech., Korea) software program (Fig. 3).

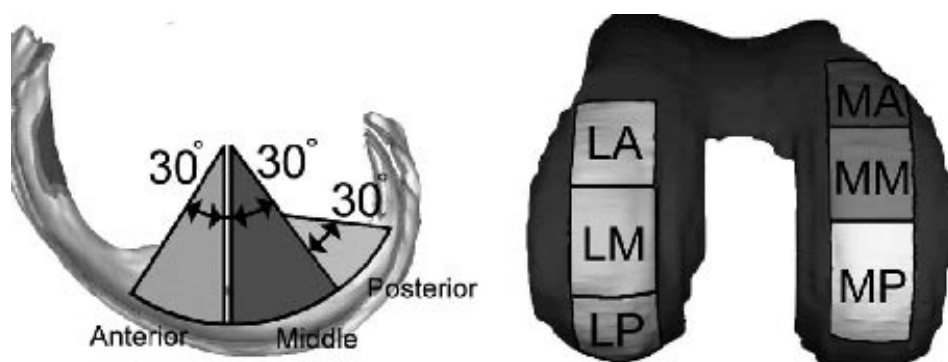


Figure 2. Selection of anterior, middle and posterior regions of the femoral cartilage. Lateral and frontal view. MA = medial condyle, anterior portion; MM = medial condyle, middle portion; MP = medial condyle, posterior portion; LA = lateral condyle, anterior portion; LM = lateral condyle, middle portion; LP = lateral condyle, posterior portion.

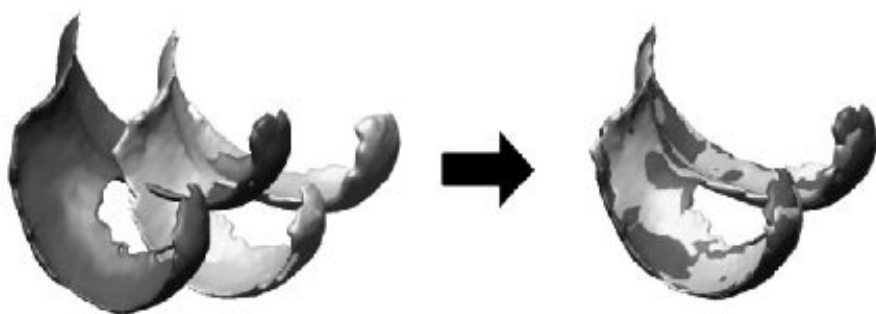


Figure 3. Femoral cartilage registration using RapidForm (Inus tech., Korea).

Statistical analyses

Data were analyzed using a multivariate repeated measures analysis of variance examining the effects of position (anterior, medial, posterior), condyle (medial vs lateral), method (3D-SPGR, FS-SSFP, Dixon SSFP), and scanner type (1.5 T, 3.0 T) on the measurement. Each knee was treated as an independent set of observations. All datasets were complete.

Results

Optimal flip angle for cartilage signal-to-noise using FS-SSFP and Dixon SSFP sequences is 30 degrees for both the 1.5 T and 3.0 T systems. For the 3D-SPGR sequences, optimal flip angle is 12 degrees for the 1.5 T system and 10 degrees for the 3.0 T system. The absolute cartilage and fluid SNR efficiencies of the three different sequences were higher at 3.0 T than at 1.5 T (Table I). For 3D-SPGR, cartilage SNR efficiencies at 3.0 T increased compared to a 1.5 T scanner by a factor of 1.83 (range: 1.40-2.09), for FS-SSFP by a factor 2.13 (range: 1.81-2.39)

and for Dixon SSFP by a factor 2.39 (range: 1.95-2.99). The Dixon SSFP sequence has the highest SNR efficiencies for cartilage and fluid. All three sequences demonstrate an increase in CNR efficiencies between cartilage and fluid and between cartilage and all of its surrounding tissue at a 3.0 T system (Table II). For 3D-SPGR at 3.0 T, CNR efficiencies between cartilage and all its surrounding tissue increased compared to a 1.5 T scanner by a factor of 2.12 (range: 1.75-2.47), for FS-SSFP by a factor 2.11 (range: 1.58-2.80) and for Dixon SSFP by a factor 2.39 (range: 2.09-2.83). Dixon SSFP images have the highest increase in CNR between cartilage and fluid, and cartilage and its surrounding tissue, as well as the highest absolute CNR on a 1.5 T and a 3.0 T MR system. Mean average cartilage thickness measured in all knees was 2.3 mm (minimum average cartilage thickness 1.4 mm, maximum average cartilage thickness 3.1 mm). There was no difference in average cartilage thickness measurements performed at the 1.5 T and 3.0 T scanners ($P = 0.80$) or between the three different sequences (3D-SPGR, FS-SSFP, Dixon SSFP) ($P = 0.79$). There was no significant effect of position (anterior, middle, posterior) or condyle (medial, lateral) on the average cartilage thickness measurements ($P > 0.05$; range: 0.33-0.99) (Table III). Cartilage SI at both field strengths varied with location (Table IV). On both the 1.5 T and the 3.0 T scanners, the lowest cartilage SNR efficiencies were measured at the tibial plateau for the 3D-SPGR and FS-SSFP sequences, and at the patella for the Dixon SSFP images. Highest cartilage SNR efficiencies at the 1.5 T scanner were for all three sequences measured at the trochlea. Highest cartilage SNR efficiencies at the 3.0 T scanner were measured at the posterior part of the femoral condyles for the 3D-SPGR and FS-SSFP sequences, and at the anterior part of the femoral condyle for the Dixon SSFP images. Cartilage SNR efficiencies varied strongly between the different knees, as shown by the minimum and maximum values per anatomic location.

Table I. Cartilage and fluid SNR efficiencies (standard deviation) of three different sequences at 1.5T and 3.0T

	Cartilage				Fluid			
	SNR efficiencies		Increase	Range	SNR efficiencies		Increase	Range
	1.5T	3.0T			1.5T	3.0T		
3D-SPGR	3.93 (0.53)	7.20 (1.28)	1.83	1.40 - 2.09	2.33 (0.36)	3.67 (0.91)	1.58	0.92 - 2.39
FS-SSFP	4.52 (0.91)	9.64 (2.38)	2.13	1.81 - 2.39	12.88 (2.77)	22.81 (9.31)	1.77	1.12 - 2.41
Dixon SSFP	5.09 (1.05)	12.15 (2.79)	2.39	1.95 - 2.99	14.64 (4.00)	33.18 (8.51)	2.27	1.89 - 2.69

Table I Cartilage and fluid SNR efficiencies (standard deviation) of three different sequences at 1.5 T and 3.0 T

Table II. Cartilage CNR efficiencies (standard deviation) of three different sequences at 1.5T and 3.0T

	Cartilage - Fluid				Cartilage - all surrounding tissue			
	CNR efficiencies		Increase	Range	CNR efficiencies		Increase	Range
	1.5T	3.0T			1.5T	3.0T		
3D-SPGR	1.60 (0.51)	3.53 (1.46)	2.21	1.24 - 4.61	2.13 (0.36)	4.52 (0.95)	2.12	1.75 - 2.47
FS-SSFP	8.37 (2.04)	13.17 (7.55)	1.57	0.44 - 2.43	3.65 (0.81)	7.71 (2.51)	2.11	1.58 - 2.80
Dixon SSFP	9.55 (3.19)	21.03 (7.61)	2.20	1.49 - 2.93	4.50 (1.04)	10.76 (2.29)	2.39	2.09 - 2.83

Table II Cartilage CNR efficiencies (standard deviation) of three different sequences at 1.5 T and 3.0 T

Table III. Average cartilage thickness (standard deviation) in millimetres at different locations in the knee measured with different sequences at different field strengths

Sequence		Medial condyle			Lateral condyle		
		Anterior	Middle	Posterior	Anterior	Middle	Posterior
		part	part	part	part	part	part
1.5T	3D-SPGR	2.0 (0.5)	2.2 (0.5)	2.3 (0.5)	2.0 (0.5)	2.3 (0.4)	2.5 (0.6)
3.0T	3D-SPGR	2.1 (0.6)	2.3 (0.5)	2.4 (0.4)	2.1 (0.3)	2.4 (0.4)	2.5 (0.5)
1.5T	FS-SSFP	1.9 (0.5)	2.3 (0.5)	2.3 (0.6)	1.9 (0.3)	2.3 (0.4)	2.5 (0.5)
3.0T	FS-SSFP	2.0 (0.5)	2.3 (0.5)	2.3 (0.4)	2.0 (0.4)	2.4 (0.3)	2.5 (0.5)
1.5T	Dixon SSFP	1.9 (0.4)	2.2 (0.4)	2.2 (0.4)	2.0 (0.3)	2.3 (0.5)	2.5 (0.6)
3.0T	Dixon SSFP	2.0 (0.6)	2.3 (0.5)	2.3 (0.5)	2.0 (0.4)	2.3 (0.5)	2.4 (0.6)

Table III Average cartilage thickness (standard deviation) in millimeters at different locations in the knee measured with different sequences at different field strengths

Table IV Cartilage SNR efficiencies at different locations in the knee on a 1.5 T and on a 3.0 T scanner

SNR (Min-Max)		Anterior	Posterior	Trochlea	Tibia	Patella
		condyle*	condyle*			
1.5 T,	3D-SPGR	4.01 (2.71-4.79)	3.99 (2.76-5.04)	4.34 (2.54-5.61)	3.55 (2.98-4.45)	4.01 (2.95-4.63)
1.5 T,	FS-SSFP	4.65 (3.27-5.75)	4.81 (3.20-6.74)	5.22 (3.36-7.01)	3.76 (2.80-4.62)	4.23 (2.78-5.84)
1.5 T,	Dixon SSFP	6.15 (3.60-8.25)	5.85 (3.47-7.88)	6.18 (3.35-8.65)	4.94 (3.66-6.13)	4.83 (2.97-7.22)
3.0 T,	3D-SPGR	6.25 (3.63-8.66)	6.65 (3.79-9.94)	6.35 (4.22-9.18)	5.55 (3.30-7.43)	5.94 (4.23-7.75)
3.0 T,	FS-SSFP	6.83 (3.17-9.61)	6.99 (3.17-12.6)	6.80 (3.83-11.5)	5.39 (3.10-7.65)	5.85 (4.04-8.97)
3.0 T,	Dixon SSFP	13.6 (8.61-18.9)	12.9 (6.79-17.4)	12.7 (8.77-16.1)	11.4 (6.13-17.2)	10.6 (5.52-15.0)

Table IV Cartilage SNR efficiencies at different locations in the knee on a 1.5 T and on a 3.0 T scanner

Min = minimum; Max = Maximum.

*Anterior or posterior portion of the femoral condyle.

Discussion

The present study demonstrates that articular cartilage imaging of the knee on a 3.0 T MR scanner shows increased cartilage SNR and CNR efficiencies compared to a 1.5 T scanner. SSFP-based techniques show the highest increase in SNR and CNR efficiency. There was no difference between average cartilage thickness measurements performed at the 1.5 T and 3.0 T scanners or between the three different sequences. The improvement in SNR efficiency varies by location, indicating the choice of coil and its sensitivity is crucial to benefit from the increase in field strength. SSFP-based techniques have higher SNR and CNR efficiencies compared to 3D-SPGR sequences on both 1.5 T and 3.0 T scanners. The main advantage of SSFP-based cartilage imaging techniques on a 1.5 T scanner, a high SNR efficiency compared with conventional techniques, have been described in literature (4,14,12). In addition the present study showed that SSFP-based cartilage imaging techniques show a greater difference in SNR efficiencies compared to conventional 3D-SPGR sequences at 3.0 T than at 1.5 T. This is important because techniques for quantifying OA surrogate endpoints, such as cartilage thickness and cartilage volume, have been developed (5,19-22). These cartilage-quantifying techniques require segmentation. Segmentation requires high contrast between cartilage and surrounding tissues, as well as high spatial resolution. Therefore, an optimal imaging technique for automatic or semi-automatic assessment of cartilage thickness and cartilage volume should have a high CNR between cartilage and its surrounding tissues, including uniform fat suppression. The present study demonstrates that not only is CNR between cartilage and fluid higher with SSFP methods than SPGR approaches, but also that CNR between cartilage and all its surrounding tissues is higher at both 1.5 T and 3.0 T. Higher CNR between cartilage and fluid, and cartilage and its surrounding tissues emphasizes the advantages of SSFP-based sequences as opposed to 3D-SPGR based sequences in the acquisition of cartilage MR images. Scanning on higher field strengths, such as 3.0 T, increases SNR efficiency by a factor of approximately 2.0. In addition, SSFP-based sequences show increased SNR efficiencies compared with conventional 3D-SPGR sequences. CNR efficiencies between cartilage and other tissue also increase by a factor 2, because the difference between SNR of different tissues increases just as the tissue itself, by a factor 2 (8). This means that scanning on a 3.0 T scanner has the advantage over the 1.5 T scanner of having a higher CNR between cartilage and surrounding tissues. Quantitative assessment of cartilage volume and cartilage thickness has already been validated successfully on a 1.5 T scanner (3,23). The present study demonstrates that average cartilage thickness measurements on a 3.0 T system do not significantly differ from measurements at 1.5 T. Because CNR efficiencies increase at 3.0 T, the accuracy and reproducibility of both semi-automatic as fully automatic cartilage segmentation software should benefit from the increase in CNR efficiencies on the 3.0 T scanner. This makes the SSFP-based sequences on a 3.0 T scanner very suitable to acquire MR images of the knee for cartilage segmentation. The fact that cartilage has the highest signal of any structure in the

knee in FS-3D-SPGR images is advantageous for cartilage segmentation algorithms, compared with SSFP acquisitions. This allows one to use a single threshold above which cartilage is defined. This initial segmentation can be refined using other segmentation techniques such as nearest neighbor or region growing. With the SSFP-based techniques both upper and lower threshold increases the subjective nature of the initial portion of the segmentation and makes this portion slightly more difficult to automate. Cartilage SI at both field strengths varied with location. The differences in cartilage SI within one knee are most likely due to the sensitivity profile of the knee coil. When cartilage is located closer to the knee coil, one can expect slightly higher SI than when cartilage is located further away from the coil. In comparing the different sequences it is therefore important to be consistent in placing the ROI when measuring cartilage SI. Another reason for the differences in cartilage SI besides the variability in coil sensitivity is that the relaxation times in cartilage can vary with location. The variation of relaxation times in cartilage can also contribute for the differences in cartilage SI within one knee. Image artifacts can also contribute or cause cartilage SI changes. An advantage of the present study is that all three sequences on both scanners were optimized for cartilage imaging beforehand (14,12,24). Therefore, we could keep the acquisition parameters of the different sequences on both scanners the same. All different images were acquired using the same matrix, the same field of view, the same section thickness, and the same bandwidth. This way we tried to make the comparison of the three different sequences as fair as possible. However, we are aware that the in-plane resolution, obtained by dividing the field of view by the image acquisition matrix, of 0.662 mm^2 , is about half the in-plane resolution used in other studies. The reason we used 256×256 resolution was to perform SSFP imaging with a relatively short TR. Going to 512 matrix would have resulted in a long TR and banding artifacts. This is a current limitation of the SSFP technique. There are approaches with SSFP which will allow us to extend the resolution to 512, including linear combination of SSFP (25) and use of VERSE pulses (26). The goal of the present study was to compare different cartilage sequences at the two different scanners, and therefore our main concern was to keep the acquisition parameters the same. Limitations of this study are that we did not validate the average cartilage thickness measurements with a gold standard. We did not correlate the average thickness measurements on 1.5 T and 3.0 T with anatomical sections of knee cartilage, arthroscopy or any other validation technique. Since we studied healthy volunteers, this paper does not address the sensitivity of the different techniques for detecting cartilage lesions. This will be addressed in future studies. Another limitation of this study is that thickness measurements were done in healthy volunteers. It may be more difficult to measure cartilage thickness in damaged, unhealthy cartilage, such as in patients with OA of the knee. The fact that we did not find a difference between average cartilage thickness measurements on a 1.5 T and a 3.0 T scanner in patients with healthy cartilage does not automatically mean there is no difference in average cartilage thickness measurements between 1.5 T and 3.0 T in OA patients. A final limitation is that

we did not account for methods, which provide quantitative evaluation of intrinsic cartilage parameters. The cartilage thickness measurements used in the present study are not able to assess the initial phase of degenerative joint diseases, as the very early beginning is characterized by alterations within the biochemical content of cartilage, not by cartilage loss or deformation. In conclusion, articular cartilage imaging of the knee on a 3.0 T MR scanner shows increased SNR and CNR efficiencies compared to a 1.5 T scanner, where SSFP-based techniques show the highest increase in SNR and CNR efficiency. There was no difference between average cartilage thickness measurements performed at the 1.5 T and 3.0 T scanners or between the three different sequences. This makes the SSFP-based sequences on a 3.0 T scanner very suitable to acquire MR images of the knee for cartilage segmentation. The improvement in SNR efficiency varies by location, indicating the choice of coil and its sensitivity is crucial to benefit from the increase in field strength.

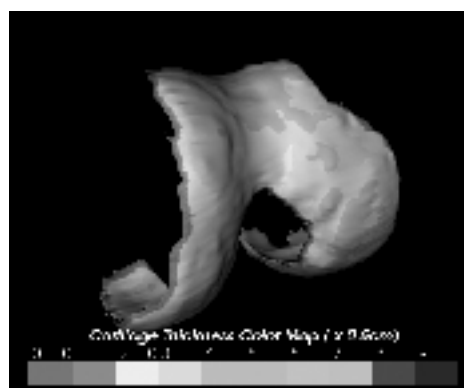
Acknowledgments

This work was funded in part by NIH R01 AR049792, NIH R01 EB0002524 and the Netherlands Organization for Scientific Research (NWO).

References

1. Harris ED Jr. The bone and joint decade: a catalyst for progress. *Arthritis Rheum* 2001;44:1969-70.
2. Peterfy CG. Imaging of the disease process. *Curr Opin Rheumatol* 2002;14:590-6.
3. Graichen H, Eisenhart-Rothe R, Vogl T, Englmeier KH, Eckstein F. Quantitative assessment of cartilage status in osteoarthritis by quantitative magnetic resonance imaging: technical validation for use in analysis of cartilage volume and further morphologic parameters. *Arthritis Rheum* 2004;50:811-6.
4. Gold GE, McCauley TR, Gray ML, Disler DG. What's new in cartilage? *Radiographics* 2003;23:1227-42.
5. Peterfy CG, van Dijke CF, Janzen DL, Gluer CC, Namba R, Majumdar S, et al. Quantification of articular cartilage in the knee with pulsed saturation transfer subtraction and fat-suppressed MR imaging: optimization and validation. *Radiology* 1994;192:485-91.
6. Stammberger T, Eckstein F, Englmeier KH, Reiser M. Determination of 3D cartilage thickness data from MR imaging: computational method and reproducibility in the living. *Magn Reson Med* 1999;41:529-36.
7. Collins CM, Smith MB. Signal-to-noise ratio and absorbed power as functions of main magnetic field strength, and definition of "90 degrees" RF pulse for the head in the birdcage coil. *Magn Reson Med* 2001; 45:684-91.
8. Gold GE, Han E, Stainsby J, Wright G, Brittain J, Beaulieu C. Musculoskeletal MRI at 3.0 T: relaxation times and image contrast. *AJR Am J Roentgenol* 2004;183:343-51.
9. Recht M, Bobic V, Burstein D, Disler D, Gold G, Gray M, et al. Magnetic resonance imaging of articular cartilage. *Clin Orthop* 2001;391(Suppl):S379-96.
10. McCauley TR, Recht MP, Disler DG. Clinical imaging of articular cartilage in the knee. *Semin Musculoskelet Radiol* 2001;5:293-304.
11. Disler DG, Peters TL, Muscoreil SJ, Ratner LM, Wagle WA, Cousins JP, et al. Fat-suppressed spoiled GRASS imaging of knee hyaline cartilage: technique optimization and comparison with conventional MR imaging. *AJR Am J Roentgenol* 1994;163:887-92.
12. Reeder SB, Pelc NJ, Alley MT, Gold GE. Rapid MR imaging of articular cartilage with steady-state free precession and multipoint fatwater separation. *AJR Am J Roentgenol* 2003;180:357-62.
13. Henkelman RM. Measurement of signal intensities in the presence of noise in MR images. *Med Phys* 1985; 12:232-3.

14. Hargreaves BA, Gold GE, Beaulieu CF, Vasanawala SS, Nishimura DG, Pauly JM. Comparison of new sequences for high-resolution cartilage imaging. *Magn Reson Med* 2003;49:700-9.
15. Kass M, Witkin A, Terzopoulos D. Snakes: active contour models. *Int J Comput Vis* 1988;1:321-31.
16. Koo S, Alexander EJ, Gold GE, Giori NJ, Andriacchi TP. Morphology and thickness in tibial and femoral cartilage at the knee is influenced by the mechanics of walking. ASME Summer Bioengineering Conference, Miami FL, June 2003 (Abstract).
17. Koo S, Dixit AN, Alexander EJ, Andriacchi TP. A rule based approach to improve cartilage thickness measurement reproducibility from knee MRI. 27th Annual Meeting of American Society of Biomechanics; 2003 (Abstract).
18. Koo S, Kornaat PR, Gold GE, Andriacchi TP. Factors influencing the accuracy of articular cartilage thickness measurement from MRI. 28th Annual Meeting of American Society of Biomechanics; 2004 (Abstract).
19. Eckstein F, Winzheimer M, Hohe J, Englmeier KH, Reiser M. Interindividual variability and correlation among morphological parameters of knee joint cartilage plates: analysis with three-dimensional MR imaging. *Osteoarthritis Cartilage* 2001;9:101-11.
20. Cicuttini F, Forbes A, Asbeutah A, Morris K, Stuckey S. Comparison and reproducibility of fast and conventional spoiled gradient-echo magnetic resonance sequences in the determination of knee cartilage volume. *J Orthop Res* 2000;18:580-4.
21. Glaser C, Faber S, Eckstein F, Fischer H, Springer V, Heudorfer L, et al. Optimization and validation of a rapid high-resolution T1-w 3D FLASH water excitation MRI sequence for the quantitative assessment of articular cartilage volume and thickness. *Magn Reson Imaging* 2001;19:177-85.
22. Cohen ZA, McCarthy DM, Kwak SD, Legrand P, Fogarasi F, Ciaccio EJ, et al. Knee cartilage topography, thickness, and contact areas from MRI: in-vitro calibration and in-vivo measurements. *Osteoarthritis Cartilage* 1999;7:95-109.
23. Mendlik T, Faber SC, Weber J, Hohe J, Rauch E, Reiser M, et al. T2 quantitation of human articular cartilage in a clinical setting at 1.5 T: implementation and testing of four multiecho pulse sequence designs for validity. *Invest Radiol* 2004;39:288-99.
24. Reeder SB, Wen Z, Yu H, Pineda AR, Gold GE, Markl M, et al. Multicoil Dixon chemical species separation with an iterative least-squares estimation method. *Magn Reson Med* 2004;51:35-45.
25. Bangarter NK, Hargreaves BA, Vasanawala SS, Pauly JM, Gold GE, Nishimura DG. Analysis of multiple acquisition SSFP. *Magn Reson Med* 2004;51: 1038-47.
26. Hargreaves BA, Cunningham CH, Nishimura DG, Conolly SM. Variable-rate selective excitation for rapid MRI sequences. *Magn Reson Med* 2004;52: 590-7.
27. Kornaat PR, Doornbos J, van der Molen AJ, Kloppenburg M, Nelissen RG, Hogendoorn PC, et al. Magnetic resonance imaging of knee cartilage using a water selective balanced steady-state free precession sequence. *J Magn Reson Imaging* 2004; 20(5):850-6.



5

Chapter 5

Comparison of quantitative cartilage measurements acquired on two 3.0T MR imaging systems from different manufacturers

Peter R Kornaat
Johan L Bloem
Scott B Reeder
Seungbum Koo
Thomas P Andriacchi
Garry E Gold.

Abstract

Purpose

To investigate the comparability of two osteoarthritis (OA) surrogate endpoints -average cartilage thickness and cartilage volume- acquired from healthy volunteers on two 3.0T magnetic resonance imaging (MRI) systems from different manufacturers.

Materials and Methods

Ten knees of five healthy volunteers were scanned on a 3.0T General Electric (GE) and a 3.0T Philips scanner using a fast three-dimensional fatsuppressed spoiled gradient (SPGR) imaging sequence. The acquisition parameters were optimized beforehand and were kept as comparable as possible on both scanners. For quantitative analysis, the average cartilage thickness and volume of the load-bearing regions of the femoral condyles were compared. Data were analyzed using a univariate repeated-measures analysis of variance (ANOVA) to examine the effects of position, condyle, and imaging system on the measurements.

Results

The average cartilage thickness and volume of the load-bearing regions of the femoral condyles did not differ between the two different 3.0T MRI systems ($P > 0.05$). There was no significant effect of position or condyle on the average cartilage thickness measurements ($P > 0.05$; range: 0.41–0.93) or cartilage volume ($P > 0.05$; range: 0.14–0.87).

Conclusion

Two OA surrogate endpoints -average cartilage thickness and cartilage volume- acquired on two 3.0T MRI systems from different manufacturers are comparable.

Introduction

The impact and consequences of osteoarthritis (OA) in the aging population of the industrialized world are very apparent in the light of the recent declaration of the Bone and Joint Decade (1), and are motivating the medical and pharmaceutical communities to develop disease-modifying drugs to prevent or delay the development of disability. Magnetic resonance imaging (MRI), with its excellent soft-tissue contrast, is the best noninvasive technique currently available for the assessment of cartilage injury and other internal rearrangements of the knee (2,3). For these reasons a number of longitudinal MR studies have been looking for findings that predict the progression of OA. Recently the National Institutes of

Health (NIH) advised the use of 3.0T MR scanners for this purpose, and several international longitudinal studies have been initiated. Different research groups use 3.0T MRI systems from different manufacturers. It is not known whether it is possible to compare OA surrogate endpoints, such as cartilage thickness and volume, acquired on these MRI systems from different manufacturers. It is also not known whether it is possible to use MRI systems from different manufacturers in the same study for the measurement of these research parameters. Therefore, the purpose of this study was to investigate the comparability of two OA surrogate endpoints acquired on a General Electric (GE) and a Philips 3.0T MRI system. We compared cartilage thickness and volume measurements in normal volunteers using threedimensional spoiled gradient-recalled echo (3D-SPGR) with fat suppression and equivalent parameters on both systems (4).

Materials and Methods

MR Acquisition

Ten knees of five healthy volunteers (five males, 28–34 years old) with no history of knee pain or prior surgery were scanned on a 3.0T GE (GE Signa VH/I; GE Healthcare, Milwaukee, WI, USA) and a 3.0T Philips (Philips Achieva; Philips Medical Systems, Best, The Netherlands) scanner. The 3.0T GE scanner was located in the United States, and the 3.0T Philips scanner was in the European Union. The local institutional review board (IRB) of one of the two hospitals approved our protocol, and informed consent was obtained for each study. The volunteers were scanned within two weeks and at the same time of day under similar conditions, as previous studies have shown that tibial cartilage deformation (5) and changes in superficial femoral weight-bearing cartilage T2 profiles (6) can occur after exercise. The bandwidths on the GE and Philips scanners are given in kHz and Hz/pixel, respectively. To convert bandwidths from one scanner to the other, the total bandwidth in Hz was divided by the acquisition matrix. The acquisition parameters of the sagittal fat-suppressed 3D-SPGR sequence on the GE system were TR/TE: 20.4/6.6 msec; FA: 10°; acquisition matrix: 320 x 320; reconstruction matrix: 512 x 512; FOV: 15 cm; section thickness: 1.5 mm; NSA: 1; bandwidth: 15.63 kHz; 64 sections in 6:58 minutes. The parameters for the Philips scanner consisted of TR/TE: 23/ 6.6 msec; FA: 10°; acquisition matrix: 320 x 320; reconstruction matrix: 512 x 512; FOV: 15 cm; section thickness: 1.5 mm; NSA: 1; bandwidth: 15.62 kHz; and 64 sections in 7:59 minutes. A transmit- receive four-channel phased array knee/foot coil (MRI Devices) was used on the GE system, and an eight-channel sensitivity encoding (SENSE) knee coil was used on the Philips system.

Optimizing Sequences

The flip angle (α) that maximizes the signal of an SPGR image for a material with a given T1 and TR (Ernst angle) (7) was calculated by the following equation:

$$= \cos^{-1} [\exp (-TR/T1)]$$

The cartilage T1 relaxation time used in this equation was 1240 msec (8). The optimum flip angle for cartilage imaging using an SPGR sequence on a 3.0T MRI system is 10°.

Average Cartilage Thickness and Volume Measurements

We used the B-spline Snakes method with manual initialization to obtain average cartilage thickness measurements of the medial and lateral femoral condyle, in order to detect the cartilage boundary on each MR image with high precision (9). The segmentation using B-spline Snakes is semiautomatic and requires manual correction, since MR images do not always have consistent brightness. The same observer performed this function for the scanners from both vendors. This interactive tool allows segmentation in a minimal amount of time (two hours) with reliable results. When the segmentation process was completed for all MR images, a 3D model was created from the segmented images using the Marching Cubes algorithm, which is a surface rendering algorithm. The Marching Cubes algorithm divides the space that contains a stack of segmented images into regular cubical cells and calculates scalar values at each grid point to create surface patches of each cell. The 3D surface models were then made by connecting these surface patches. The Laplacian smoothing algorithm was used to regularize the surface points (10). On average the 3D model used 80,000 points for the cartilage–bone and 80,000 points for the cartilage–soft tissue surface interface. To calculate the cartilage thickness in this 3D model, the closest point on the cartilage–bone surface was found for each point at the articular surface. We divided the femoral cartilage into six regions to examine the average cartilage thickness and volume. These regions were defined based on the load-bearing areas of the knee during normal gait (11,12). The average thickness and volume were calculated for each region. The reproducibility and accuracy of the method were tested in our previous studies (8,9). To ensure that the average cartilage thickness and volume were measured at identical regions for both cartilage models obtained from the different MR machines, we aligned the two cartilage models on each other using the Rapid- Form (Inus Technology, Inc., South Korea) software program. Figure 1 shows an example of a cartilage thickness map from both scanners on the same volunteer.

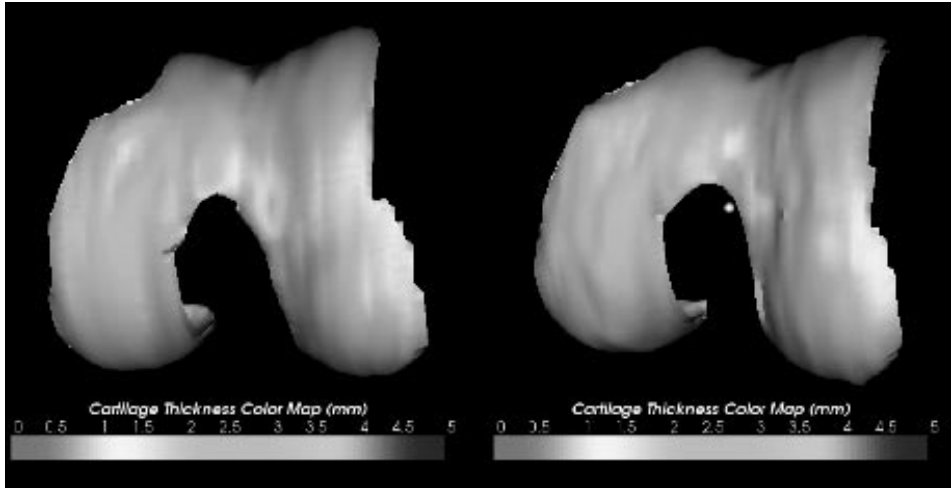


Figure 1. Cartilage thickness maps of a knee based on images from one volunteer scanned with (a) 3.0T GE and (b) 3.0T Philips systems.

Statistical Analyses

Data were analyzed using a univariate repeated-measures analysis of variance (ANOVA) to examine the effects of position (anterior, medial, or posterior), condyle (medial vs. lateral condyle), and MRI system (GE or Philips) on the measurement. Each knee was treated as an independent set of observations. All data sets were complete.

Results

Figure 2 shows an example of an MR image of the left knee of one volunteer acquired on the 3.0T GE and 3.0T Philips MRI systems. The mean average cartilage thickness of the 10 knees was 2.51 mm (minimum average cartilage thickness: 1.44 mm, maximum average cartilage thickness: 4.29 mm). The mean difference of the cartilage thickness measurements was 0.19 mm (maximum: 0.88 mm; minimum: 0.00 mm). There was no difference in average cartilage thickness measurements ($P = 0.61$) or cartilage volume ($P = 0.51$) obtained on the 3.0T GE or 3.0T Philips MRI system. There was no significant effect of position (anterior, middle, or posterior) or condyle (medial or lateral) on the average cartilage thickness measurements ($P > 0.05$; range: 0.41–0.93) or cartilage volume ($P > 0.05$; range: 0.14–0.87; Table 1).

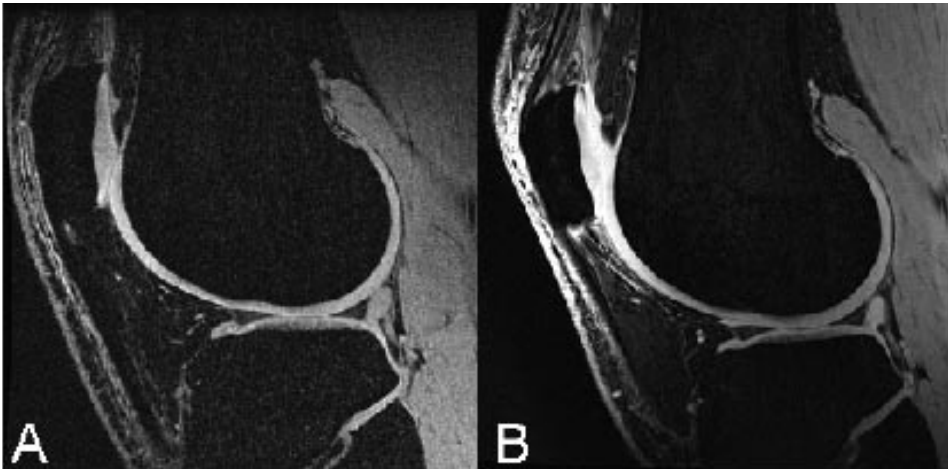


Figure 2. Sagittal fat-suppressed 3D SPGR images of a knee acquired on (a) 3.0T GE and (b) 3.0T Philips systems. Both images were acquired from the same volunteer.

Table 1. Average cartilage thickness (mm) of weight bearing regions in the knee on different MR imaging systems in 5 volunteers.

		Medial Conyle						Lateral condyle					
		Anterior		Middle		Posterior		Anterior		Middle		Posterior	
		GE	Philips	GE	Philips	GE	Philips	GE	Philips	GE	Philips	GE	Philips
Volunteer 1	Left Knee	1.75	1.79	2.51	2.23	2.16	2.05	1.92	1.87	1.93	1.94	1.44	1.80
	Right Knee	1.95	1.87	2.02	1.91	2.04	1.71	1.66	1.89	2.37	2.38	2.28	2.34
Volunteer 2	Left Knee	1.73	2.08	2.07	2.70	1.92	2.80	2.60	2.88	2.62	2.76	2.28	2.35
	Right Knee	2.50	2.84	2.43	2.29	2.14	2.05	2.17	2.26	2.86	2.77	2.93	2.75
Volunteer 3	Left Knee	1.97	1.79	3.25	2.79	3.45	3.13	2.87	2.94	3.65	3.40	3.58	3.50
	Right Knee	2.55	2.33	3.17	3.21	3.33	3.06	1.78	1.91	4.29	4.21	3.68	3.75
Volunteer 4	Left Knee	1.96	1.79	2.66	2.42	2.55	2.29	2.27	2.08	2.67	2.42	2.50	2.27
	Right Knee	1.87	2.07	2.19	2.22	2.26	2.01	2.41	2.27	2.96	2.88	2.64	2.38
Volunteer 5	Left Knee	2.41	2.32	2.70	3.05	2.78	2.88	3.09	3.05	2.17	2.81	2.44	3.01
	Right Knee	3.06	3.11	2.83	2.81	2.84	2.84	2.42	2.47	3.10	3.09	2.60	2.72

Table 1 Average Cartilage Thickness (mm) of Weight Bearing Regions in the Knee on Different MR Imaging Systems in five Volunteers

Discussion

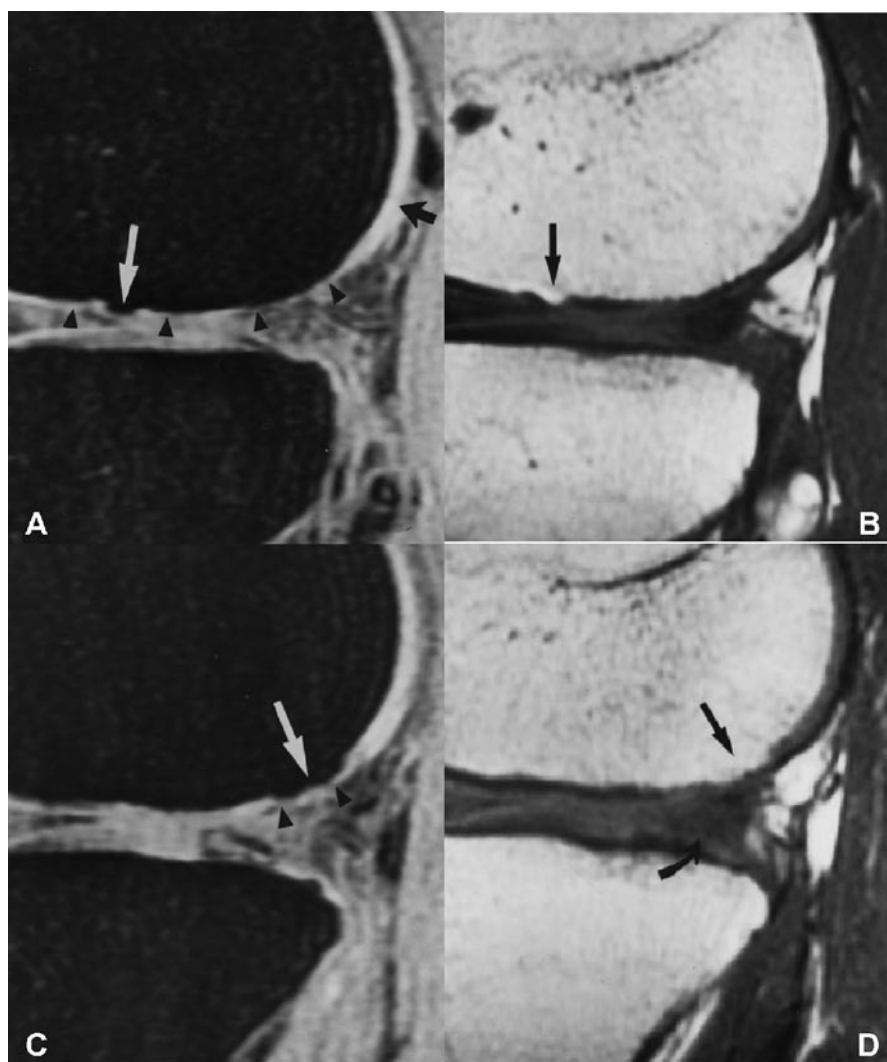
The present study shows that two OA surrogate endpoints -average cartilage thickness and cartilage volume- of weight-bearing regions acquired on two 3.0T MRI systems from different manufacturers are comparable. This is an important finding because interest in multicenter studies of OA, which are likely to use 3.0T MR scanners from different manufacturers, has recently increased. A major focus of these OA multicenter studies is to monitor decreasing hyaline cartilage

thickness, a hallmark of OA. In the only previous report on this subject in the literature, Morgan et al (13) compared total cartilage volumes acquired on 1.5T GE, 1.0T Siemens, and 1.5T Philips MRI systems. They concluded that although there were small systematic differences in the measurements of knee cartilage volume, the three MRI systems gave broadly similar results. That finding is in agreement with the present study; however, in the present study no systematic differences in the measurements were found. Another difference between that study and the present one is that the present study reports on cartilage volumes of the weightbearing areas instead of total knee cartilage volumes (including the non-weight-bearing areas). In addition to cartilage volumes, the present study reports the average cartilage thickness of the weight-bearing areas. The weight-bearing areas of the femoral condyles are an interesting OA surrogate endpoint because cartilage damage in osteoarthritic patients occurs predominantly in the weight-bearing areas of the femoral condyles. Measuring average cartilage thickness and volumes in the weightbearing areas is also a more sensitive tool for detecting cartilage changes compared to measurements on all of the cartilage of the knee. Another difference between the two studies is that the present study compares 3.0T MRI systems instead of 1.0T and 1.5T MRI systems. Although 1.5T MRI systems are widely used for cartilage imaging, it is advisable to use 3.0T MRI systems for new longitudinal OA research studies. An advantage of the present study is that the sequence was optimized for cartilage imaging beforehand. Therefore, the acquisition parameters for the different sequences on both scanners were kept the same. Images on both systems were acquired using the same matrix, FOV, section thickness, and bandwidth. In this way we tried to make the comparison of the two different MRI systems as fair as possible. Another advantage of the present study is that a 512 x 512 reconstruction matrix was used, as opposed to a 256 x 256 matrix. Consequently, we achieved an increased in-plane resolution and were able to perform reliable and accurate measurements of cartilage thickness. An alternative method for imaging cartilage thickness and volume is steady-state free precession (SSFP) imaging (14). We chose not to use SSFP imaging sequences because they result in increased susceptibility artifacts at higher field strengths (specifically 3.0T). Furthermore, it would be difficult to compare SSFP sequences between the GE and Philips MRI systems. The product SSFP sequence on a GE system uses chemical fat suppression, while water excitation is used on a Philips system. This made the SSFP sequences difficult to compare between the two different MRI systems. A disadvantage of the present study is that cartilage thickness and volume measurements were obtained in healthy volunteers. It may be more difficult to measure cartilage thickness in damaged, unhealthy cartilage, such as in patients with OA of the knee. The fact that we did not find different average cartilage thickness measurements between the two different MRI systems in patients with healthy cartilage does not necessarily mean there is no difference in average cartilage thickness measurements between the two MRI systems in OA patients. Another disadvantage is that only two 3.0T MRI systems from different manufacturers were compared in a small data set.

Another disadvantage is that only average cartilage thickness and volume were compared. Other morphological parameters, such as osteophytes, cysts, bone marrow edema, meniscal defects, and effusion were not compared. This will be addressed in future studies. In conclusion, the present study shows that two OA surrogate endpoints- average cartilage thickness and cartilage volume- acquired on two 3.0T MRI systems from different manufacturers are comparable.

References

1. Harris Jr ED. The bone and joint decade: a catalyst for progress. *Arthritis Rheum* 2001;44:1969–1970.
2. Gold GE, McCauley TR, Gray ML, Disler DG. What's new in cartilage? *Radiographics* 2003;23:1227–1242.
3. Vincken PW, ter Braak BP, van Erkel AR, et al. Effectiveness of MR imaging in selection of patients for arthroscopy of the knee. *Radiology* 2002;223:739–746.
4. Eckstein F, Westhoff J, Sittek H, et al. In vivo reproducibility of three-dimensional cartilage volume and thickness measurements with MR imaging. *AJR Am J Roentgenol* 1998;170:593–597.
5. Eckstein F, Lemberger B, Gratzke C, et al. In vivo cartilage deformation after different types of activity and its dependence on physical training status. *Ann Rheum Dis* 2005;64:291–295.
6. Mosher TJ, Smith HE, Collins C, et al. Change in knee cartilage T2 at MR imaging after running: a feasibility study. *Radiology* 2005; 234:245–249.
7. Ernst RR, Anderson WA. Application of Fourier transform spectroscopy to magnetic resonance. *Rev Sci Instrum* 1966;37:93–102.
8. Gold GE, Han E, Stainsby J, Wright G, Brittain J, Beaulieu C. Musculoskeletal MRI at 3.0 T: relaxation times and image contrast. *AJR Am J Roentgenol* 2004;183:343–351.
9. Kass M, Witkin A, Terzopoulos D. Snakes: active contour models. *Int J Comput Vision* 1988;1:321–331.
10. Koo S, Alexander EJ, Gold GE, Giori NJ, Andriacchi TP. Morphology and thickness in tibial and femoral cartilage at the knee is influenced by the mechanics of walking. In: *Proceedings of the ASME Summer Bioengineering Conference*, Miami, FL, USA, 2003.
11. Koo S, Dixit AN, Alexander EJ, Andriacchi TP. A rule based approach to improve cartilage thickness measurement reproducibility from knee MRI. In: *Proceedings of the 27th Annual Meeting of the American Society of Biomechanics*, Toledo, OH, USA, 2003.
12. Koo S, Kornaat PR, Garry GE, Andriacchi TP. Factors influencing the accuracy of articular cartilage thickness measurement from MRI. In: *Proceedings of the 28th Annual Meeting of the American Society of Biomechanics*, Portland, OR, USA, 2004.
13. Morgan SR, Waterton JC, Maciewicz RA, et al. Magnetic resonance imaging measurement of knee cartilage volume in a multicentre study. *Rheumatology (Oxford)* 2004;43:19–21.
14. Kornaat PR, Reeder SB, Koo S, et al. MR imaging of articular cartilage at 1.5T and 3.0T: comparison of SPGR and SSFP sequences. *Osteoarthritis Cartilage* 2005;13:338–344.



6

Chapter 6

Central Osteophytes in the Knee: Prevalence and Association with Cartilage Defects on MR Imaging

Thomas R McCauley
Peter R Kornaat
Won-Hee Jee

Abstract

Objective

The objective of this study was to determine the prevalence and location of central osteophytes in patients referred for MR imaging of the knee and the relationship of central osteophytes to articular cartilage defects, marginal osteophytes, meniscal tears, and anterior cruciate ligament tears as seen on MR imaging.

Materials and methods

Two hundred consecutive patients referred for MR imaging of the knee were evaluated for central osteophytes, articular cartilage defects, marginal osteophytes, meniscal tears, and anterior cruciate ligament tears. A 1.5-T scanner was used, and assessments were made by consensus of two experienced musculoskeletal radiologists. Seven patients were excluded, leaving 193 patients in the study population.

Results

The prevalence of central osteophytes in the knee was 15% (35 central osteophytes in 29 patients). Patients with central osteophytes were older (mean age, 52 years versus 38 years), weighed more (mean weight, 204 lb [92 kg] versus 174 lb [78 kg]), had more articular cartilage defects (mean, 4.3 versus 1.3), and had more marginal osteophytes (mean, 3.9 versus 1.1) than patients without central osteophytes ($p < 0.0001$, Student's t test). Patients with central osteophytes were more likely to have a meniscal tear ($p = 0.004$, chi-square test), but they were not more likely to have an anterior cruciate ligament tear. All central osteophytes were associated with articular cartilage defects at the same location, which were full or near-full thickness on MR imaging for 32 of 35 central osteophytes.

Conclusion

Central osteophytes are common in patients referred for MR imaging of the knee. When central osteophytes are seen in the knee there is a high likelihood of an associated full thickness or near-full thickness articular cartilage defect.

Introduction

Osteoarthritis is characterized by loss of articular cartilage and changes in bone including marginal osteophytes, subchondral sclerosis, and remodeling of bone [1]. Although marginal osteophytes are almost always present in patients with osteoarthritis, the appearance of osteophytic outgrowths in the central

portions of the articular space is a less well-recognized finding. These osteophytic outgrowths are termed "central osteophytes" [1–4]. We frequently see central osteophytes on MR examinations of the knee, and central osteophytes often are associated with focal articular cartilage defects. The purpose of our study was to determine the prevalence and location of central osteophytes in patients referred for MR imaging of the knee and to determine the relationship of central osteophytes to articular cartilage defects, marginal osteophytes, meniscal tears, and anterior cruciate ligament tears.

Materials and Methods

We evaluated clinical knee MR examinations from 200 consecutive patients who were referred for MR imaging of the knee over a 15-week period. Seven patients were excluded from the study because metal artifacts degraded image quality in six patients and fat suppression was inadvertently omitted on the fat-suppressed three-dimensional spoiled gradient-echo sequence in one patient. This left 193 patients in the study population: 83 females and 110 males. The patients ranged in age from 11 to 86 years (mean age, 40 years), and their average weight was 179 lb (81 kg; range, 95–310 lb [43–140 kg]). The study was approved by our institution's review board for human studies. Informed consent was not necessary because of the retrospective design of the study. All patients were imaged with a 1.5-T superconducting magnet (Signa; General Electric Medical Systems, Milwaukee, WI) using our routine clinical protocol that includes the following sequences: axial fat-suppressed fast spin-echo images (TR/effective TE, 4000/20; 4-mm thick; 0.5-mm intersection gap; 16-cm field of view; 256 x 256 matrix; echo train length, 10; 1 excitation); sagittal T1-weighted spinecho images (TR range/TE, 450–600/14; 3.3-mm thick; no gap; 16-cm field of view; 256 x 192 matrix; 1 excitation); coronal fast spin-echo images (TR/effective TEs, 3000/20 and 80; 3.3-mm thick; 0.3-mm intersection gap; 14-cm field of view; 256 x 256 matrix; echo train length, 10; 1 excitation); sagittal fast spin-echo T2-weighted images through the anterior cruciate ligament (TR/effective TE, 2000/84; 3-mm thick; 0.3-mm intersection gap; 14-cm field of view; 256 x 160 matrix; echo train length, 10; 2 excitations); and fat-suppressed three-dimensional spoiled gradient-echo images in the sagittal plane that were also reformatted in the axial plane (TR/TE, 40/6; 1.5-mm thick; 14-cm field of view; 256 x 160 matrix; 0.75 excitations; flip angle, 40°; 60 images).

Two experienced musculoskeletal radiologists reviewed all images by consensus for the presence of focal articular cartilage defects, central osteophytes, marginal osteophytes, meniscal tears, and anterior cruciate ligament tears. Central osteophytes and articular cartilage defects were assigned to one of 10 locations: the medial or lateral femoral condyle; the medial or lateral tibial plateau; the medial facet, lateral facet, or median ridge of the patella; or the medial part, lateral part, or midline of the trochlear groove. A central osteophyte was recorded as associated with an articular cartilage defect when it was subjacent to the defect or at the margin of the defect. Articular cartilage defects were graded using a

modification of the following method proposed by Shahriaree [5]: grade 0, absent (no abnormality in signal intensity or morphology); grade 1, signal abnormality (signal intensity was abnormal but the cartilaginous surface appeared intact); grade 2, less than 50% reduction of cartilage thickness; grade 3, 50% or greater reduction of cartilage thickness; grade 4, full thickness or near-full thickness cartilage defect (cartilage defects with either no high signal intensity over the cortex or a very thin rim of high signal intensity); and grade 5, same findings as grade 4 with associated underlying subchondral marrow signal abnormality. The depth of cartilage loss was measured by estimating the actual cartilage contour in relation to the expected normal cartilage contour. Osteophytes were identified when focal excrescences extended from the cortical surface either with signal that was the same as the cortex or covered with signal that was the same as cortex and containing marrow signal. Osteophytes were identified as marginal when at the margin of the joint and as central when surrounded by articular cartilage on all sides. The size of each osteophyte was compared with that of adjacent articular cartilage with a normal MR imaging appearance. Central osteophytes were assessed using the following scale: grade 0, none; grade 1, small (<50% of cartilage thickness); grade 2, moderate (50–100% of cartilage thickness); and grade 3, large (>100% of cartilage thickness). The configuration of each central osteophyte was categorized as to whether it completely filled the base of the cartilage defect or incompletely filled the base of the cartilage defect. The locations of central osteophytes were categorized as weight-bearing versus non-weight-bearing surfaces. Weight-bearing surfaces were defined as the tibial plateau and the articular surfaces of the femoral condyles between the posterior margin of the posterior horn of the meniscus and the anterior margin of the anterior horn of the meniscus. The presence or absence of a rim of high signal covering the surface of the osteophyte on the fat-suppressed three-dimensional spoiled gradient-echo images was determined for each central osteophyte. The presence or absence of marginal osteophytes was determined at each of seven sites in the knee: the medial femoral condyle, the lateral femoral condyle, the medial tibial plateau, the lateral tibial plateau, the patella, the medial margin of the trochlear groove, or the lateral margin of the trochlear groove. The maximum size of a marginal osteophyte at each of these sites was assessed using the following scale: grade 0, none; grade 1, minimal (<1 mm); grade 2, small (1–3 mm); grade 3, moderate (>3–5 mm); and grade 4, large (>5 mm). Size was measured from the base to the tip of the osteophyte. For statistical analysis, the ages, weights, number of hyaline cartilage defects, and number of sites with marginal osteophytes for patients with and without central osteophytes were compared using the unpaired two-tailed Student's *t* test. The difference in the prevalence of central osteophytes in male versus female patients and the association of central osteophytes with meniscal tears and anterior cruciate ligament tears were compared using the chi-square test. Spearman's rank correlation coefficient was used to determine whether there was a correlation between the grade of central osteophytes and the maximum grade of marginal osteophytes. To quantitate the severity of changes

of osteoarthritis, the mean number of articular cartilage defects, the number of sites with marginal osteophytes, and the highest grade of marginal osteophyte in each patient were determined. These values for patients with central osteophytes were compared with patients with marginal osteophytes alone (i.e., patients with marginal osteophytes without central osteophytes). The unpaired two-tailed Student's *t* test was used for number of articular cartilage defects and number of marginal osteophytes, and the Mann-Whitney test was used for grade of marginal osteophytes. For all comparisons, a *p* value of 0.5 or less was considered significant.

Results

In the 193 patients, 35 central osteophytes were detected in 29 patients (15% prevalence). Twenty-five patients had one central osteophyte, two patients had two central osteophytes, and two patients had three central osteophytes in one knee. The size of the 35 central osteophytes was grade 1 (<50% of cartilage thickness) for 12 central osteophytes and grade 2 (50–100% of cartilage thickness) for 23 central osteophytes; no central osteophytes were defined as grade 3 (>100% of cartilage thickness). Of the 35 central osteophytes, 22 (63%) incompletely filled the base of the cartilage defect (Fig. 1), and 13 (37%) completely filled the base of the cartilage defect (Figs. 1–3). Central osteophytes were found at all locations in the knee (Table 1). Twenty-three (66%) of the 35 central osteophytes were located at a non-weight-bearing area, and 12 (34%) central osteophytes were located at a weight-bearing area. Patients with central osteophytes were older (mean age, 52 years; range, 19–78 years) and weighed more (mean weight, 204 lb [92 kg]; range, 140–285 lb [63–128 kg]) than patients without central osteophytes (mean age, 38 years; range, 11–86 years; mean weight, 174 lb [78 kg]; range, 95–310 lb [43–140 kg]) ($p < 0.0001$, *t* test). The mean age of patients with central osteophytes was higher than that of patients with marginal osteophytes alone (52 years versus 47 years); however, this difference did not reach statistical significance ($p = 0.09$, Student's *t* test). The mean weight of patients with central osteophytes was higher than that of patients with marginal osteophytes alone (mean, 204 lb [92 kg] versus 181 lb [81 kg]) ($p = 0.013$, Student's *t* test). There was no difference in the prevalence of central osteophytes between female versus male patients ($p > 0.05$, chi-square test), with central osteophytes in 19% of the female patients and in 12% of the male patients. Eighteen (51%) of the 35 central osteophytes were associated with grade 4 articular cartilage defects, and 14 (40%) of the 35 were associated with grade 5 defects (Fig. 4). Only two central osteophytes were associated with grade 3 articular cartilage defects, and one central osteophyte was associated with a grade 2 defect. Thus, 91% of the central osteophytes occurred in association with articular cartilage defects graded as full thickness or near-full thickness, and no central osteophyte was associated with a normal appearance of the adjacent or overlying articular cartilage. Patients with central osteophytes had more articular cartilage defects at other locations in the knee (mean, 4.3) than patients with marginal osteophytes alone (mean, 2.7)

($p = 0.007$, Student's t test) and those without central osteophytes (mean, 1.3) ($p < 0.0001$, Student's t test) (Fig. 2). High-signal-intesity tissue covered the surface of 91% (32/35) of the central osteophytes on fat-suppressed three-dimensional spoiled gradient-echo images (Figs. 1 and 2); only three were not covered by a rim of high signal (Fig. 3). Only three patients (10%) with central osteophytes did not have marginal osteophytes. More marginal osteophytes were present in patients with central osteophytes (mean, 3.9 sites) than in those with marginal osteophytes alone (mean, 2.6 sites) ($p = 0.011$, Student's t test) or in those without central osteophytes (mean, 1.1 sites) ($p < 0.0001$, Student's t test; Fig. 2). Patients with central osteophytes had larger marginal osteophytes (mean grade, 2.3) than patients with marginal osteophytes alone (mean grade, 1.7) ($p = 0.001$, Mann-Whitney test). Increased size of the central osteophytes was associated with increased size of the largest marginal osteophyte in the knee (Spearman's rank correlation coefficient = 0.46 with $p = 0.022$). Patients with central osteophytes were more likely to have a meniscal tear than were patients without central osteophytes ($p = 0.004$, chi-square test), but they were not more likely to have a meniscal tear than patients with marginal osteophytes alone ($p = 0.15$, chi-square test). A meniscal tear occurred in 69% (20/29) of the patients with central osteophytes, 40% (66/164) of the patients without central osteophytes, and 53% (36/68) of the patients with marginal osteophytes alone. There was no significant relationship between central osteophytes and anterior cruciate ligament tears; anterior cruciate ligament tears were present in 14% (4/29) of the patients with central osteophytes and in 15% (24/164) of the patients without central osteophytes ($p > 0.05$).

Table I Location and Grade of Central Osteophytes

Location	Grade			Total
	1	2	3	
Medial femoral condyle	1	2	0	3
Medial tibial plateau	0	2	0	2
Lateral femoral condyle	2	6	0	8
Lateral tibial plateau	1	0	0	1
Patella medial facet	3	4	0	7
Patella median ridge	1	1	0	2
Patella lateral facet	2	1	0	3
Medial trochlear groove	1	1	0	2
Midline trochlear groove	1	3	0	4
Lateral trochlear groove	0	3	0	3
Total central osteophytes	12	23	0	35

Table 1 Location and Grade of Central Osteophytes
Grade indicates size of central osteophytes. Grade 1 = small osteophyte (<50% of cartilage thickness), grade 2 = moderate osteophyte (50–100% of cartilage thickness), and grade 3 = large osteophyte (>100% of cartilage thickness).

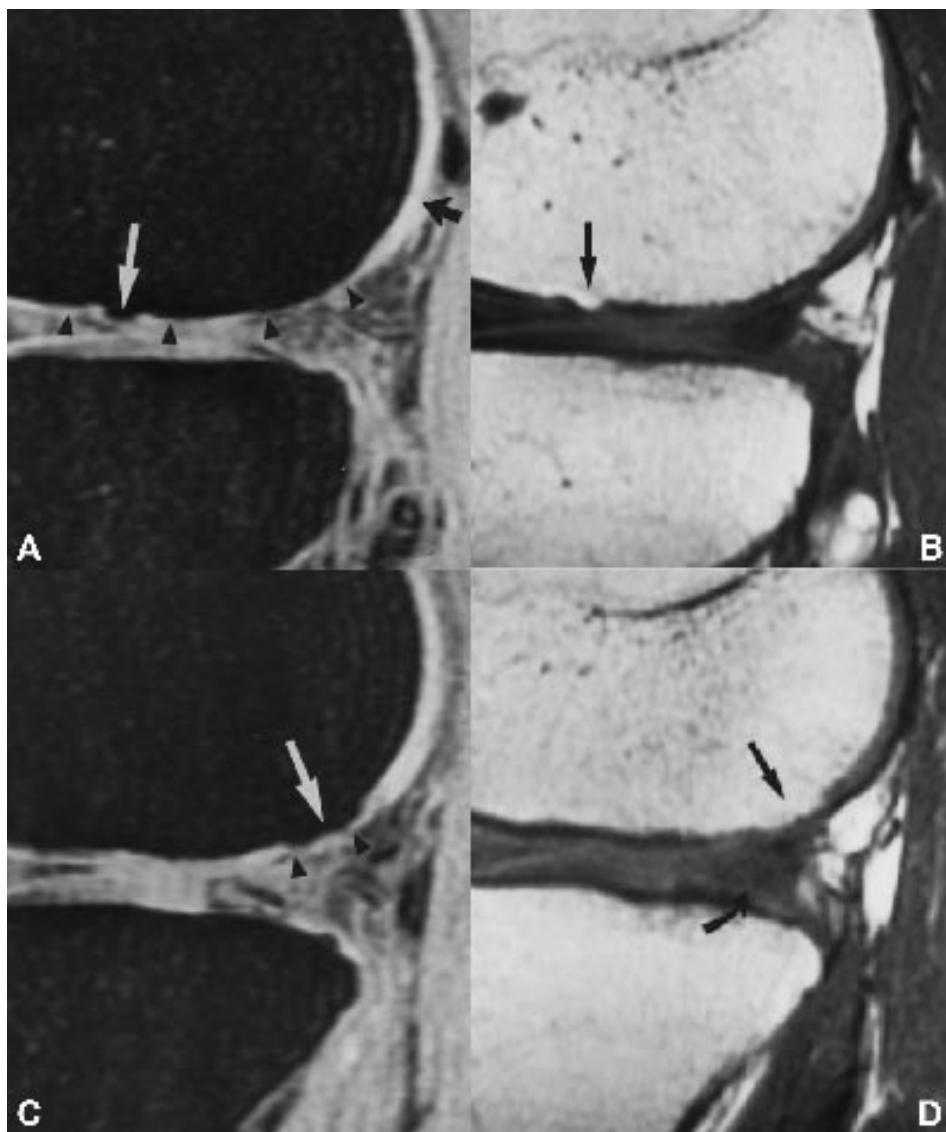


Figure 1 A B C D 46-year-old man with two central osteophytes associated with grade 4 articular cartilage defects. A, Fat-suppressed three-dimensional spoiled gradient-echo MR image (TR/TE, 40/6; flip angle, 40°) shows central osteophyte (white arrow) at lateral femoral condyle incompletely filling base of cartilage defect (arrowheads). Normal articular cartilage, which has high signal intensity on fat-suppressed three-dimensional spoiled gradient-echo MR images, is seen posteriorly (black arrow). B, Sagittal T1-weighted MR image (600/14) obtained at same location as A shows fat signal in central osteophyte (arrow). C, Fat-suppressed three-dimensional spoiled gradient-echo MR image (40/6; flip angle, 40°) shows central osteophyte (arrow) completely filling base of cartilage defect (arrowheads). D, Sagittal T1-weighted MR image (600/14) obtained at same location as A shows fat signal in central osteophyte (straight arrow). Complex tear can be seen in posterior horn of medial meniscus (curved arrow). Note thin layer of high signal intensity covers surface of osteophytes in A and C, and note that both osteophytes involve weight-bearing surface of condyle.

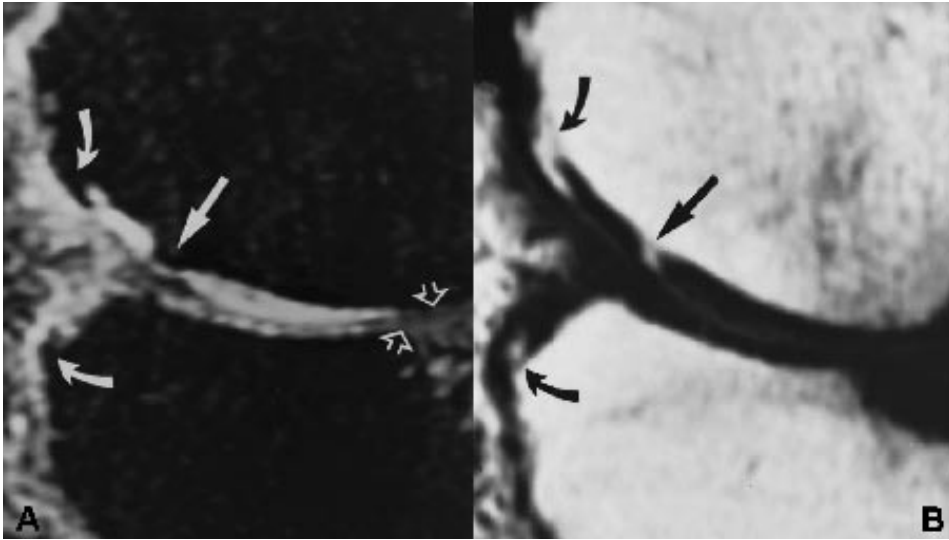


Figure 2 A B 59-year-old woman with central osteophyte at medial femoral condyle that fills base of articular cartilage defect. A, Sagittal fat-suppressed three-dimensional spoiled gradient-echo MR image (TR/TE, 40/6; flip angle, 40°) shows central osteophyte (solid straight arrow) and marginal osteophytes (curved arrows). Full-thickness articular cartilage defects (open arrows) that are separate from central osteophyte can be seen at femoral condyle and tibial plateau along with subchondral signal abnormality beneath tibial plateau defect. B, Sagittal T1-weighted MR image (600/14) shows central osteophyte (straight arrow) and marginal osteophytes (curved arrows) with fat signal from marrow extending into osteophytes.

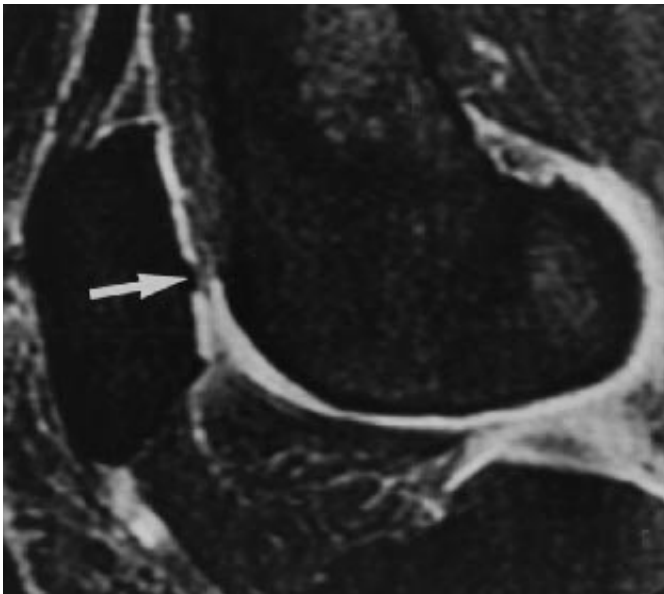


Figure 3 50-year-old woman with central osteophyte (arrow) at lateral facet of patella on sagittal fat-suppressed three-dimensional spoiled gradient-echo MR image (TR/TE, 40/6; flip angle, 40°). This is one of only three of 35 central osteophytes not covered by thin layer of high signal intensity.

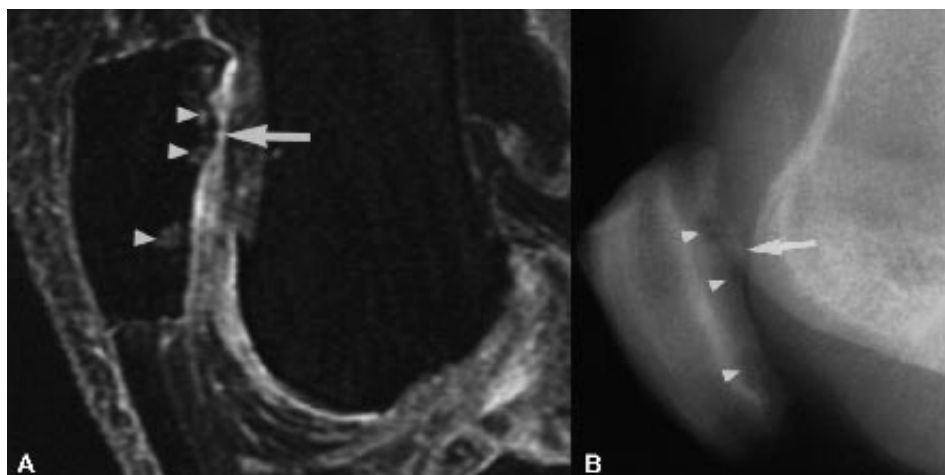


Figure 4 A B 54-year-old woman with central osteophyte at patella. A, Sagittal fat-suppressed three-dimensional spoiled gradient-echo MR image (TR/TE, 40/6; flip angle, 40°) shows subarticular osteophyte (arrow) with extensive articular cartilage loss at patella and trochlear groove and underlying foci of increased subchondral signal (arrowheads). B, Lateral radiograph shows subarticular osteophyte (arrow) with subarticular lucencies (arrowheads) corresponding to subarticular signal abnormalities shown in A.

Discussion

Few reports have been published about central osteophytes. Only three imaging studies of central osteophytes were found from an electronic search of the literature [2–4], with only one of these three studies reporting the use of MR imaging [2]. However, because we found the prevalence of central osteophytes in the knee was 15% on MR imaging, central osteophytes are commonly seen. The prior study that examined MR imaging of central osteophytes limited to the femur found a prevalence of 14% (9/63) [2], which is similar to the 10.4% (20/193) prevalence we found at this site (Table 1). We found central osteophytes at all cartilage surfaces in the knee. We found that central osteophytes frequently occurred at weight-bearing areas (34%). This finding is in contrast to the findings of previous studies, which concluded that central osteophytes rarely occur in weight-bearing areas of the joint [3, 4]; however, our finding agrees with that of a prior study of femoral specimens [2], which found 24% (32/136) of central osteophytes at the weight-bearing surface of the femoral condyles. All the central osteophytes occurred in association with a cartilage defect, most (91%) of which were graded as full or near-full thickness (grade 4 or 5). A prior study found 73% of central osteophytes were accompanied by an overlying articular cartilage abnormality on MR imaging [2]. The prevalence of articular cartilage abnormality in our study is higher most likely because of the use of an MR imaging sequence designed specifically for articular cartilage evaluation. Our results indicate detection of central osteophytes with any imaging modality makes it probable that an adjacent articular cartilage defect, which usually is full thickness or near-full

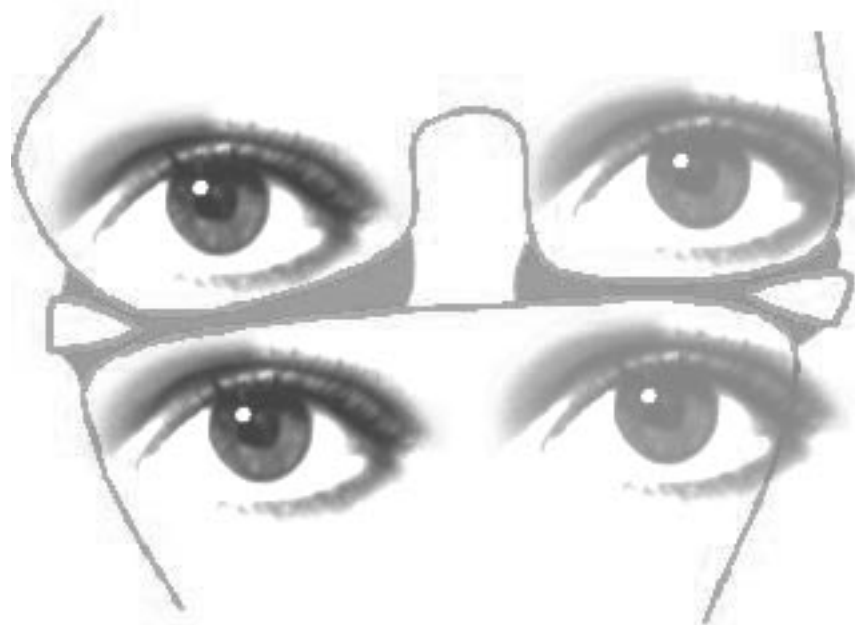
thickness, is present. When central osteophytes are seen in the knee on radiographs, CT scans, or MR images obtained without cartilage-specific sequences, an adjacent articular cartilage defect should be assumed to be present. It has been suggested that MR imaging is more sensitive for detection of central osteophytes than radiographs because the curved articular surfaces often lead to obscuration of central osteophytes on radiographs [2, 3]. We found a rim of high-signal-intensity tissue covers the surface of almost all central osteophytes on fat-suppressed three-dimensional spoiled gradient-echo images. We do not have histologic proof of the nature of this tissue. We believe it most likely is a thin rim of cartilage on the basis of previous histologic descriptions that indicate overlying cartilage is required for development of central osteophytes and is seen overlying most central osteophytes [1, 2, 6]. The covering tissue along with osteophytes either being present at the margin of cartilage defects or filling the base of cartilage defects would explain the fact that our referring orthopedic surgeons rarely report seeing central osteophytes at arthroscopy. The inability to see central osteophytes at arthroscopy is consistent with the pathologic description that central osteophytes are usually not visible on inspection of the articular surface but are visible with longitudinal sectioning of the articular surface [6]. Of the 35 central osteophytes, 13 (37%) diffusely filled the base of the cartilage defect. Central osteophytes with a diffuse configuration can lead to an underestimation of the depth of cartilage loss at arthroscopy. Identification of these osteophytes is important for cartilage therapies, such as chondrocyte transplantations, because the central osteophyte decreases the volume available for placement of cells and the volume available for regrowth of cartilage. The presence of central osteophytes is associated with more severe changes of osteoarthritis than marginal osteophytes alone, as indicated by more numerous articular cartilage defects and larger and more numerous marginal osteophytes. Marginal osteophytes have previously been shown to be associated with knee pain [7]. Future studies are needed to determine whether central osteophytes are associated with more severe symptoms or a worse prognosis than are marginal osteophytes alone. Increased weight and age are known predisposing factors for osteoarthritis [8] and likely account for the association seen between central osteophytes and increased weight and age. Despite the association of central osteophyte formation with increased age, the youngest patient with a central osteophyte was only 19 years old, which indicates that central osteophytes can occur in young patients. Meniscal tears have been shown to predispose patients to develop osteoarthritis, likely accounting for the association between central osteophytes and meniscal tears [9]. The lack of association of central osteophytes with anterior cruciate ligament tears is surprising given the known association between anterior cruciate ligament tears and osteoarthritis [9]. It is possible that the mechanism of development of osteoarthritis caused by an anterior cruciate ligament tear differs from that caused by a meniscal tear, thus resulting in the lack of association with central osteophyte formation. Alternatively, the lack of association possibly occurred because of factors not controlled in this study.

We did not determine the time interval between anterior cruciate ligament injury and MR examination, and we did not assess the degree of instability, both of which could influence the association between the presence of central osteophytes and anterior cruciate ligament tears. Proposed explanations for the development of osteophytes include aging, mechanical instability of the joint, proliferative response caused by adjacent synovial membrane inflammation, and tissue response to stretching at the insertion site of the joint capsule [2, 4, 10–12]. These factors are believed to induce production of chemical or hormonal transducers including insulin, insulinlike growth factor–1, and transforming growth factor– β , which have been found to stimulate osteophyte growth [10–16]. Unlike marginal osteophytes, central osteophytes do not have an adjacent joint capsule or synovium, and, thus, stretching of the joint capsule and the adjacent synovial inflammation are not responsible for their formation. The exact mechanism or mechanisms resulting in formation of central osteophytes and marginal osteophytes have not yet been determined, and future studies are needed to determine whether similar mechanisms are responsible for formation of both types of osteophytes. One limitation of this study is that we did not have arthroscopic or pathologic confirmation of our findings. Arthroscopic confirmation of central osteophytes is not possible because central osteophytes are generally not visible at arthroscopy, which is most likely because of the thin layer of covering cartilage and because of their morphology. Our referring orthopedic surgeons report seeing central osteophytes only when they débrided the overlying tissue. Our referring orthopedic surgeons rarely use débridement in their treatment of articular cartilage defects and, thus, rarely visualize subarticular osteophytes. The diffuse form of central osteophytes would not be expected to be visible even with débridement because they fill the base of the cartilage defect (Fig. 3). Despite the inability to obtain arthroscopic correlation, the MR imaging findings are typical of osteophytes seen at the margins of the knee, and the configuration and appearance of the osteophytes agree with prior studies [2, 3]. Although cartilage defects were not arthroscopically confirmed, the fat-suppressed three-dimensional spoiled gradient-echo imaging sequence used in this study has been shown to be accurate for detection of cartilage defects [17, 18]. An MR imaging grading system similar to that used in this study showed good concordance with arthroscopic grade in a prior study [18]. Consensus interpretation was used in this study because the study was designed to determine the prevalence of central osteophytes and their association with cartilage defects and other MR imaging findings rather than to determine the accuracy or interobserver reliability for MR imaging. We also did not design this study to compare different MR imaging sequences because this was not the goal of this investigation. In conclusion, central osteophytes are commonly found in patients referred for MR imaging of the knee and are associated with cartilage defects at the same location that are usually full thickness or near-full thickness. Thus, when central osteophytes are identified in the knee on radiographs, CT scans, or MR images obtained without articular cartilage-specific sequences, it is likely that an associated articular cartilage defect

is present. Central osteophytes are associated with more severe changes of osteoarthritis than are marginal osteophytes alone, including a greater number of articular cartilage defects and a greater number and larger size of marginal osteophytes. Future studies are needed to determine whether central osteophytes are associated with more severe symptoms of osteoarthritis or a worse prognosis.

References

1. Resnick D. Degenerative disease of extraspinal locations. In: Resnick D. *Diagnosis of bone and joint disorders*, 3rd ed. Philadelphia: Saunders, 1995 :1261–1371
2. Abraham-Zadeh R, Yu JS, Resnick D. Central (interior) osteophytes of the distal femur: imaging and pathologic findings. *Invest Radiol* 1994 ;29: 1001–1005
3. Kindynis P, Haller J, Kang HS, et al. Osteophytosis of the knee: anatomic, radiologic, and pathologic investigation. *Radiology* 1990 ;174:841–846
4. Varich L, Pathria M, Resnick D, et al. Patterns of central acetabular osteophytosis in osteoarthritis of the hip . *Invest Radiol* 1993 ;28:1120–1127
5. Shahriaree H. Chondromalacia. *Contemp Orthop* 1985 ;11:27–39
6. Jaffe HL. Metabolic, degenerative, and inflammatory diseases of bones and joints . Philadelphia: Lea & Febiger, 1972 :735–778
7. Cicuttini FM, Baker J, Hart DJ, Spector TD. Association of pain with radiological changes in different compartments and views of the knee joint. *Osteoarthritis Cartilage* 1996 ;4: 143–147
8. Hochberg MC. Epidemiologic considerations in the primary prevention of osteoarthritis. *J Rheumatol* 1991 ;18:1438–1440
9. Roos H, Adalberth T, Dahlberg L. Osteoarthritis of the knee after injury to the anterior cruciate ligament or meniscus: the influence of time and age. *Osteoarthritis Cartilage* 1995 ;3:261–267
10. Moskowitz RW, Goldberg VM. Studies of osteophyte pathogenesis in experimentally induced osteoarthritis. *J Rheumatol* 1987 ;14:311–320
11. van Osch GJ, van der Kraan PM, van Valburg AA, van den Berg WB. The relation between cartilage damage and osteophyte size in a murine model for osteoarthritis in the knee. *Rheumatol Int* 1996 ;16:115–119
12. Buckwalter JA, Mankin HJ. Articular cartilage: degeneration and osteoarthritis, repair, regeneration, and transplantation. *J Bone Joint Surg Am* 1997 ;79-A:612–632
13. Horn CA, Bradley JD, Brandt KD, Kreipke DL, Slowman SD, Kalasinski LA. Impairment of osteophyte formation in hyperglycemic patients with type II diabetes mellitus and knee osteoarthritis. *Arthritis Rheum* 1992 ;35:336–342
14. Schouten JS, van den Ouweland FA, Valkenburg HA, Lamberts SW. Insulin-like growth factor-1: a prognostic factor of knee osteoarthritis. *Br J Rheumatol* 1993 ;32:274–280
15. van Beuningen HM, van der Kraan PM, Arntz OJ, van den Berg WB. Transforming growth factor-beta 1 stimulates articular chondrocyte proteoglycan synthesis and induces osteophyte formation in the murine knee joint. *Lab Invest* 1994 ;71:279–290
16. van den Berg WB. Growth factors in experimental osteoarthritis: transforming growth factor beta pathogenic? *J Rheumatol Suppl* 1995 ;43:143–145
17. McCauley TR, Disler DG. MR imaging of articular cartilage. *Radiology* 1998 ;209:629–640
18. Disler DG, McCauley TR, Kelman CG, et al. Fatsuppressed three-dimensional spoiled gradient-echo MR imaging of hyaline cartilage defects in the knee: comparison with standard MR imaging and arthroscopy. *AJR* 1996 ;167: 127–132



7

Chapter 7

The relationship between the MRI
features of mild osteoarthritis in
the patellofemoral and tibiofemoral
compartment of the knee

Peter R Kornaat
Naghmeh Riyazi
Margreet Kloppenburg
Iain Watt
Johan L Bloem

Abstract

The aim of this work was to demonstrate the relationship between osteoarthritic changes seen on magnetic resonance (MR) images of the patellofemoral (PF) or tibiofemoral (TF) compartments in patients with mild osteoarthritis (OA) of the knee. MR images of the knee were obtained in 105 sib pairs (210 patients) who had been diagnosed with OA at multiple joints. Entry criteria included that the degree of OA in the knee examined should be between a Kellgren and Lawrence score of 2 or 3. MR images were analyzed for the presence of cartilaginous lesions, bone marrow edema (BME) and meniscal tears. The relationship between findings in the medial and lateral aspects of the PF and TF compartments was examined. The number of cartilaginous defects on either side of the PF compartment correlated positively with number of cartilaginous defects in the ipsilateral TF compartment (odds ratio, OR, 55, confidence interval, CI, 7.8–382). The number of cartilaginous defects in the PF compartment correlated positively with ipsilateral meniscal tears (OR 3.7, CI 1.0–14) and ipsilateral PF BME (OR 17, CI 3.8–72). Cartilaginous defects in the TF compartment correlated positively with ipsilateral meniscal tears (OR 9.8, CI 2.5–38) and ipsilateral TF BME (OR 120, CI 6.5–2,221). Osteoarthritic defects lateralize or medialize in the PF and TF compartments of the knee in patients with mild OA.

Introduction

The impact and consequences of osteoarthritis (OA) in the ageing population of the industrialized world are very apparent in light of the recent declaration of the Bone and Joint Decade [1]. The impact and magnitude of OA motivates the medical and pharmaceutical communities to develop disease-modifying drugs to prevent or delay the development of disability. For these reasons a number of longitudinal studies have been initiated looking for findings that may predict the progression of OA. One of such study has started in our research institute [2]. Part of this includes detailed assessment of sequential magnetic resonance (MR) images of the knee. MRI, with its excellent soft-tissue contrast, is the best noninvasive technique currently available for the assessment of cartilage injury and other internal derangement of the knee [3–5]. Preliminary assessment of the MR images suggested a tendency of osteoarthritic defects to medialize or lateralize in the knee compartments. Such a tendency may be of importance in further advancing insight into the pathogenesis of OA. Medialization and lateralization of OA defects is described in the literature. A recent study reports a relationship between bone marrow edema (BME) lesions in the subarticular bone and ipsilateral radiographic progression [6]. Medial BME lesions were related to medial progression and lateral lesions to lateral progression, but not to the contralateral

compartment. Radiographic progression was defined as an increase at follow-up in medial or lateral joint space narrowing. However, whether BME predicted ipsilateral progression of joint space narrowing was due to cartilaginous loss in the tibiofemoral (TF) compartment or to other factors, such as meniscal tears, was not discussed. Further, it is not known whether osteoarthritic defects in the patellofemoral (PF) compartment correlate with ipsilateral BME. As mechanical factors are believed to be essential to the pathogenesis of knee OA [7], and recent studies show limb misalignment as a potent risk factor for structural progression of TF and PF OA [8, 9], it was felt it was important to investigate the distribution of cartilaginous defects, BME and meniscal tears in the knee in patients with mild OA. Therefore, this study examines the hypothesis that OA defects in the medial compartment of the PF or TF joints correlate with each other, and vice versa, and, further, that OA defects in the lateral compartments are found to correlate similarly.

Materials and methods

Patients

The present study is part of the ongoing Genetics, Osteoarthritis and Progression (GARP) study [2]. The primary goal of the GARP study is the identification of genetic determinants of OA susceptibility and progression in patients aged between 40 and 70 years with familial generalized OA. Only 35% of the patients had symptomatic knee OA, defined as pain or stiffness on most days of the prior month with osteophytes on radiographs. Radiographic knee OA, defined by a Kellgren and Lawrence score greater than 1, was diagnosed in 47% of the patients. As the purpose of the MR study was to assess progression of OA, no images were made of a knee with a Kellgren and Lawrence score of grade 4. Global TF radiographic severity was scored using the Kellgren and Lawrence grading system, in which 0 is normal, 1 is possible osteophyte lipping, 2 is definite osteophytes and possible joint space narrowing, 3 is moderate/ multiple osteophytes, definite joint space narrowing, some sclerosis, and possible bony attrition, and 4 is large osteophytes, marked joint space narrowing, severe sclerosis, and definite bony attrition [10]. MRI of the knee was performed successfully in 205 out of 210 patients (105 sib pairs). One patient was excluded owing to claustrophobia, another had a large knee that did not fit into the knee coil, and in three patients image quality was inadequate owing to motion artifacts. Written informed consent was obtained from each patient prior to the study. The study was approved by our institution's medical ethical review board.

MR acquisition

Knees were imaged using a dedicated knee coil in a 1.5-T superconducting magnet (Philips Medical Systems, Best, The Netherlands). Each examination consisted of the following: coronal proton density and T2-weighted dual spin echo (SE)

images (with a repetition time, TR, of 2,200, an echo time, TE, of 20/80, 5-mm slice thickness, 0.5-mm intersection gap, 160-mm field of view, and 205×256 acquisition matrix); sagittal proton density and T2-weighted dual SE images (TR 2,200, TE 20/80, 4-mm slice thickness, 0.4-mm intersection gap, 160-mm field of view, 205×256 acquisition matrix); sagittal 3 DT1-weighted spoiled gradient echo (GE) frequency-selective fat-suppressed images (TR 46, TE 2.5, flip angle 40°, 3.0-mm slice thickness, slice overlap 1.5 mm, no gap, 180-mm field of view, 205×256 acquisition matrix); and axial proton density and T2-weighted turbo SE fat-suppressed images (TR 2500, TE 7.1/40, echo train length 6, 2-mm slice thickness, no gap, 180-mm field of view, 205×256 acquisition matrix). The total acquisition time (including the initial survey sequence) was 30 min.

MR interpretation

All MR images were analyzed by means of consensus between two readers. During the assessment, the readers were blinded to radiographic results, patient symptoms and patient age. The knee OA scoring system (KOSS) was used to assess osteoarthritic defects [11]. Cartilaginous defects and BME were assigned to any one, or a combination of, the following anatomical locations: the crista patellae; medial or lateral patellar facet; the medial or lateral trochlear facets; the medial or lateral femoral condyle; and the medial or lateral tibial plateaus. The medial and lateral menisci were reviewed for the presence of meniscal tears.

Cartilaginous defects were graded as diffuse or focal. Both coronal and sagittal SE images and sagittal GE images were used to assess the TF cartilage. Axial turbo SE images and sagittal GE and SE images were used to assess PF cartilage. The surface extent of a diffuse or focal cartilaginous defect was estimated by its maximal diameter and was graded as follows: grade 0, absent; grade 1, minimal (less than 5 mm); grade 2, moderate (5–10 mm); grade 3, severe (more than 10 mm). The depth of a cartilaginous defect was graded using a modification of the Yulish classification [12]: grade 0, absent (no abnormality in signal intensity or morphology); grade 1, less than 50% reduction of cartilage thickness; grade 2, 50% or greater reduction of cartilage thickness; grade 3, full thickness or nearly full thickness cartilage defect.

BME was defined as an ill-defined area of increased signal intensity on T2-weighted images in the subchondral cancellous bone, extending away from the articular surface 1539 over a variable distance, or at places where traction edema occurs [13]. The lesions were graded as follows: grade 0, absent; grade 1, minimal (diameter less than 5 mm); grade 2, moderate (diameter 5 mm–2 cm); grade 3, severe (diameter more than 2 cm). A meniscal tear was defined as a region of intermediate signal intensity on proton density-weighted images within the meniscus, communicating with its superior or inferior surfaces or inner margin, on more than one slice [14].

Statistical analysis

The medial PF compartment was defined as the medial patellar facet and the medial part of the trochlear groove. The lateral PF compartment was defined as the lateral patellar facet and the lateral part of the trochlear groove. Defects at the median ridge of the patella did not contribute to either the medial or lateral part of the patella. The medial TF compartment was defined as the medial femoral condyle and the medial tibial plateau; the lateral TF compartment was defined as the lateral femoral condyle and the lateral tibial plateau. In order to quantify cartilaginous defects in different compartments of the knee, the depth of each cartilage defect was added. To quantify BME the grade of each lesion was added. Odds ratios (OR) with 95% confidence intervals (CI) were used to examine the association between osteoarthritic defects in various anatomic compartments of the knee.

Results

The basic characteristics of the study population are shown in Table 1. The frequency distribution of osteoarthritic defects in the population studied is shown in Tables 2 and 3. Table 4 shows the distribution of cartilage defects in the PF and TF compartments. In total, 38 of 205 patients did not have any cartilage defects in either the PF or the TF compartment. This means that in 167 patients a cartilage defect was present in either the PF or the TF compartment. Fiftyfour of the 167 patients (33%) had an asymmetric distribution of diffuse and focal cartilage defects in both the PF and the TF compartment. Of these, 41 showed medialization of cartilaginous defects in both their PF and TF compartments and eight showed lateralization. The tendency of cartilaginous defects to medialize or lateralize in the PF and TF compartment is significant (OR 55, CI 7.8–382). Cartilaginous defects are 3.3 times (73/22) more common in the medial TF compartment than in the lateral TF compartment, and 2.9 times (76/26) more common in the medial PF compartment compared with the lateral side. Table 5 demonstrates the presence of meniscal tears in patients with an asymmetric distribution of cartilaginous defects in both anatomical compartments of the knee. Meniscal tears are more often located on the ipsilateral side in patients with an asymmetric distribution of cartilaginous defects. The association between PF cartilaginous defects and ipsilateral meniscal tears (OR 3.7, CI 1.0–15) and the association between TF cartilaginous defects and ipsilateral meniscal tears (OR 9.8, CI 2.5–38) is significant. Tables 6 and 7 show the distribution of cartilaginous defects and BME in the PF and TF compartments of the knee. Forty-six of 205 patients had an asymmetric distribution of cartilaginous defects and an asymmetric distribution of BME in the PF compartment of the knee. In 22 patients cartilaginous defects and BME occurred on the medial side of the PF compartment. In 15 patients cartilaginous defects and BME occurred on the lateral side of the PF compartment. The association between PF cartilaginous defects and ipsilateral PF BME was significant (OR 17, CI 3.8–72). The association between cartilaginous defects and BME at the ipsilateral side of the knee was stronger for the TF compartment (OR 120, CI 6.5–2221).

Table 1.Characteristics of population studied (patients with symptomatic osteoarthritis at multiple joints) (n=205)

	Range	Median
Age (years)	43 - 77	60
Weight (kg)	54 - 116	74
Height (cm)	152 - 191	169
Body Mass Index	20-40	26
Gender (female)		163 (80) ^a
Knee pain (yes)		121 (59) ^a
Knee stiffness (yes)		97 (47) ^a
Knee OA ^b (yes)		71 (35) ^a
Radiographic OA ^c (yes)		97 (47) ^a

Table 1 Characteristics of the population studied (patients with symptomatic osteoarthritis at multiple joints) (n=205)

^a Percentage in parentheses

^b Pain or stiffness on most days of the prior month with osteophytes on radiographs

^c Defined by a Kellgren and Lawrence score above 1 [10]

Table 2. Frequency distribution of osteoarthritic abnormalities in the population studied (n=205)

Number of patients with osteoarthritic abnormalities in the knee per group ^a	
Cartilage defects	167 (81)
Diffuse cartilage defects	152 (74)
Focal cartilage defects	64 (31)
Bone marrow edema	86 (42)
Meniscal tears	137 (67)

Table 2 Frequency distribution of osteoarthritic abnormalities in the population studied (n=205)

^aPercentage in parentheses

Table 3 Frequency distribution of osteoarthritic abnormalities in the population studied (n=205)

Frequency distribution of abnormal findings per patient for each category of abnormalities

	Range	Median
Cartilage defects (max 18)	0 - 10	4
Diffuse cartilage defects (max 9)	0 - 9	3
Focal cartilage defects (max 9)	0 - 4	0
Bone marrow edema (max 9)	0 - 5	1
Meniscal tears (max 6)	0 - 6	1

Table 3 Frequency distribution of osteoarthritic abnormalities in the population studied (n=205)

Max = maximum number of lesions scored per patient

Table 4. Distribution of cartilage defects in the patellofemoral and femorotibial compartment

		Tibiofemoral compartment				Total
		Medial > Lateral ^a	Lateral > Medial ^b	Medial = Lateral ^c	No Defects ^d	
Patellofemoral Compartment	Medial > Lateral *	41	2	15	18	76
	Lateral > Medial **	3	8	8	7	26
	Medial = Lateral ***	12	5	11	5	33
	No defects ****	17	7	8	38	70
	Total	73	22	42	68	205

Table 4 Distribution of cartilage defects in the patellofemoral and tibiofemoral compartments

^a More cartilage defects were present at the medial side than at the lateral side of the anatomical compartment.

^b More cartilage defects were present at the lateral side than at the medial side of the anatomical compartment.

^c The same number of cartilage defects were present at the medial and the lateral sides of the anatomical compartment.

^d No cartilage defects were present at either the medial side or the lateral side of the anatomical compartment.

Table 5. Location of meniscal tears in patients with an asymmetric distribution of cartilage defects in the femorotibial and patellofemoral compartment

	Difuse and focal cartilage defects			
	Patellofemoral compartment		Femorotibial compartment	
	Medial > Lateral ^a	Lateral > Medial ^b	Medial > Lateral ^a	Lateral > Medial ^b
Medial meniscal tear	28	4	32	4
Lateral meniscal tear	15	8	9	11
No tear	33	14	32	7
Total	76	26	73	22

Table 5 Location of meniscal tears in patients with an asymmetric distribution of cartilage defects in the femorotibial and patellofemoral compartment

^a More cartilage defects were present at the medial side than at the lateral side of the anatomical compartment.

^b More cartilage defects were present at the lateral side than at the medial side of the anatomical compartment.

Table 6. Association between bone marrow edema and cartilage defects in the patellofemoral compartment

		Cartilage defects at the patellofemoral compartment				Total
		Medial > Lateral ^a	Lateral > Medial ^b	Medial = Lateral ^c	No defects ^d	
Bone marrow edema at the patellofemoral compartment	Medial > Lateral	22	4	3	1	30
	Lateral > Medial	5	15	7	3	30
	Medial = Lateral	5	0	0	0	5
No defects		44	7	23	66	140
Total		76	26	33	70	205

Table 6 Association between bone marrow edema and cartilage defects in the patellofemoral compartment

^a More cartilage defects were present at the medial side than at the lateral side of the anatomical compartment.

^b More cartilage defects were present at the lateral side than at the medial side of the anatomical compartment.

^c The same number of cartilage defects were present at the medial and the lateral sides of the anatomical compartment.

^d No cartilage defects were present at either the medial or the lateral side of the anatomical compartment.

Table 7. Association between bone marrow edema and cartilage defects in the femorotibial compartment

		Cartilage defects at the femorotibial compartment				Total
		Medial > Lateral ^a	Lateral > Medial ^b	Medial = Lateral ^c	No defects ^d	
Bone marrow edema at the femorotibial compartment	Medial > Lateral	20	1	1	3	25
	Lateral > Medial	1	6	2	2	11
	Medial = Lateral	1	1	0	0	2
No defects		51	14	39	63	167
Total		73	22	42	68	205

Table 7 Association between bone marrow edema and cartilage defects in the femorotibial compartment

^a More cartilage defects were present at the medial side than at the lateral side of the anatomical compartment.

^b More cartilage defects were present at the lateral side than at the medial side of the anatomical compartment.

^c The same number of cartilage defects were present at the medial and the lateral sides of the anatomical compartment.

^d No cartilage defects were present at either the medial or the lateral side of the anatomical compartment.

Discussion

This study confirms a tendency for cartilaginous defects to medialize or lateralize in the PF and TF anatomical compartments of the knee in a substantial proportion of patients with mild OA of the knee. It demonstrates also the association between a meniscal tear and an ipsilateral cartilaginous defect in the TF compartment of the knee, and, not commonly known, an association between a meniscal tear and an ipsilateral cartilaginous defect in the PF compartment of the knee. Lastly, it demonstrates that cartilaginous defects and BME medialize or lateralize in the PF or TF compartments of the knee (Fig. 1). One explanation for the finding of medialization or lateralization of the PF and TF compartments of the knee may be due to a disturbance of load transmission through the knee joint. In a longitudinal study by Sharma et al. [8], patients with varus alignment were at high risk of medial progression of knee OA, while limbs with valgus alignment were equally at risk of lateral progression. The accepted mechanism for the effect of malalignment is that increased stress on one side of a joint leads to cartilage loss [6]. Elahi et al. [9] found an association between varus and valgus malalignment and PF OA on radiographs. Valgus malalignment leads to an increase in the force on the lateral patellar facet and is associated with lateral OA of the PF compartment. Similarly, varus malalignment leads to an increase in the force on the medial patellar facet and is associated with medial OA of the PF compartment. Medial TF cartilaginous defects are associated

with varus malalignment of the knee and therefore increase the force on the medial patellar facet associated with medial OA of the medial PF compartment. Similarly cartilaginous lesions in the lateral TF compartment increase the risk of OA of the lateral PF compartment. The association between a meniscal tear and cartilaginous defects on the ipsilateral side of the TF compartment of the knee has been described previously [15–17]. Articular cartilage defects in the TF compartment can occur secondary to meniscal tears and it is believed that treatment of meniscal tears can prevent progression of articular cartilage damage. In these studies cartilaginous defects associated with ipsilateral tears of the meniscus were assessed in the TF compartment but not in the PF compartment. In the present study an association was shown between meniscal tears and ipsilateral cartilaginous defects not only in the TF compartment, but also in the PF compartment of the knee. Two possible explanations are suggested for the association between ipsilateral cartilaginous lesions in the PF compartment and meniscal tears. Firstly, it may be due to a disturbance of load transmission through the knee joint: valgus malalignment owing to lateral meniscal tears leading to an increase in the load on the lateral patellar facet and resulting in lateral OA of the PF compartment. Varus malalignment due to medial meniscal tears would lead to an increase in the force on the medial patellar facet and medial OA of the PF compartment. Secondly, lateral meniscal tears may lead to lateral TF cartilaginous defects. These, in combination with a lateral meniscal tear, may lead to valgus malalignment. Valgus malalignment resulting in an increase in the force on the lateral patellar facet is thus associated with lateral OA of the PF compartment. Similarly, a medial meniscal tear may lead to varus malalignment and an increase in the force on the medial patellar facet associated with medial OA of the PF compartment. The relation between cartilaginous defects in the TF compartment and ipsilateral BME in patients with symptomatic knee OA has been described by Felson et al. [6]. In that study a relationship was found between BME lesions in subarticular bone and ipsilateral radiographic progression. Radiographic progression was defined as increases in medial or lateral joint space narrowing at follow-up. Medial BME lesions were related to medial progression and lateral lesions to lateral progression. It was concluded that BME is a potent risk factor for structural deterioration in knee OA, and that its relation to progression is explained in part by its association with limb alignment. In that study cartilaginous defects associated with ipsilateral BME were assessed in the TF compartment by radiographs but not in the PF compartment. In the present study not only was an association found between cartilaginous defects and ipsilateral BME lesions in the TF compartment, but also in the PF compartment of the knee. A limitation of this study is that limb malalignment was not assessed radiographically. Limb malalignment has been reported to be a potent risk factor for structural progression of OA [8]. However, the purpose of the present study was to investigate the distribution of OA defects seen on MR images of the knee and weight-bearing, dynamic imaging was not available in our research institute. Another limitation of this study is that it is a cross-

sectional study; thus, a longitudinal evaluation of these associations was not possible. For example, it remains unknown whether BME occurred before or after an ipsilateral cartilaginous defect. Another limitation of this study is that we did not use recently improved cartilage imaging sequences, such as steady-state free-precession sequences [3, 18, 19]. Therefore, we might have underestimated the presence of small focal cartilage defects [20]. By design, only patients with mild OA were included in the present study; hence, it is not known if the same findings also apply for a patient population with severe OA. It is possible that the medialization and lateralization of OA defects demonstrated in the present study in patients with mild OA of the knee would be obscured in patients with severe OA of the knee. In conclusion, osteoarthritic defects are shown to lateralize or medialize in the PF and TF compartments of the knee in a subset of patients with generalized OA. Thus, this study supports the concept that a specific compartment of a joint may be susceptible to the development of OA owing to local mechanical and biochemical factors.

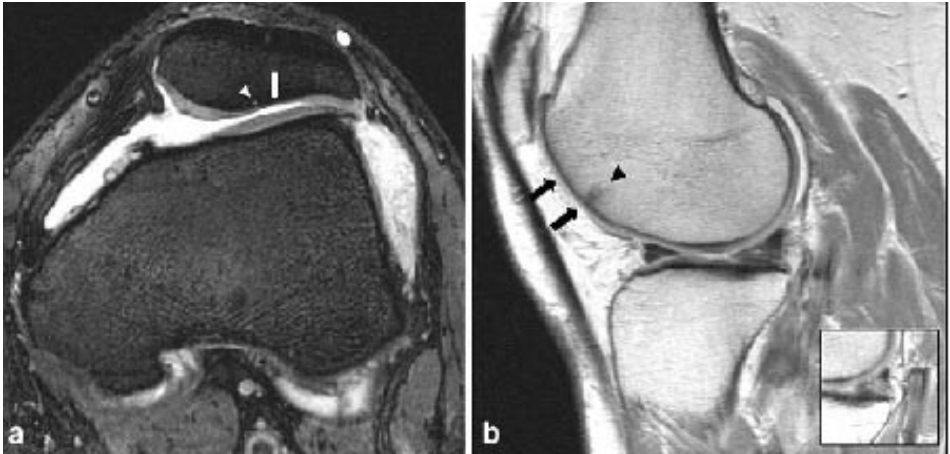


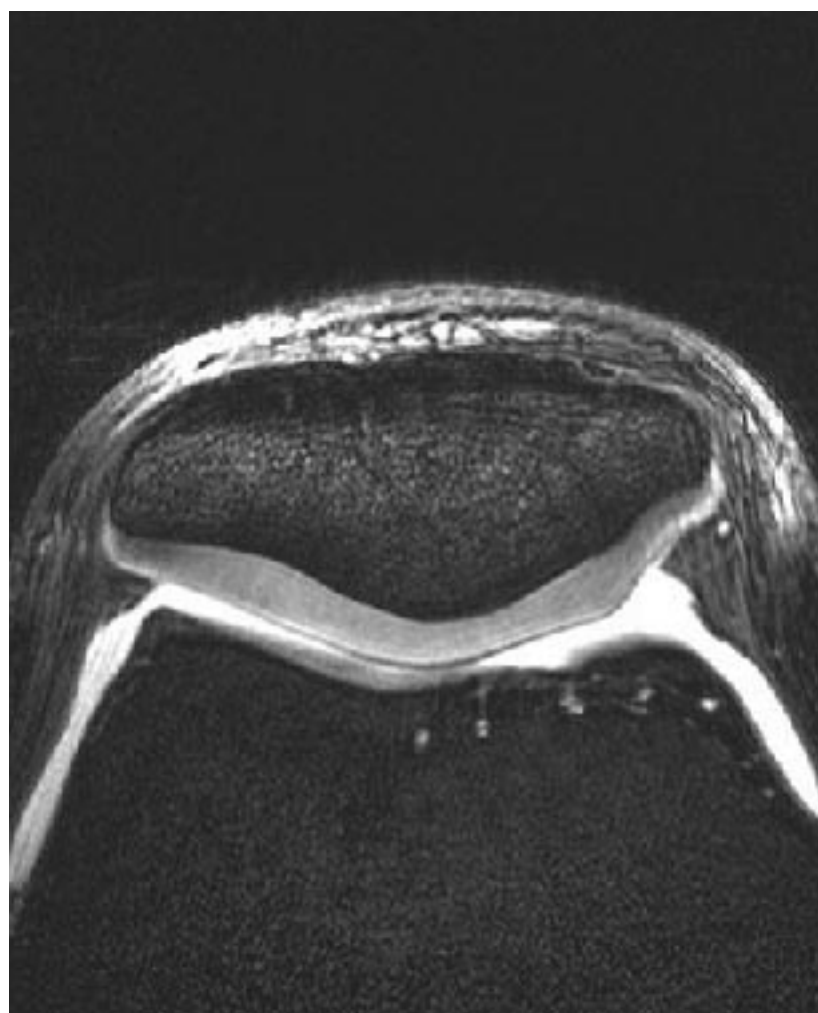
Figure 1 Images of the same patient. Lateralization of defects. a Axial water-selective steadystate free-precession image. Patellar cartilage thinning at the lateral facet of the patella (white arrow) with a small focal subchondral high signal intensity lesion (white arrowhead). b Sagittal proton-densityweighted images. Cartilage thinning (black arrows) and bone marrow edema (black arrowhead) at the lateral facet of the trochlear groove. A meniscal tear in the posterior horn of the lateral meniscus is best seen in the next slice (inset).

Acknowledgements

Pfizer, Groton, CT, USA, provided generous support for this work. The authors would like to acknowledge the support of the cooperating hospitals and the referring rheumatologists, orthopedic surgeons and general practitioners in our region.

References

1. Harris ED Jr (2001) The bone and joint decade: a catalyst for progress. *Arthritis Rheum* 44(9):1969–1970
2. Riyazi N, Meulenbelt I, Kroon HM et al (2004) Evidence for familial aggregation of hand, hip and spine osteoarthritis (OA) but not knee OA in siblings with OA at multiple sites: the GARP study. *Ann Rheum Dis* Sep 30 (Epub ahead of print) PMID:15458958
3. Gold GE, McCauley TR, Gray ML, Disler DG (2003) What's new in cartilage? *Radiographics* 23(5):1227–1242
4. Guermazi A, Zaim S, Taouli B et al (2003) MR findings in knee osteoarthritis. *Eur Radiol* 13(6):1370–1386
5. Vincken PW, ter Braak BP, van Erkel AR et al (2002) Effectiveness of MR imaging in selection of patients for arthroscopy of the knee. *Radiology* 223 (3):739–746
6. Felson DT, McLaughlin S, Goggins J et al (2003) Bone marrow edema and its relation to progression of knee osteoarthritis. *Ann Intern Med* 139 (5 Pt 1):330–336
7. Sharma L, Lou C, Felson DT et al (1999) Laxity in healthy and osteoarthritic knees. *Arthritis Rheum* 42 (5):861–870
8. Sharma L, Song J, Felson DT et al (2001) The role of knee alignment in disease progression and functional decline in knee osteoarthritis. *JAMA* 286(2):188–195
9. Elahi S, Cahue S, Felson DT et al (2000) The association between varus–valgus alignment and patellofemoral osteoarthritis. *Arthritis Rheum* 43 (8):1874–1880
10. Kellgren JH, Lawrence RC (1957) Radiographic assessment of osteoarthritis. *Ann Rheum Dis* 16:494–502
11. Kornaat PR, Ceulemans RY, Kroon HM et al (2004) MRI assessment of knee osteoarthritis: Knee Osteoarthritis Scoring System (KOSS)—inter-observer and intra-observer reproducibility of a compartment-based scoring system. *Skeletal Radiol* Oct 8 (Epub ahead of print) PMID:15480649
12. Yulish BS, Montanez J, Goodfellow DB et al (1987) Chondromalacia patellae: assessment with MR imaging. *Radiology* 164(3):763–766
13. Mink JH, Deutsch AL (1989) Occult cartilage and bone injuries of the knee: detection, classification, and assessment with MR imaging. *Radiology* 170 (3 Pt 1):823–829
14. Stoller DW, Martin C, Crues JV III et al (1987) Meniscal tears: pathologic correlation with MR imaging. *Radiology* 163(3):731–735
15. Dandy DJ, Jackson RW (1975) Meniscectomy and chondromalacia of the femoral condyle. *J Bone Joint Surg Am* 57(8):1116–1119
16. Lewandrowski KU, Muller J, Schollmeier G (1997) Concomitant meniscal and articular cartilage lesions in the femorotibial joint. *Am J Sports Med* 25(4):486–494
17. Roos H, Lauren M, Adalberth T et al (1998) Knee osteoarthritis after meniscectomy: prevalence of radiographic changes after twenty-one years, compared with matched controls. *Arthritis Rheum* 41(4):687–693
18. Hargreaves BA, Gold GE, Beaulieu CF et al (2003) Comparison of new sequences for high-resolution cartilage imaging. *Magn Reson Med* 49 (4):700–709
19. Mohr A, Priebe M, Taouli B et al (2003) Selective water excitation for faster MR imaging of articular cartilage defects: initial clinical results. *Eur Radiol* 13(4):686–689
20. Kornaat PR, Doornbos J, van der Molen AJ et al (2004) Magnetic resonance imaging of knee cartilage using a water selective balanced steady-state free precession sequence. *J Magn Reson Imaging* 20(5):850–856



8

Chapter 8

Magnetic resonance imaging in knees of patients with osteoarthritis at multiple sites: association with clinical findings

Peter R Kornaat
Johan L Bloem
Ruth YT Ceulemans
Naghmeh Riyazi
Frits R Rosendaal
Rob G Nelissen
Wayne O Carter
Marie-Pierre Helio Le Graverand
Margreet Kloppenburg

Abstract

Purpose

To evaluate prospectively in patients with osteoarthritis (OA) the association between clinical features and structural abnormalities found at magnetic resonance (MR) imaging of their knees.

Materials and Methods

The study has been approved by our institution's medical ethical review board. Written informed consent was obtained from each patient prior to the study. MR images of the knee were obtained from 205 (20% (42/205) males, aged 47-77 years; mean age 60 years) of 210 patients who had been diagnosed with symptomatic OA at multiple joint sites. MR images were analyzed for various osteoarthritic abnormalities. All patients were interviewed concerning pain and stiffness in the knee to be imaged. Odds ratios (OR) with 99% confidence intervals (CI) were used to associate the different osteoarthritic findings with clinical features.

Results

A large joint effusion was associated with pain (OR: 9.99; CI: 1.28-149) and stiffness (OR: 4.67; CI: 1.26-26.1). The presence of an osteophyte in the patellofemoral compartment (OR: 2.25; CI: 1.06-4.77) was associated with pain. All other imaging findings including focal or diffuse cartilaginous abnormalities, subchondral cysts, bone marrow edema, subluxation of the meniscus, meniscal tears, or Baker's cysts were unassociated with symptoms.

Conclusion

Our study demonstrated that only a few number of associations exist between clinical symptoms and structural findings found on MR images of the knee in patients with OA.

Introduction

Osteoarthritis (OA) of the knee is a major cause of disability among the ageing population of the industrialized world. A major hallmark of OA is cartilage loss. The exact cause of knee pain in patients with OA remains enigmatic because hyaline cartilage does not contain pain fibres and as such cannot be the direct cause of pain in OA. Pain fibres are present in other structures in the knee including the joint capsule, the periosteum, insertional sites of ligaments and muscles, the outer third of the menisci and, possibly, the synovium (1;2) but their role is uncertain. Radiographs remain the usual means of assessing osteoarthritic

changes in the knee and their association with clinical features, such as knee pain. However, the association between osteoarthritic findings on radiographs and clinical features is poor (3). Magnetic resonance (MR) imaging allows another perspective of the structural abnormalities associated with OA and has been associated with clinical features, including knee pain. Reported findings include the association between knee pain and joint effusion and synovial thickening (4), bone marrow edema (5), osteophytes (6;7), minimal cartilage lesions (8), alterations in patellar cartilage volume (9) and periarticular lesions including bursitis and iliotibial band syndrome (10). Controversy remains about the aetiology of knee pain in patients with OA. Prior studies demonstrate a poor association between knee pain and cartilaginous defects, however, other studies demonstrate an association between the two (9). Bone marrow edema has been associated with clinical symptoms in a study by Felson et al. (5) whereas this was not found by Link et al. (8). In most studies, knee pain was associated with only one or a limited number of structural abnormalities, or have been based on small population samples (8). Thus, the purpose of our study was to evaluate prospectively in patients with osteoarthritis (OA) the association between clinical features and structural abnormalities found at magnetic resonance (MR) imaging of their knees.

Patients and methods

Pfizer Inc., Groton, CT, USA provided financial support for this work, however, authors who are not employees for Pfizer Inc. had control of inclusion of all data and information that might present a conflict of interest.

Patients

The present prospective study is part of the ongoing GARP (Genetics, Osteoarthritis and Progression) study (11). The primary goal of the GARP study is the identification of genetic susceptibility determinants to OA and disease progression in patients aged between 40 and 70 years with generalized OA. Patients diagnosed by rheumatologists, orthopaedic surgeons and general practitioners were informed of the ongoing study by mail. Interested probands were sent a mailed questionnaire about demographic data, medical history, symptoms and signs of OA and family history of OA. Subsequently, eligible probands were requested to introduce a sibling "with joint complaints". Between August 2000 and March 2003, 105 sibling pairs, were included in the GARP-MRI study. Probands and siblings were required to have symptomatic OA in at least two or more of the following joints sites: hands, spine (cervical or lumbar), knees or hips. All sibling pairs who fulfilled the criteria were included (210 patients). In this study 35% (71/205) of the patients had symptomatic knee OA, defined as pain or stiffness on most days of the prior month at study entry, and osteophytes on radiographs. Radiographic knee OA, defined as a Kellgren and Lawrence score of greater than grade 1, was diagnosed in 47% (97/205) of the patients (12). As the purpose of the MR study was to assess progression of OA, no images were made of a knee that already had a maximum Kellgren and Lawrence score of

grade 4 (12). MR imaging of the knee was performed successfully in 205 (20% (42/205) males, aged 47-77 years; mean age 60 years) of 210 patients. The 210 patients consisted of 105 sibling pairs. Five patients were excluded. The remaining 205 patients consisted of 100 sibling pairs and 5 non-siblings. One patient was excluded due to claustrophobia, another had a large knee that would not fit into the knee-coil, and in three image quality was inadequate due to motion artefacts. Written informed consent was obtained from each patient prior to the study. The study has been approved by our institution's medical ethical review board.

Clinical assessment

All patients were interviewed and underwent a physical examination by a medical doctor (NR) with 3 years of experience. Questions concerning the presence of knee pain and knee stiffness were answered. There was a single question in the questionnaire regarding these findings: do you have knee pain and knee stiffness on most days of the prior month (yes/no). Some patients had hip OA as well as knee OA. Referred pain from the ipsilateral hip may have been a confounder for pain in the knee, however, hip OA occurred in only 14 out of the 205 patients (7%).

MR acquisition

Knees were imaged using a transmit-receive 4-channel knee coil in a 1.5 T superconducting magnet (Philips Medical Systems, Best, the Netherlands). Each examination consisted of: coronal intermediate weighted and T2-weighted dual spin echo (SE) images (with repetition time (TR) of 2200; echo time (TE) of 20/80; Number of Signal Averages (NSA) 2; 5 mm slice thickness; 0.5 mm intersection gap; 160 mm field of view; 256 acquisition matrix, 18 slices); sagittal intermediate weighted and T2-weighted dual SE images (TR 2200; TE 20/80; NSA 2; 4 mm slice thickness; 0.4 mm intersection gap; 160 mm field of view; 256 acquisition matrix, 20 slices); sagittal 3D T1-weighted spoiled gradient echo (GE) frequency selective fat suppressed images (TR 46; TE 2.5; NSA 1; flip angle 40°; 3.0 mm slice thickness; slice overlap 1.5 mm; no gap; 180 mm field of view; 256 acquisition matrix, 80 slices); and axial intermediate weighted and T2-weighted turbo spin echo (TSE) fat suppressed images (TR 2500; TE 7.1/40; NSA 2; 2 mm slice thickness; no gap; 180 mm field of view; 256 acquisition matrix, 62 slices). Total acquisition time (including the initial survey sequence) was 30 minutes.

MR interpretation

All MR images were analyzed by means of consensus between three readers (PK, RC, JB) with 3, 15, 25 years of experience, using a comprehensive score form (13). During the assessment, the readers were blinded to radiographic results, patients symptoms and patient age. Cartilaginous defects, osteophytes, subchondral cysts and bone marrow edema were assigned to any one or more of the following anatomic locations: the crista patellae, medial or lateral patellar facets, the medial or lateral trochlear articular facets, the medial or lateral femoral condyles, the

medial or lateral tibial plateaux. The medial and lateral menisci were reviewed for the presence of tears and extrusion from the joint line (subluxation). Joint effusion, synovitis and Baker's cysts were noted.

Cartilaginous defects were graded as diffuse, or focal cartilaginous. Both coronal and sagittal SE images and sagittal GE images were used to assess the tibiofemoral cartilage. Axial turbo SE images and sagittal GE and SE images were used to assess patellofemoral cartilage. The surface extent of a diffuse or focal cartilage defect was estimated by its maximal diameter and graded as follows: grade 0, absent; grade 1, minimal (<5mm); grade 2, moderate (5-10mm); grade 3, severe (>10mm). The depth of a cartilaginous defect was graded using a modification of the Yulish classification (14): grade 0, absent (no abnormality in signal intensity or morphology); grade 1, less than 50% reduction of cartilage thickness; grade 2, 50% or greater reduction of cartilage thickness; grade 3, full thickness or near full thickness cartilage defect.

Osteophytes were defined as focal bony excrescences, seen on axial, sagittal or coronal images, extending from a cortical surface. Osteophytes were further specified as being marginal, intercondylar or central in location. A central osteophyte arose from the subchondral bone plate and was surrounded, but not necessarily covered by articular cartilage. Osteophytes were graded using the following scale: grade 0, absent; grade 1, minimal (<3mm); grade 2, moderate (3-5mm); grade 3, severe (>5mm). Size was measured from the base to the tip of the osteophyte (15). A marginal osteophyte was counted in each compartment (except at the crista patellae). Intercondylar osteophytes were counted at the medial and lateral femoral condyle. Thus, a maximum of 10 marginal and intercondylar osteophytes combined could be counted. A central osteophyte was counted in each compartment: a maximum of 9 central osteophytes could be scored.

Subchondral cysts were defined as well-defined foci of high signal intensity on T2-weighted images, in the cancellous bone underlying the joint cartilage. Their greatest dimension was measured and they were graded as follows: grade 0, absent; grade 1, minimal (<3mm); grade 2, moderate (3-5mm); grade 3, severe (>5mm).

Bone marrow edema was defined as an ill-defined area of increased signal intensity on T2 weighted GE images in the subchondral cancellous bone, extending away from the articular surface over a variable distance, or at places where traction edema occurs (16). The lesions were graded as follows: grade 0, absent; grade 1, minimal (diameter <5mm); grade 2, moderate (diameter 5mm-2cm); grade 3, severe (diameter >2cm).

A meniscal tear was defined as a region of intermediate signal intensity on intermediate-weighted images within the meniscus, communicating with its superior or inferior surface or inner margin, on more than one slice

Meniscal subluxation was defined as protrusion over the edge of the tibial plateau on coronal intermediate-weighted images and was graded as follows: grade 0, absent; grade 1, minimal (<1/3 width of the meniscus bulging); grade 2, moderate

(1/3-2/3 meniscal width involved); grade 3, severe (>2/3 meniscal width involved). Presence of a knee joint effusion was evaluated on T2-weighted coronal, sagittal and axial sequences. A small, physiological sliver of synovial fluid was not recorded. A small effusion was present when a small amount of fluid distended one or two of the joint recesses, moderate effusion when more than two joint recesses were partially distended, and massive when there was full distension of all the joint recesses. Joint recesses evaluated are the lateral-, medial- and suprapatellar recesses.

A Baker's cyst, or a distended gastrocnemial-semimembranosal bursa was diagnosed when a circumscribed mass with intermediate signal intensity on intermediate-weighted and high signal intensity on T2-weighted dual SE sequences was observed, originating from the posteromedial tibiofemoral joint space, extending between the tendons of the medial head of the gastrocnemius and the semimembranosus and dissecting either caudally, cranially or both. Bursal distension was classified as minimal, moderate or severe.

Statistical Analysis

In the cross-sectional analyses, odds ratios with 99% confidence intervals (CI) were used to associate the presence or absence of pain and stiffness with the presence or absence of the various osteoarthritic abnormalities. Since multiple test were performed a $p\text{-value} \leq 0.01$ was considered significant. Because sibling pairs were included in the study, Spearman rank correlation coefficients were used to exclude a potential family effect between the sibling pairs. The Spearman rank correlation coefficient was 0.058 ($p=0.57$) for pain and 0.16 ($p=0.12$) for stiffness. Spearman rank correlation coefficient ranged from -0.09 to 0.35 for the different imaging parameters. Since the Spearman rank correlation coefficient showed that the clinical findings and imaging parameters were not associated between the sibpairs, they were considered as independent patients (PK, MK, FR). Logistic regression analysis was used to adjust for intra-family effect and for the most important risk factors of OA: age, sex, and body mass index (BMI). Stata software version 7.0 (Stata College Station, TX) was used for this purpose.

Results

The overall characteristics of the patients were similar in both groups (table 1). The frequency distribution of osteoarthritic lesions in the studied population showed that cartilage defects and osteophytes were the lesions seen most commonly on MR images of the knee (table 2). Cartilage defects: no association was found between any of the cartilage defects and pain or stiffness (table 3). Neither did we find an association between the sub-group of grade 2 cartilage defects and pain (OR: 1.88; CI: 0.50-7.06; $p=0.22$) or stiffness (OR: 2.06; CI: 0.57-7.43; $p=0.14$). Osteophytes: the presence of osteophyte in the entire knee did not associate with either of the two clinical features of pain and stiffness. However,

the presence of an osteophyte in the patellofemoral compartment associated with pain only (OR: 2.25; CI: 1.06-4.77; $p=0.005$). No association between the grade of an osteophyte and knee pain (OR: 1.70; CI: 0.52-5.50; $p=0.25$) or stiffness (OR: 1.60; CI: 0.52-4.91; $p=0.28$) was found. The number of osteophytes (any grade), however, associated with pain when there were more than four osteophytes in the entire knee (OR: 2.80; CI: 1.28-6.12; $p=0.001$). An association was found between central osteophytes and stiffness in the knee (OR: 2.25; CI: 0.93-5.41; $p=0.016$), however, the p -value did not reach significance. No association between central osteophytes and knee pain was found (OR: 1.65; CI: 0.67-4.10; $p=0.15$). Bone marrow edema: bone marrow edema was not associated with pain or stiffness, in particular no association was found between the grade (grade 2 and 3) of bone marrow edema and knee pain (OR: 1.13; CI: 0.41-3.11; $p=0.76$) or stiffness (OR: 1.30; CI: 0.48-3.55; $p=0.50$). Sixty-four out of 121 patients (53%) with knee pain had bone marrow edema in the entire knee and 38 out of 84 patients (45%) without knee pain had bone marrow edema in the entire knee. Menisci: similarly, no association was found between meniscal defects and pain or stiffness and, in particular no association was found between lesions of the medial (OR: 1.47; CI: 0.71-3.08; $p=0.44$) and lateral menisci (OR: 0.96; CI: 0.46-2.00; $p=0.88$) with knee pain. Effusion: an association was found between moderate and massive effusion (grade 2 and 3) and knee pain (OR: 9.99; CI: 1.28-149; $p=0.008$), and between moderate to severe effusion (grade 2 and 3) and stiffness (OR: 4.67; CI: 1.26-26.1; $p=0.01$) (Figure 1). Baker's cyst: the presence of a Bakers cysts did not associate with clinical findings. Neither did we find an association between severe (grade 2 and 3) Bakers cysts and pain (OR: 1.90; CI: 0.56-6.40; $p=0.17$) and stiffness (OR: 1.88; CI: 0.61-5.76; $p=0.14$). Odds ratios and confidence intervals did not change essentially when adjusting for intra-family effect and for the most important risk factors of OA: age, sex, and BMI.

Table 1. Characteristics of population studied (patients with symptomatic OA at multiple joints) (n = 205)

	Range	Median
Age (years)	43 - 77	60
Weight (kg)	54 - 116	74
Height (cm)	152 - 191	169
Body Mass Index	20 - 40	26
		n
Gender (female)		163 (80)*
Knee pain (yes)		121 (59)*
Knee stiffness (yes)		97 (47)*
Knee osteoarthritis ** (yes)		71 (35)*
Radiographic knee osteoarthritis *** (yes)		97 (47)*

Table 1. Characteristics of population studied (patients with symptomatic OA at multiple joints) (n = 205)

* % in brackets

** Defined as pain or stiffness on most days of the prior month with osteophytes on radiographs

*** Defined by a Kellgren and Lawrence score > 1

Table 2a. Frequency distribution of osteoarthritic abnormalities seen on MR images in studied population. Number of patients with osteoarthritic abnormalities in the knee per group

	Patients
Diffuse and focal cartilage defects	175 (85)*
Diffuse cartilage defects	167 (81)*
Focal cartilage defects	75 (37)*
Osteophytes	174 (85)*
Central osteophytes	47 (23)*
Subchondral cysts	89 (43)*
Bone Marrow Edema (BME)	102 (50)*
BME grade 2 and 3	36 (18)*
Meniscal Tears	138 (67)*
(Sub) Luxation of the meniscus	74 (36)*
Effusion	112 (55)*
Effusion grade 2 and 3	15 (7)*
Bakers cysts	96 (47)*

Table 2a. Frequency distribution of osteoarthritic abnormalities seen on MR images in studied population. Number of patients with osteoarthritic abnormalities in the knee per group

* % in brackets.

Table 2. Frequency distribution of abnormal findings per patient for each category of abnormalities

	Median	Min	Max
Diffuse and focal cartilage defects	3	0	18
Diffuse cartilage defects	3	0	9
Focal cartilage defects	0	0	9
Osteophytes	4	0	10
Central osteophytes	0	0	9
Subchondral cysts	0	0	9
Bone Marrow Edema	0	0	9
Meniscal Tears	1	0	6
(Sub) Luxation of the meniscus	0	0	2
Effusion	0	0	1
Bakers cysts	0	0	1

Table 2. Frequency distribution of abnormal findings per patient for each category of abnormalities

Max = maximum amount of lesions that can be scored per patient
Min = minimum amount of lesions that can be scored per patient

Table 3. Association of basic MR imaging findings and clinical findings in 205 patients

MR Imaging finding	Clinical findings					
	Pain			Stiffness		
	p-value	OR	99% CI	p-value	OR	99% CI
Cartilage defects	0.78	1.12	(0.40-3.14)	0.45	1.35	(0.48-3.82)
Focal defects only	0.83	1.07	(0.50-2.28)	0.51	1.21	(0.57-2.56)
Diffuse defects only	0.11	1.79	(0.70-4.55)	0.19	1.61	(0.62-4.20)
In PF compartment	0.21	1.52	(0.64-3.61)	0.35	1.37	(0.57-3.26)
In TF compartment	0.20	1.47	(0.68-3.17)	0.11	1.62	(0.75-3.50)
Osteophytes	0.91	1.05	(0.38-2.91)	0.36	1.44	(0.52-4.04)
Central osteophytes	0.15	1.65	(0.67-4.10)	0.02	2.25	(0.93-5.41)
In PF compartment	0.00	2.25	(1.06-4.77)†	0.03	1.83	(0.88-3.81)
In TF compartment	0.64	1.19	(0.46-3.09)	0.97	0.99	(0.38-2.56)
Subchondral cysts	0.06	1.71	(0.81-3.63)	0.44	1.25	(0.60-2.59)
In PF compartment	0.06	1.83	(0.80-4.16)	0.92	1.03	(0.47-2.25)
In TF compartment	0.72	1.14	(0.44-2.92)	0.08	1.88	(0.74-4.77)
BME	0.28	1.36	(0.65-2.84)	0.11	1.57	(0.76-3.25)
In PF compartment	0.35	1.31	(0.62-2.79)	0.48	1.22	(0.58-2.56)
In TF compartment	0.36	1.38	(0.55-3.48)	0.08	1.83	(0.75-4.47)
Meniscal tear	0.44	1.26	(0.58-2.74)	0.14	0.64	(0.30-1.39)
(Sub) Luxation of the meniscus	0.92	1.03	(0.48-2.21)	0.10	1.63	(0.76-3.46)

Effusion grade 2 and 3	0.01	9.99	(1.13-149)†	0.01	4.67	(1.11-26.14)†
Baker cysts	0.07	1.68	(0.80-3.53)	0.32	1.32	(0.64-2.73)

Table 3. Association of basic MR imaging findings and clinical findings in 205 patients
MR = Magnetic Resonance; OR = Odds Ratio; CI = Confidence Interval; † = $p \leq 0.01$

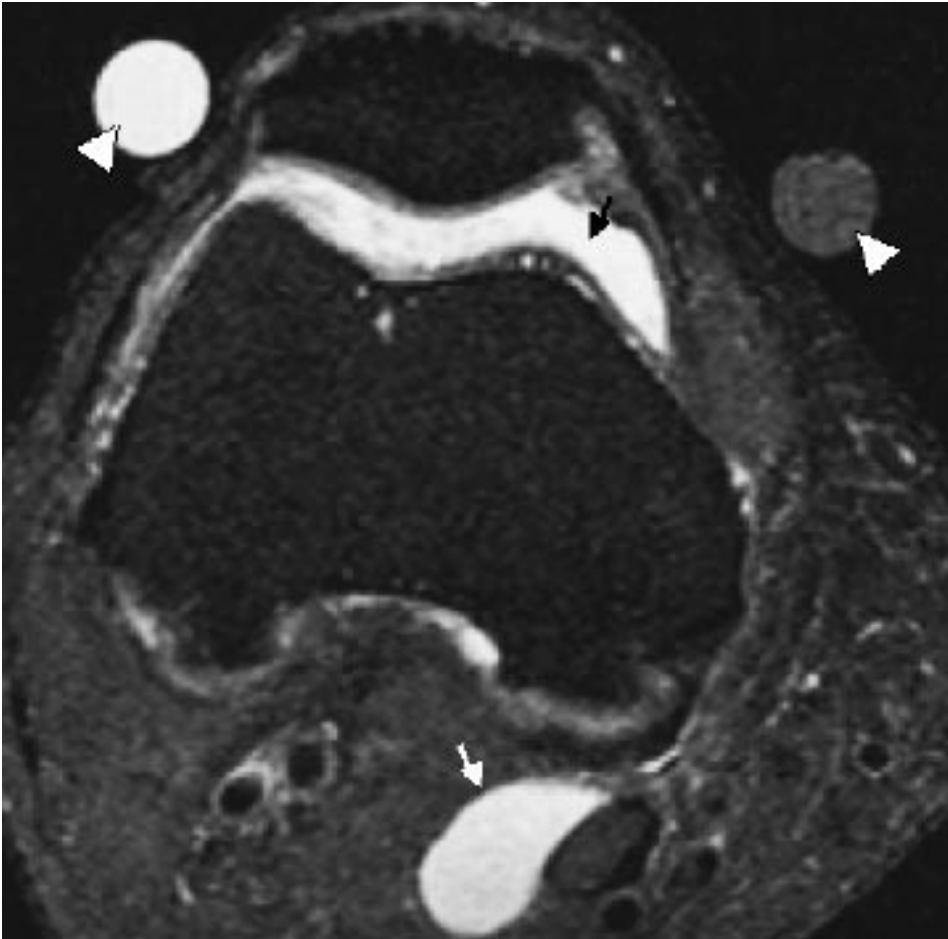


Figure 1. Transverse T2-weighted (2500/40) MR image shows a moderate joint effusion (black arrow) associated with pain and stiffness of the knee. Please note the presence of a Baker's cyst (white arrow) and the presence of an external marker (white arrowhead).

Discussion

Although different grades and types of structural abnormality in the various anatomical compartments of the knee were comprehensively analyzed, and associated with pertinent clinical features, a remarkably small number of associations were found between the findings on MR images and knee pain or stiffness. An association between osteophytes and knee pain was found only when

an osteophyte was located in the patellofemoral compartment or when more than four (median) osteophytes anywhere in the knee were present. Boegard et al. reported an association between osteophytes at the inferior pole of the patella and knee pain (7). The same authors found also an association between knee pain and osteophytes at the medial tibial plateau (6). The frequency of central osteophytes in our study was 23% (47/205 patients) and, in concordance with literature (15), almost all central osteophytes (20/23 osteophytes) were associated with a full thickness cartilage defect. A association between central osteophytes and knee stiffness was suggested ($p = 0.02$), but central osteophytes were not associated with knee pain. These findings were described also in the study by Link et al. where an association between central osteophytes and knee stiffness, but not knee pain, was found (8). We did not find in our study an association between the presence, severity or frequency of bone marrow edema and pain or stiffness of the knee. These findings are supported by studies from Link et al. (8) and Sowers et al. (17), but are in contrast to results published by Felson et al. (5). In the latter study it was concluded that bone marrow edema on MRI was strongly associated with the presence of pain in knee OA. Felson et al. reported on 401 patients with radiographically diagnosed OA. Seventy eight percent of 351 patients with knee pain had bone marrow edema whereas only 30% of 50 patients without knee pain had bone marrow edema. In our study 64 out of 121 patients (53%) with knee pain had bone marrow edema in the entire knee and 38 out of 84 patients (45%) without knee pain had bone marrow edema in the entire knee. These numbers show a clear disparity in prevalence of bone marrow edema in the different populations. In the present study, patients with moderate (Kellgren and Lawrence score <4) OA as well as patients with no radiographic knee OA (but OA in hands, spine or hips) were included, whereas in the study by Felson and colleagues patients with more severe radiographic OA (Kellgren and Lawrence grade 2-4) were included. Another association found between structural abnormalities seen on MR of the knee and clinical features was that between grade 2 and 3 (moderate and massive) joint effusion and knee pain or knee stiffness. In the literature a controversy exists about the association between joint effusion and knee pain. Hill et al. found that moderate and severe effusions (grade 2 and 3) were significantly more common among those with knee pain compared to those without in patients with knee OA (4). But Link et al. reported no significant association between the presence or the amount of joint effusion and clinical features. They did, however, find a trend toward higher pain scores in patients with joint effusion (8). An explanation for the association between pain and joint effusion is given in different studies by the suggestion that capsular distention is the cause of knee pain (4;18;19). No association was found between number and grades of cartilage defects with clinical features. As anticipated, this conforms to literature (8) since hyaline cartilage does not contain pain fibers and thus cartilage cannot be the direct cause of pain in OA (1). In a study by Link et al. (8) most symptoms were found in patients with grade IIa ($<50\%$ cartilage loss) cartilage lesions. They hypothesized that clinical symptoms are most substantial at

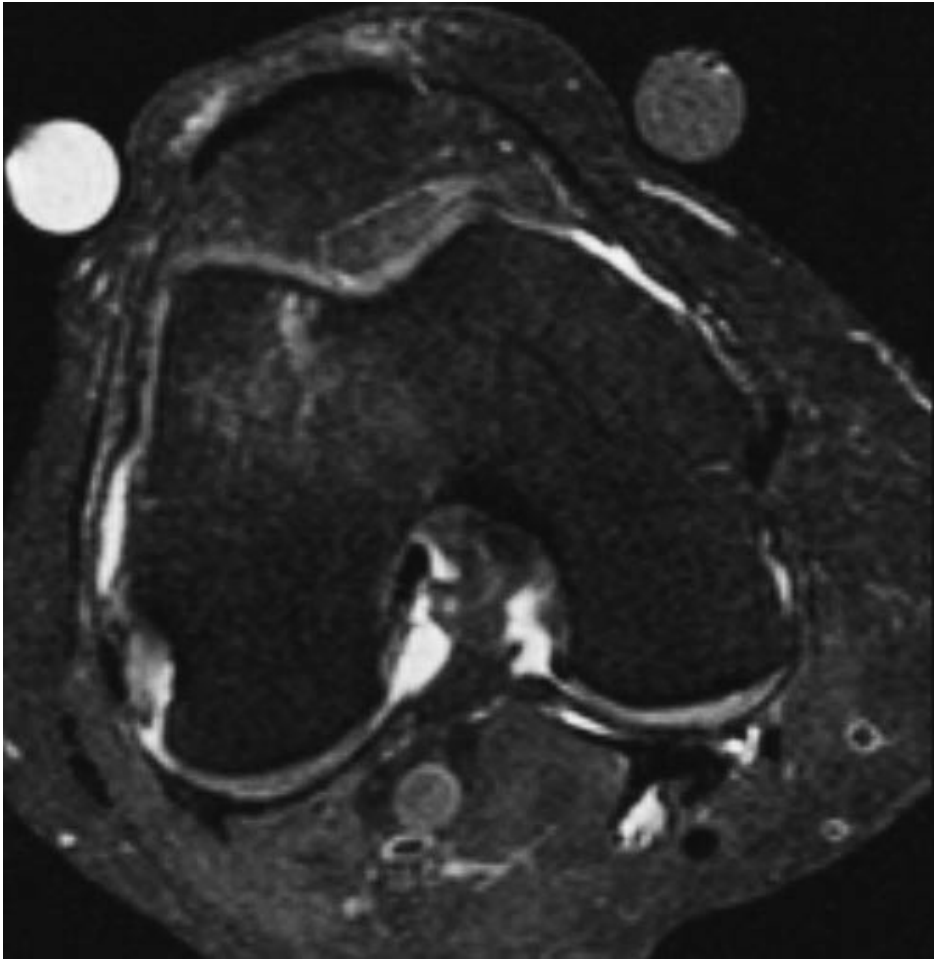
the onset of OA, when cartilage defects occur. In that study they found that when cartilage damage progressed (grade 3 cartilage defects), a trend toward less pain and stiffness was shown, which may potentially be explained by the knee becoming more accustomed to the cartilage damage. These results could not be confirmed in the present study as no difference was found between grade 0 and grade 2 (>50% cartilage loss - full thickness cartilage loss) cartilage defects. No association was found between meniscal tears in patients with OA and clinical features. This is supported by other studies which have reported that patients with or without a meniscal tear do not have significantly different levels of pain and disability (8;20). Neither was an association found between the presence or grade of a Baker's cysts and clinical features. This too has been reported popliteal cysts being as common in patients with knee pain as in those without (4). Our study examined a broad spectrum of structural abnormalities found on MR imaging of the knee with clinical features in a large, unique, study population. Unique because the population is based on siblings and not all patients included did have knee OA. The fact that patients were family related may have introduced an artefact. However, Spearman rank coefficients showed no family related correlation of the most important parameters such as pain and stiffness. A limitation of the study is the lack of a reference standard such as arthroscopy. However, MR sequences have been successfully used to evaluate cartilage and non-cartilaginous joint structures (21-24) with accuracies for cartilage imaging of more than 90% (25;26). Another limitation is that the recently improved cartilage imaging sequences such as steady-state free precession sequences were not used (27-29). Thus, the presence of small focal cartilage defects might have been underestimated. A further limitation is that some patients had hip OA as well as knee OA. Although referred pain from the hip may have been a confounder, hip OA occurred in only 14 out of the 205 patients (7%). Lastly, we did not correct for the presence of intrasubstance degeneration of the meniscus when meniscal tears were associated with clinical features. Intra substance degeneration of the meniscus might be associated with knee pain (30). In conclusion, this study demonstrates only a few number of associations between structural abnormalities found on MR images of the knee and clinical features in patients with OA. Moderate and massive joint effusion was associated with both knee pain and knee stiffness. The presence of a patellofemoral osteophyte and the presence of >4 osteophytes in the entire knee did associate with knee pain only. Focal or diffuse cartilaginous abnormalities, subchondral cysts, bone marrow edema, subluxation of the meniscus, meniscal tears, or Baker's cysts are not associated with pain and stiffness.

References

1. Heppelmann B. Anatomy and histology of joint innervation. *J Peripher Nerv Syst* 1997; 2(1):5-16.
2. Dye SF, Vaupel GL, Dye CC. Conscious neurosensory mapping of the internal structures of the human knee without intraarticular anesthesia. *Am J Sports Med* 1998; 26(6):773-777.
3. Lawrence JS, Bremner JM, Bier F. Osteo-arthritis. Prevalence in the population and relationship between symptoms and x-ray changes. *Ann Rheum Dis* 1966; 25(1):1-24.

4. Hill CL, Gale DG, Chaisson CE, Skinner K, Kazis L, Gale ME et al. Knee effusions, popliteal cysts, and synovial thickening: association with knee pain in osteoarthritis. *J Rheumatol* 2001; 28(6):1330-1337.
5. Felson DT, Chaisson CE, Hill CL, Totterman SM, Gale ME, Skinner KM et al. The association of bone marrow lesions with pain in knee osteoarthritis. *Ann Intern Med* 2001; 134(7):541-549.
6. Boegard T, Rudling O, Petersson IF, Jonsson K. Correlation between radiographically diagnosed osteophytes and magnetic resonance detected cartilage defects in the tibiofemoral joint. *Ann Rheum Dis* 1998; 57(7):401-407.
7. Boegard T, Rudling O, Petersson IF, Jonsson K. Correlation between radiographically diagnosed osteophytes and magnetic resonance detected cartilage defects in the patellofemoral joint. *Ann Rheum Dis* 1998; 57(7):395-400.
8. Link TM, Steinbach LS, Ghosh S, Ries M, Lu Y, Lane N et al. Osteoarthritis: MR imaging findings in different stages of disease and correlation with clinical findings. *Radiology* 2003; 226(2):373-381.
9. Hunter DJ, March L, Sambrook PN. The association of cartilage volume with knee pain. *Osteoarthritis Cartilage* 2003; 11(10):725-729.
10. Hill CL, Gale DR, Chaisson CE, Skinner K, Kazis L, Gale ME et al. Periarticular lesions detected on magnetic resonance imaging: prevalence in knees with and without symptoms. *Arthritis Rheum* 2003; 48(10):2836-2844.
11. Riyazi N, Meulenbelt I, Kroon HM, Runday KH, Hellio Le Graverand MP, Rosendaal FR et al. Evidence for familial aggregation of hand, hip, and spine but not knee osteoarthritis in siblings with multiple joint involvement: the GARP study. *Ann Rheum Dis* 2005; 64(3):438-443.
12. Kellgren JH, Lawrence RC. Radiographic assessment of osteoarthritis. *Ann Rheum Dis* 1957; 16:494-502.
13. Kornaat PR, Ceulemans RY, Kroon HM, Riyazi N, Kloppenburg M, Carter WO et al. MRI assessment of knee osteoarthritis: Knee Osteoarthritis Scoring System (KOSS)-inter-observer and intra-observer reproducibility of a compartment-based scoring system. *Skeletal Radiol* 2005; 34(2):95-102.
14. Yulish BS, Montanez J, Goodfellow DB, Bryan PJ, Mulopulos GP, Modic MT. Chondromalacia patellae: assessment with MR imaging. *Radiology* 1987; 164(3):763-766.
15. McCauley TR, Kornaat PR, Jee WH. Central osteophytes in the knee: prevalence and association with cartilage defects on MR imaging. *AJR Am J Roentgenol* 2001; 176(2):359-364.
16. Mink JH, Deutsch AL. Occult cartilage and bone injuries of the knee: detection, classification, and assessment with MR imaging. *Radiology* 1989; 170(3 Pt 1):823-829.
17. Sowers MF, Hayes C, Jamadar D, Capul D, Lachance L, Jannausch M et al. Magnetic resonance-detected subchondral bone marrow and cartilage defect characteristics associated with pain and X-ray-defined knee osteoarthritis. *Osteoarthritis Cartilage* 2003; 11(6):387-393.
18. Creamer P, Hunt M, Dieppe P. Pain mechanisms in osteoarthritis of the knee: effect of intraarticular anesthetic. *J Rheumatol* 1996; 23(6):1031-1036.
19. Likar R, Schafer M, Paulak F, Sittl R, Pipam W, Schalk H et al. Intraarticular morphine analgesia in chronic pain patients with osteoarthritis. *Anesth Analg* 1997; 84(6):1313-1317.
20. Bhattacharyya T, Gale D, Dewire P, Totterman S, Gale ME, McLaughlin S et al. The clinical importance of meniscal tears demonstrated by magnetic resonance imaging in osteoarthritis of the knee. *J Bone Joint Surg Am* 2003; 85-A(1):4-9.
21. Recht M, Bobic V, Burstein D, Disler D, Gold G, Gray M et al. Magnetic resonance imaging of articular cartilage. *Clin Orthop* 2001;(391 Suppl):S379-S396.
22. Peterfy CG. Scratching the surface: articular cartilage disorders in the knee. *Magn Reson Imaging Clin N Am* 2000; 8(2):409-430.
23. Eckstein F, Reiser M, Englmeier KH, Putz R. In vivo morphometry and functional analysis of human articular cartilage with quantitative magnetic resonance imaging—from image to data, from data to theory. *Anat Embryol (Berl)* 2001; 203(3):147-173.
24. Vincken PW, ter Braak BP, van Erkel AR, de Rooy TP, Mallens WM, Post W et al. Effectiveness of MR imaging in selection of patients for arthroscopy of the knee. *Radiology* 2002; 223(3):739-746.

25. Disler DG, McCauley TR, Kelman CG, Fuchs MD, Ratner LM, Wirth CR et al. Fat-suppressed three-dimensional spoiled gradient-echo MR imaging of hyaline cartilage defects in the knee: comparison with standard MR imaging and arthroscopy. *AJR Am J Roentgenol* 1996; 167(1):127-132.
26. Bredella MA, Tirman PF, Peterfy CG, Zarlingo M, Feller JF, Bost FW et al. Accuracy of T2-weighted fast spin-echo MR imaging with fat saturation in detecting cartilage defects in the knee: comparison with arthroscopy in 130 patients. *AJR Am J Roentgenol* 1999; 172(4): 1073-1080.
27. Gold GE, McCauley TR, Gray ML, Disler DG. What's new in cartilage? *Radiographics* 2003; 23(5):1227-1242.
28. Hargreaves BA, Gold GE, Beaulieu CF, Vasanawala SS, Nishimura DG, Pauly JM. Comparison of new sequences for high-resolution cartilage imaging. *Magn Reson Med* 2003; 49(4): 700-709.
29. Kornaat PR, Doornbos J, van der Molen AJ, Kloppenburg M, Nelissen RG, Hogendoorn PC et al. Magnetic resonance imaging of knee cartilage using a water selective balanced steady-state free precession sequence. *J Magn Reson Imaging* 2004; 20(5):850-856.
30. Biedert RM. Treatment of intrasubstance meniscal lesions: a randomized prospective study of four different methods. *Knee Surg Sports Traumatol Arthrosc* 2000; 8(2):104-108.



9

Chapter 9

Bone marrow edema lesions change in volume in the majority of patients with osteoarthritis; association with clinical features

Peter R Kornaat
Margreet Kloppenburg
Ruby Sharma
Stella A Scheepers-Botha
Marie-Pierre Hellio Le Graverand
L Napoleon Coene
Johan L Bloem
Iain Watt

Abstract

Purpose

It has been suggested that bone marrow edema (BME) in the knee is associated with progression of osteoarthritis (OA). The purpose of our study is to evaluate prospectively, in patients with OA, changes of BME over two years and its relationship with clinical features.

Materials and Methods

Our institution's medical ethical review board approved the study. Written informed consent was obtained from each patient prior to the study. Magnetic resonance (MR) images of the knee were obtained from 182 (20% male; aged 43-76 years; mean age 59 years) patients who had been diagnosed with familial symptomatic OA at multiple joint sites. MR images were made at baseline and at 2 years follow-up. MR images were analysed by 2 experienced readers on a validated subjective scoring system for total volume of BME and cysts. Symptoms and function were assessed by the Western Ontario and McMaster Universities Osteoarthritis index (WOMAC) after 2 years. Odds ratios (OR's) with 99% confidence intervals (CI's) and linear mixed models with fixed effects were used to associate BME changes with clinical features.

Results

132 patients (75%) had BME at any point in time. A total of 327 BME lesions were recorded. Total volume of BME changed in 90 patients (66%). Volume changed in 147 BME lesions (45%): there appeared 69 (21%) new lesions, 32 (10%) lesions disappeared, 26 (8%) increased, and 20 (6%) decreased in volume. A total of 222 cysts were documented in 182 patients (55%). Seventy (32%) cystic lesions in 56 patients (30%) changed in size. If a cystic lesion changed in size, it changed in the same way, either an increase or decrease, as did an associated BME lesion (OR: 37; CI: 6-210). Increase or decrease of BME volume, over a 2 year time period were not associated with severity of WOMAC scores.

Conclusion

In patients with OA, BME volume fluctuates in the majority of patients over a 2 year time period. These changes are not associated with severity of WOMAC scores at the study end point.

Introduction

Knee osteoarthritis (OA) is a chronic progressive joint disease, leading to pain and loss of function in a considerable proportion of patients, with great impact and consequences in the ageing population of the industrialized world. Disease markers need to be identified in order to predict and quantify progression. Magnetic resonance (MR) imaging is a promising imaging modality of this entity because of its ability to assess the whole joint in vivo and depict lesions that are associated with OA. One of the possible markers in OA is bone marrow edema (BME). Unfortunately, the role of BME in OA is controversial, as contradictory results have been reported. BME detected with MR imaging has been associated with clinical symptoms in patients with OA (1;2). However, other studies reported no association between BME and clinical symptoms (3-5). Further, the role of BME as a marker for progression of OA is open to discussion. In an study by Felson et al., BME was associated with progression of OA as assessed by joint space narrowing on conventional radiographs (6). On the other hand, in a study by Phan et al., changes in BME did not significantly change with progression of disease assessed by Western Ontario and McMaster Universities Osteoarthritis (WOMAC) scores (4). The purpose of our study is to evaluate prospectively, in patients with OA, changes of BME over two years and its relationship with clinical features.

Patients and methods

Pfizer Inc., Groton, CT, USA provided financial support for this work, however, authors who are not employees for Pfizer Inc. had control of inclusion of all data and information that might present a conflict of interest.

Patients

The present prospective study is part of the ongoing GARP (Genetics, Osteoarthritis and Progression) study (7). The primary goal of the GARP study is the identification of genetic susceptibility determinants to OA and disease progression in middle-aged sib pairs with OA at multiple joint sites. Patients were required to have symptomatic OA in at least two or more of the following joints sites: hands, spine (cervical or lumbar), knees or hips. Complete written informed consent was obtained from each patient prior to the study. Our institution's medical ethical review board has approved the study. MR image sets of the knee were obtained in 182 patients at study entry and after 2 years (5). In this study 39% (71/182) of the patients had symptomatic knee OA in their imaged knee, defined as pain or stiffness on most days in the month prior to study entry, and osteophytes on radiographs. As the purpose of the MR study was to assess progression of OA, no images were made of a knee that already had a maximum Kellgren and Lawrence score of grade 4 (8).

Clinical assessment

Clinical data were assessed by structured questionnaires and all patients were interviewed and underwent a physical examination by a research medical doctor.

The WOMAC was used to assess self-reported pain, stiffness and physical functioning of the imaged knee (9).

MR acquisition

Knees were imaged using a transmit-receive 4-channel knee coil in a 1.5 T superconducting magnet (Philips Medical Systems, Best, the Netherlands). Each examination consisted of: coronal proton density and T2-weighted dual spin echo (SE) images (with repetition time (TR) of 2200; echo time (TE) of 20/80; Number of excitations per data line (NEX) 2; 5 mm slice thickness; 0.5 mm intersection gap; 160 mm field of view; 256x205 acquisition matrix, 18 slices); sagittal proton density and T2-weighted dual SE images (TR 2200; TE 20/80; NEX 2; 4 mm slice thickness; 0.4 mm intersection gap; 160 mm field of view; 256x205 acquisition matrix, 20 slices); sagittal 3D T1-weighted spoiled gradient echo (GE) frequency selective fat suppressed images (TR 46; TE 2.5; NEX 1; flip angle 40°; 3.0 mm slice thickness; slice overlap 1.5 mm; no gap; 180 mm field of view; 256 acquisition matrix, 80 slices); and axial proton density and T2-weighted turbo spin echo (TSE) fat suppressed images (TR 2500; TE 7.1/40; NEX 2; 2 mm slice thickness; no gap; 180 mm field of view; 256 acquisition matrix, 62 slices). Total acquisition time (including the initial survey sequence) was 30 minutes.

MR interpretation

All MR images were analyzed by means of consensus between three readers (RS, PK, IW) with 1, 5, 25 years of experience, using a comprehensive score form (10). During the assessment, the readers were blinded to radiographic results, patient symptoms and patient age. In cases of disagreement between the readers the more conservative, less severe, score was recorded. All MR images were scored in chronological order. BME was assigned to any one or more of the following anatomic locations: the crista patellae, medial or lateral patellar facets, the medial or lateral trochlear articular facets, the medial or lateral femoral condyles, the medial or lateral tibial plateaux.

BME was defined as an ill-defined area of increased signal intensity on T2-weighted images in the subchondral cancellous bone, extending away from the articular surface over a variable distance, or at places where traction edema occurs (11). The lesions were graded as follows: grade 0, absent; grade 1, minimal (diameter <5 mm); grade 2, moderate (diameter 5 mm-2 cm); grade 3, severe (diameter > 2cm). A total BME score of the knee was calculated by adding all grades of each BME lesion in the knee. Maximum possible knee score was 27 (grade 3 times 9 anatomic locations). In the total study a maximum of 1638 BME lesions (182 patients times 9 anatomic locations) could be scored.

Subchondral cysts were defined as well-defined foci of high signal intensity, with low signal intensity margins, on T2-weighted images, in the cancellous bone underlying the joint cartilage. Their greatest dimension was measured and they were graded as follows: grade 0, absent; grade 1, minimal (<3 mm); grade 2, moderate (3-5 mm); grade 3, severe (>5 mm). A total score of the knee was

calculated by adding all grades of each cystic lesion in the knee. Maximum possible knee score was 27 (grade 3 times 9 anatomic locations). In the total study a maximum of 1638 cystic lesions (182 patients times 9 anatomic locations) could be scored.

Statistical Analysis

Odds ratios (OR's) with 99% confidence intervals (CI's) were used to show the association between BME volume changes with cystic volume changes. The difference in WOMAC scores between patients without BME (group A) and patients with BME lesions (group B: unchanged BME lesions over 2 years, group C: increasing volume of BME lesions over 2 years, group D: decreasing volume of BME lesions over 2 years) was calculated by linear mixed models in SPSS for Windows, version 12.0 (SPSS Inc, Chicago, Ill) with a random intercept to adjust for the familial effect within sib pairs. Adjustments were made for age, sex and body mass index (BMI). Estimates of fixed effects were reported with 95% confidence intervals (CI95). The estimates represent the magnitude of the difference in the mean WOMAC score between patients with versus without BME lesions over 2 years (PK,SB).

Results

A total of 182 patients were monitored over a period of 2 years (table 1). Forty-six (25%) patients did not have BME lesions, thus 136 patients (75%) had one or more BME lesions at any time. In 46 (34%) of these patients BME scores did not fluctuate whereas it changed in the other 90 (66%) patients: The total BME score per individual patient increased in 54 (40%) patients. It decreased in 27 patients (20%), and total BME score remained unchanged in nine (7%) patients. Individual BME scores did change in this last group without resulting in a change of the total BME score. A total of 327 BME lesions were detected from a possible total of 1638 lesions (table 2). One hundred forty seven (45%) BME lesions changed: 69 new lesions appeared on the second MR (21%), 26 (8%) increased, 20 (6%) decreased in volume, and 32 (10%) were no longer visible on the second MR scan (Figure 1). Note that more lesions appeared or increased than decreased or disappeared. One hundred (55%) patients had one or more cystic lesions at any time. In 44 (44%) of these patients, total cystic score did not fluctuate over time, whereas in the other 56 (56%) patients the total cystic score did change in size. In 36 of these 56 patients (64%) the cystic score increased, it decreased in 18 patients (32%), and the total cystic score remained unchanged irrespective of changes on the level of individual cysts in two patients (4%). A total of 222 cystic lesions were detected from a possible total of 1638 sites (table 2). Seventy cystic lesions (32%) changed: 32 new cysts appeared on the second MR (46%), 14 (20%) increased, six (8%) decreased in volume, and 18 (26%) were no longer visible on the second MR. Cystic and BME lesions were both present in the same anatomic location (associated lesions) in 191 cases. A change of BME or cystic lesions was associated with a change in volume of an adjacent cystic or BME lesion (OR: 6.2; 3.2-12.3).

In 47 cases both BME lesions and cystic lesions changed. When cystic and BME lesions were both present in the same anatomic location, volume changes (increase or decrease) were in same direction (OR: 37; CI: 6-210) (table 2). Onehundredfiftyseven (86%) patients completed a WOMAC questionnaire of the imaged knee at two years. The WOMAC pain and functions scores for patients without and with BME lesions over 2 years are shown in figure 2a and 2b respectively. The mean WOMAC scores did not differ between the different patient groups; even when BME lesions completely disappeared, lower WOMAC scores were not recorded. The mean difference in WOMAC pain scores between patients with unchanged BME lesions, with increasing BME lesions and with decreasing BME lesions compared to patients without BME were 2 (95CI -8 to 12), 2 (95CI -8 to 11) and 1 (95CI -11 to 12) respectively (Figure 2a). The mean difference in WOMAC function scores between patients with unchanged BME lesions, with increasing BME lesions and with decreasing BME lesions compared to patients without BME were -2 (95CI -12 to 8), -4 (95CI -13 to 6) and -4 (95CI -15 to 8) respectively (Figure 2b).

Table 1. Patient characteristics (n=182)

	At baseline	
Age years, median (range)	59	(43 - 76)
Female sex, (%)	157	(80%)
Body mass index (kg/m ²), median (range)	25.7	(20.2 - 40.0)
Symptomatic knee OA, No. (%)*	71	(39%)
Kellgren & Lawrence Score 0 / 1 / 2 / 3 / 4, No.	65 / 61 / 67 / 12 / 0	
	Over 2 years	
Bone marrow edema, No. (%)**	128	(70%)
Grade 0 / 1 / 2 / 3 ***	54 / 56 / 62 / 10	
Cysts, No. (%)**	100	(55%)
Grade 0 / 1 / 2 / 3 ***	82 / 60 / 37 / 3	
	At 2 Years	
WOMAC Pain scores, median (range)****	13	(0 - 99)
WOMAC Stiffness scores, median (range)****	18	(0 - 99)
WOMAC Function scores, median (range)****	14	(0 - 98)

Table 1. Patient characteristics (n=182)

WOMAC = Western Ontario and McMaster Universities Osteoarthritis index; OA = osteoarthritis

* defined as pain or stiffness on most days of the month prior to study entry, in combination with osteophytes on radiographs

** during 2 years

*** maximal grade per patient

**** n = 157

Table 2. Cystic and BME lesions in 9 anatomic locations per patient changing over 2 years in 182 patients (n=1638)

Bone marrow edema						
		No BME	No change	Increase	Decrease	Total
Cysts	No cyst	1280	77	38	21	1416
	No change	24	87	24	17	152
	Increase	2	11	30	3	46
	Decrease	5	5	3	11	24
	Totals	1311	180	95	52	1638

Table 2. Cystic and BME lesions in 9 anatomic locations per patient changing over 2 years in 182 patients (n=1638)

BME = Bone marrow edema

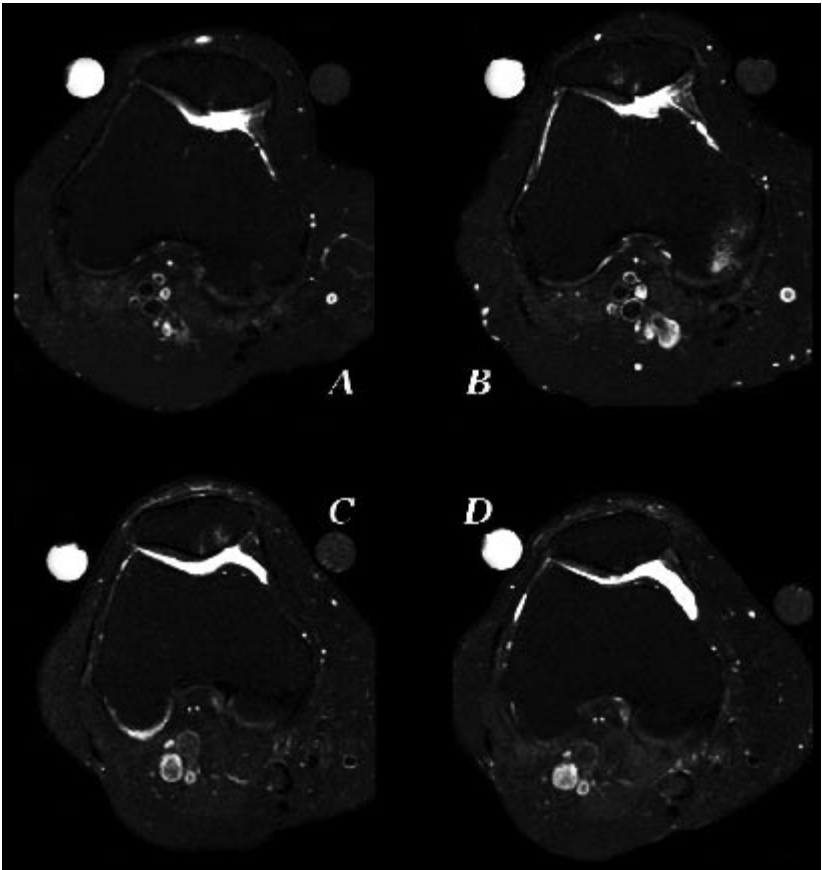


Figure 1. Axial T2-weighted turbo spin echo fat suppressed images. Increase (A= at baseline, B= after two years) in volume of bone marrow edema over 2 years at the crista patella and at the medial femoral condyle. Decrease (C= at baseline, D= after two years) in volume of bone marrow edema over 2 years at the crista and medial part of the patella.

Figure 2a

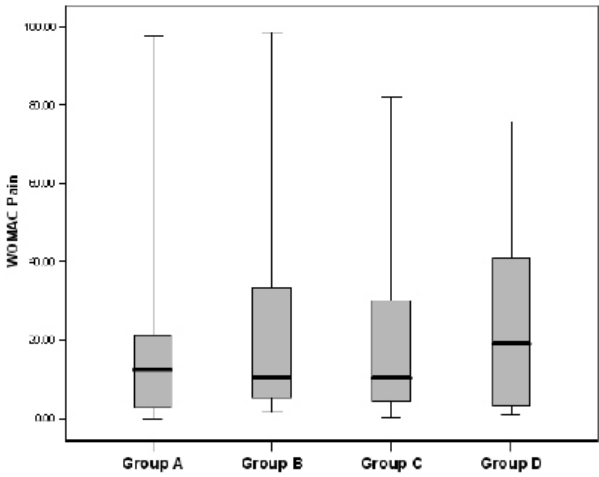


Figure 2a. Association between Western Ontario and McMaster Universities Osteoarthritis pain scores and bone marrow edema. Group A: patients with no bone marrow edema; group B: patients in whom bone marrow edema lesions did not change over 2 years; group C: patients in whom bone marrow edema lesions increased in volume over 2 years; group D: patients in whom bone marrow edema lesions decreased in volume over 2 years. Boxplots show the median, interquartile range, minimum and maximum values.

Figure 2b

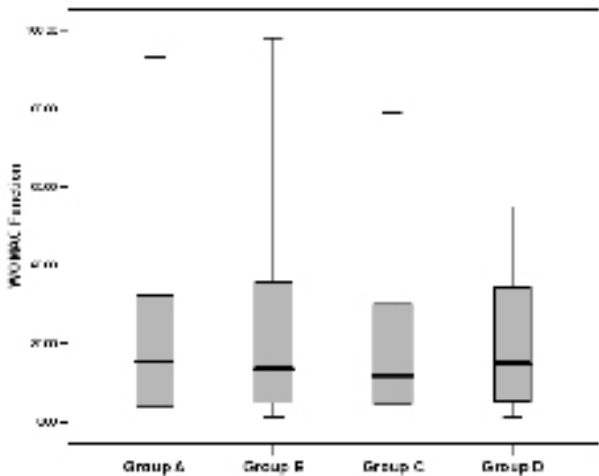


Figure 2b. Association between Western Ontario and McMaster Universities Osteoarthritis function scores and bone marrow edema. Group A: patients with no bone marrow edema; group B: patients in whom bone marrow edema lesions did not change over 2 years; group C: patients in whom bone marrow edema lesions increased in volume over 2 years; group D: patients in whom bone marrow edema lesions decreased in volume over 2 years. Boxplots show the median, interquartile range, minimum and maximum values.

Discussion

The majority (75%) of patients with familial OA at multiple sites have BME lesions visualized when two sequential MR scans are made with a two year time interval. In the majority (66%) of these patients with BME lesions, the total volume of BME changed over this two year time period. Our study demonstrates also that cysts and BME fluctuations are associated. However, no association existed between changes in BME and severity of WOMAC scores after 2 years.

The finding, that BME lesions fluctuate in 66% of the patients, indicates that BME is part of a dynamic process in OA. BME is not a constant finding, as opposed to hyaline cartilage loss for example. Thus, it is important to realize that the finding of BME lesions in patients with OA represents only a single snapshot in time. This versatility of BME has been noted before (4). It is also interesting and important to see that 10% of BME areas disappear completely. This is particularly noteworthy if BME is an inclusion criterion, or outcome parameter, or surrogate endpoint in drug trials or clinical outcome studies.

The second finding of the present study is when cysts and BME are in close proximity; the direction in which they change is identical. This is an interesting finding as the role of cysts in OA is unclear. Their exact pathophysiology is uncertain, as is their prognostic significance. A recent study by Carrino et al. also showed a change in cyst size was always accompanied by a change in edema-like signal size (12). That study also showed subchondral cysts develop in pre-existing regions of subchondral bone marrow edema-like signal.

The third finding is that changes in BME are not predictive of severity of WOMAC scores. Patients in which BME increased do not have a higher WOMAC score, than patients with a decrease in BME volume. Even when BME completely disappeared, lower WOMAC scores were not recorded. Previous work has demonstrated that pain, assessed by WOMAC scores, was not related significantly to changes in BME (4). However, in the study by Felson et al., BME is associated with progressive radiographic knee OA and pain (1;6). Cross sectional associations between BME and clinical findings are controversial (1-5). Hence, a lack of clarity about the relationship between changes in BME and WOMAC scores is not surprising. Phan et al have suggested that the complexity of pain physiology and the difficulty of pain evaluation, as well as the fact that patients experience pain differently, may explain these findings (4). Another important factor might be the stage of OA in the patients being studied. Pain might for instance be associated with BME in a more developed stage of the disease and less so earlier on. OA in the population of Felson (1) has more advanced knee OA than the GARP population (7) as the population of Felson did consist of knee OA patients only, whereas the GARP population consists of patients with familial OA at multiple sites. A considerable proportion of patients in the present study did not have symptomatic radiographic knee OA of the imaged knee, and consequently average WOMAC scores in the present population were low (table 1). Nevertheless, associations between BME and clinical findings are controversial and BME may ultimately be excluded as a factor in pain sensation.

The present study has a number of limitations. Firstly, not all the patients that had a complete MRI follow up filled out the WOMAC signal knee score forms. Secondly, the fact that these patients were first-degree relatives may have introduced an artefact. However, a linear regression, with robust standard errors that clustered on pairs, excluded this possibility. Thirdly, although referred pain from the hip may have been a confounder, hip OA occurred in only 7% of the patients and was not thought a contributory factor. In conclusion, in patients with knee OA, BME is shown to be a versatile parameter over time that is not predictive of pain.

References

1. Felson DT, Chaisson CE, Hill CL, Totterman SM, Gale ME, Skinner KM et al. The association of bone marrow lesions with pain in knee osteoarthritis. *Ann Intern Med* 2001; 134(7): 541-549.
2. Cicuttini F, Wluka A, Hankin J, Wang Y. Longitudinal study of the relationship between knee angle and tibiofemoral cartilage volume in subjects with knee osteoarthritis. *Rheumatology (Oxford)* 2004; 43(3):321-324.
3. Link TM, Steinbach LS, Ghosh S, Ries M, Lu Y, Lane N et al. Osteoarthritis: MR imaging findings in different stages of disease and correlation with clinical findings. *Radiology* 2003; 226(2):373-381.
4. Phan CM, Link TM, Blumenkrantz G, Dunn TC, Ries MD, Steinbach LS et al. MR imaging findings in the follow-up of patients with different stages of knee osteoarthritis and the correlation with clinical symptoms. *Eur Radiol* 2005;1-11.
5. Kornaat PR, Bloem JL, Ceulemans RYT, Riyazi N, Rosendaal FR, Nelissen RG et al. The association between clinical features and magnetic resonance imaging findings of the knee in patients with osteoarthritis. *Radiology* 2006; 239(3):811-817.
6. Felson DT, McLaughlin S, Goggins J, LaValley MP, Gale ME, Totterman S et al. Bone marrow edema and its relation to progression of knee osteoarthritis. *Ann Intern Med* 2003; 139 (5 Pt 1):330-336.
7. Riyazi N, Meulenbelt I, Kroon HM, Runday KH, Hellio le Graverand MP, Rosendaal FR et al. Evidence for familial aggregation of hand, hip, and spine but not knee osteoarthritis in siblings with multiple joint involvement: the GARP study. *Ann Rheum Dis* 2005; 64(3):438-443.
8. Kellgren JH, Lawrence RC. Radiographic assessment of osteoarthritis. *Ann Rheum Dis* 1957; 16:494-502.
9. Bellamy N, Buchanan WW, Goldsmith CH, Campbell J, Stitt LW. Validation study of WOMAC: a health status instrument for measuring clinically important patient relevant outcomes to antirheumatic drug therapy in patients with osteoarthritis of the hip or knee. *J Rheumatol* 1988; 15(12):1833-1840.
10. Kornaat PR, Ceulemans RY, Kroon HM, Riyazi N, Kloppenburg M, Carter WO et al. MRI assessment of knee osteoarthritis: Knee Osteoarthritis Scoring System (KOSS)-inter-observer and intra-observer reproducibility of a compartment-based scoring system. *Skeletal Radiol* 2005; 34(2):95-102.
11. Mink JH, Deutsch AL. Occult cartilage and bone injuries of the knee: detection, classification, and assessment with MR imaging. *Radiology* 1989; 170(3 Pt 1):823-829.
12. Carrino JA, Blum J, Parellada JA, Schweitzer ME, Morrison WB. MRI of bone marrow edema-like signal in the pathogenesis of subchondral cysts. *Osteoarthritis Cartilage* 2006.



10

Chapter 10

Summary and General Conclusion
Samenvatting en Algemene Conclusie
Curriculum Vitae

Summary

Chapter 1 provides a general introduction to the thesis. The purpose of the thesis is to explore and optimize a scoring form and also MR imaging techniques to acquire potentially important data from patients with OA of the knee and to investigate a possible association between these data and clinical findings in patients with OA of the knee. Ultimate goal of the efforts made, is to find any possible progressors for OA.

In Chapter 2 a scoring system for quantifying osteoarthritic changes of the knee, as identified by MR imaging, as well as its inter- and intra-observer reproducibility was developed in order to monitor medical therapy in research studies. Two independent observers evaluated 25 consecutive MR examinations of the knee in patients with previously defined clinical symptoms and radiological signs of osteoarthritis. Images were scored for the presence of cartilaginous lesions, osteophytes, subchondral cysts, bone marrow edema, and for meniscal abnormalities. Presence and size of effusion, synovitis and Baker's cyst were recorded. All parameters were ranked on a previously defined, semiquantitative scale, reflecting increasing severity of findings. Kappa, weighted kappa and intraclass correlation coefficient (ICC) were used to determine inter- and intra-observer variability. Inter-observer reproducibility was good (ICC value 0.77). Inter- and intra-observer reproducibility for individual parameters was good to very good. It was concluded that the presented comprehensive MR scoring system for osteoarthritic changes of the knee has a good to very good inter-observer and intra-observer reproducibility. Thus the score form with its definitions can be used for standardized assessment of osteoarthritic changes to monitor medical therapy in research studies.

In Chapter 3 an optimized water selective balanced steady-state free precession sequence (WS-bSSFP) was compared with conventional MR sequences in imaging cartilage of osteoarthritic knees. Flip angles of sagittal and axial WS-bSSFP sequences were optimized in three volunteers. Subsequently, the knees of 10 patients with generalized osteoarthritis were imaged using sagittal and axial WS-bSSFP and conventional MR imaging techniques. Contrast-to-noise ratios (CNR) between cartilage and its surrounding tissues was calculated to quantitatively analyze the various sequences. Using dedicated software the accuracy of cartilage volume measurements with anatomic sections of the tibial plateau was assessed. CNR efficiency between cartilage and its surrounding tissue using WS-bSSFP was maximal with a 20-25 degrees flip angle. A WS-bSSFP sequence is superior to conventional MR imaging sequences in imaging cartilage of the knee in patients with osteoarthritis.

In Chapter 4 SPGR and SSFP sequences were compared regarding optimal imaging of articular cartilage at 1.5T and 3.0T. Articular cartilage signal-to-noise ratio (SNR), CNR, and thickness measurements on a 1.5T and a 3.0T MR scanner

were compared using three-dimensional spoiled gradient recalled echo (3D-SPGR) and two 3D steady-state free precession (SSFP) sequences. Both knees of five volunteers were scanned at 1.5 T and at 3.0 T using a transmit-receive quadrature extremity coil. Each examination consisted of a sagittal 3D-SPGR sequence, a sagittal fat suppressed 3D-SSFP (FS-SSFP) sequence, and a sagittal Dixon 3D-SSFP sequence. For quantitative analysis, we compared cartilage SNR and CNR efficiencies, as well as average cartilage thickness measurements. For 3D-SPGR, cartilage SNR efficiencies at 3.0T increased compared to those at 1.5T by a factor of 1.83 (range: 1.40-2.09). In comparison to 3D-SPGR, the SNR efficiency of FS-SSFP increased by a factor of 2.13 (range: 1.81-2.39) and for Dixon SSFP by a factor of 2.39 (range: 1.95-2.99). For 3D-SPGR, CNR efficiencies between cartilage and its surrounding tissue increased compared to those at 1.5 T by a factor of 2.12 (range: 1.75-2.47), for FS-SSFP by a factor 2.11 (range: 1.58-2.80) and for Dixon SSFP by a factor 2.39 (range 2.09-2.83). Average cartilage thicknesses of load bearing regions were not different at both field strengths or between sequences ($P>0.05$). Mean average cartilage thickness measured in all knees was 2.28 mm. It was concluded that articular cartilage imaging of the knee on a 3.0 T MR scanner shows increased SNR and CNR efficiencies compared to a 1.5 T scanner, where SSFP-based techniques show the highest increase in SNR and CNR efficiency. There was no difference between average cartilage thickness measurements performed at the 1.5 T and 3.0 T scanners or between the three different sequences.

Chapter 5 investigates the comparability of two OA surrogate endpoints, average cartilage thickness and cartilage volume, acquired from healthy volunteers on two 3.0T MR imaging systems from different manufacturers. Ten knees of five healthy volunteers were scanned on a 3.0T General Electric (GE) and a 3.0T Philips scanner using a fast three-dimensional fatsuppressed spoiled gradient (SPGR) imaging sequence. The acquisition parameters were optimized beforehand and were kept as comparable as possible on both scanners. For quantitative analysis, the average cartilage thickness and volume of the load-bearing regions of the femoral condyles were compared. Data were analyzed using a univariate repeated-measures analysis of variance (ANOVA) to examine the effects of position, condyle, and imaging system on the measurements. The average cartilage thickness and volume of the load-bearing regions of the femoral condyles did not differ between the two different 3.0T MRI systems. There was no significant effect of position or condyle on the average cartilage thickness measurements. It was concluded that two OA surrogate endpoints, average cartilage thickness and cartilage volume, acquired on two 3.0T MR imaging systems from different manufacturers are comparable.

In Chapter 6 the prevalence and location of central osteophytes in patients referred for MR imaging of the knee and the relationship of central osteophytes to other derangements as seen on MR imaging was determined. Two hundred

consecutive patients referred for MR imaging of the knee were evaluated for central osteophytes, articular cartilage defects, marginal osteophytes, meniscal tears, and anterior cruciate ligament tears. A 1.5-T scanner was used, and assessments were made by consensus of two experienced musculoskeletal radiologists. Seven patients were excluded, leaving 193 patients in the study population. The prevalence of central osteophytes in the knee was 15% (35 central osteophytes in 29 patients). Patients with central osteophytes were older (mean age, 52 years versus 38 years), weighed more (mean weight, 92 kg versus 78 kg), had more articular cartilage defects (mean, 4.3 versus 1.3), and had more marginal osteophytes (mean, 3.9 versus 1.1) than patients without central osteophytes. Patients with central osteophytes were more likely to have a meniscal tear, but they were not more likely to have an anterior cruciate ligament tear. All central osteophytes were associated with articular cartilage defects at the same location, which were full or near-full thickness on MR imaging for 32 of 35 central osteophytes. It was concluded that central osteophytes are common in patients referred for MR imaging of the knee. When central osteophytes are seen in the knee there is a high likelihood of an associated full thickness or near-full thickness articular cartilage defect.

In Chapter 7 the relationship between osteoarthritic changes seen on MR images of the patellofemoral (PF) or tibiofemoral (TF) compartments in patients with mild OA of the knee was investigated. MR images of the knee were obtained in 105 sib pairs (210 patients) who had been diagnosed with OA at multiple joints. Entry criteria included that the degree of OA in the knee examined should be between a Kellgren and Lawrence score of 2 or 3. MR images were analyzed for the presence of cartilaginous lesions, bone marrow edema (BME) and meniscal tears. The relationship between findings in the medial and lateral aspects of the PF and TF compartments was examined. The number of cartilaginous defects on either side of the PF compartment correlated positively with number of cartilaginous defects in the ipsilateral TF compartment (odds ratio, OR, 55, confidence interval, CI, 7.8-382). The number of cartilaginous defects in the PF compartment correlated positively with ipsilateral meniscal tears (OR 3.7, CI 1.0-14) and ipsilateral PF BME (OR 17, CI 3.8-72). Cartilaginous defects in the TF compartment correlated positively with ipsilateral meniscal tears (OR 9.8, CI 2.5-38) and ipsilateral TF BME (OR 120, CI 6.5-2,221). Osteoarthritic defects lateralize or medialize in the PF and TF compartments of the knee in patients with mild OA.

Chapter 8 describes prospectively in patients with OA the association between clinical features and structural abnormalities found at MR imaging of their knees. MR images of the knee were obtained from 205 (20% (42/205) males, aged 43-77 years; mean age 60 years) of 210 patients who had been diagnosed with symptomatic OA at multiple joint sites. MR images were analyzed for various osteoarthritic abnormalities. All patients were interviewed concerning pain and stiffness in the knee to be imaged. A large joint effusion was associated with

pain (OR: 9.99; CI: 1.28-149) and stiffness (OR: 4.67; CI: 1.26-26.1). The presence of an osteophyte in the patellofemoral compartment (OR: 2.25; CI: 1.06-4.77) was associated with pain. All other imaging findings including focal or diffuse cartilaginous abnormalities, subchondral cysts, bone marrow edema, subluxation of the meniscus, meniscal tears, or Baker's cysts were unassociated with symptoms. The study demonstrated that only a few number of associations exist between clinical symptoms and structural findings found on MR images of the knee in patients with OA.

It has been suggested that BME in the knee is associated with progression of osteoarthritis. Chapter 9 describes changes of BME over two years, in patients with OA, and its relationship with clinical features. MR images of the knee were obtained from 182 (20% male; aged 43-76 years; mean age 59 years) patients who had been diagnosed with familial symptomatic OA at multiple joint sites. MR images were made at baseline and at 2 years follow-up. MR images were analysed by 2 experienced readers on a validated subjective scoring system for total volume of BME and cysts. Symptoms and function were assessed by the WOMAC after 2 years. OR's with 99% CI's and linear mixed models with fixed effects were used to associate BME changes with clinical features. 132 patients (75%) had BME at any point in time. A total of 327 BME lesions were recorded. Total volume of BME changed in 90 patients (66%). Volume changed in 147 BME lesions (45%): there appeared 69 (21%) new lesions, 32 (10%) lesions disappeared, 26 (8%) increased, and 20 (6%) decreased in volume. A total of 222 cysts were documented in 182 patients (55%). Seventy (32%) cystic lesions in 56 patients (30%) changed in size. If a cystic lesion changed in size, it changed in the same way, either an increase or decrease, as did an associated BME lesion (OR: 37; CI: 6-210). Increase or decrease of BME volume, over a 2 year time period were not associated with severity of WOMAC scores. It was concluded that in patients with OA, BME volume fluctuates in the majority of patients over a 2 year time period. These changes are not associated with severity of WOMAC scores at the study end point.

General conclusion

Starting with the more technical aspect of the thesis, the present thesis describes how to optimize the assessment of osteoarthritis (OA) related morphology and pathology in the knee using magnetic resonance (MR) imaging instead of conventional radiographs. A comprehensive score form, the Knee Osteoarthritis Score System (KOSS), has been developed and validated specifically for the assessment of structures possibly involved in the process of knee OA. Together with another comprehensive knee OA score form, called Whole Organ Magnetic Resonance Imaging score (WORMS), no other forms for this purpose are described in literature (1).

Regarding the investigation, comparison and optimising of state of the art cartilage imaging sequences, basically two types of sequences, relevant for cartilage MR imaging, have been studied. These two types of sequences are conventional Spoiled Gradient (SPGR) and relatively newer Steady State Free Precession (SSFP) type of sequences. As higher field systems, typically 3.0 Tesla (T), have become more prevalent in the clinical setting and longitudinal MR imaging studies are performed on both a 1.5T and 3.0T scanners, both field strengths were studied. The author's general conclusion regarding cartilage imaging sequences used for knee OA studies is to be conservative in using SSFP types of sequences on higher field strengths, typically 3.0T. However, SSFP types of sequences do have advantages over conservative SPGR sequences on lower field strengths (1.5T) regarding cartilage imaging.

Osteoarthritis of the knee is a chronic progressive joint disease leading to pain and loss of function in a considerable proportion of patients with great impact and consequences in the ageing population of the industrialized world (2). Clinical symptoms and radiographs of the knee are normally used to monitor osteoarthritic changes in the knee. However, the correlation between radiographic osteoarthritic findings and clinical features is poor (3). Therefore, various longitudinal MR imaging studies have started to clarify the controversy mentioned. Does MR imaging of the knee tell us more about the relation between osteoarthritic structural findings and clinical features?

According to the present thesis, the answer is "No". Most of the data presented in this thesis is based on a 1.5T longitudinal MR study called the "Genetica, Artrose & Progressie" (GARP) study. In the GARP study MR imaging findings were associated with clinical features of patients with OA, and it was concluded that there were no strong associations between the most important OA imaging findings and clinical features of patients with OA.

These findings contrasted some important publications in literature (4). Especially the fact that there was no association between bone marrow edema (BME) and clinical features is a contrasting finding. Also the finding that changes in BME are not predictive of severity of Western Ontario and McMaster Universities Osteoarthritis (WOMAC) scores is controversial (5). Patients in which BME increased do not have a higher WOMAC score, than patients with a decrease in BME volume. Even when BME completely disappeared, lower WOMAC scores were not recorded. However, in the study by Felson et al., BME is associated with progressive radiographic knee OA and pain (4;6). Cross sectional associations between BME and clinical findings are controversial (4;6-10). Hence, a lack of clarity about the relationship between changes in BME and WOMAC scores is not surprising. Phan et al have suggested that the complexity of pain physiology and the difficulty of pain evaluation, as well as the fact that patients experience pain differently, may explain these findings (9). Another important factor might be the

stage of OA in the patients being studied. Pain might for instance be associated with BME in a more developed stage of the disease and less so earlier on. OA in the population of Felson (4) has more advanced knee OA than the GARP population (11) as the population of Felson did consist of knee OA patients only, whereas the GARP population consists of patients with familial OA at multiple sites. A considerable proportion of patients in the present study did not have symptomatic radiographic knee OA of the imaged knee, and consequently average WOMAC scores in the present population were low. Nevertheless, associations between BME and clinical findings are controversial and BME may ultimately be excluded as a factor in pain sensation.

The finding that BME lesions fluctuate in 66% of the patients, indicates that BME is part of a dynamic process in OA. BME is not a constant finding, as opposed to hyaline cartilage loss for example. Thus, it is important to realize that the finding of BME lesions in patients with OA represents only a single snapshot in time. This versatility of BME has been noted before (9). It is also interesting and important to see that 10% of BME areas disappear completely. This is particularly noteworthy if BME is an inclusion criterion, or outcome parameter, or surrogate endpoint in drug trials or clinical outcome studies.

These controversial findings are important findings with regards to future clinical trials, as it urges conservatism with regards to the idea of BME being an outcome measure for progression of the disease. Therefore, the current theses also strongly recommend a further quest to identify ideal parameters to quantify the progression of the disease.

References

1. Peterfy CG, Guermazi A, Zaim S, Tirman PF, Miaux Y, White D et al. Whole-Organ Magnetic Resonance Imaging Score (WORMS) of the knee in osteoarthritis. *Osteoarthritis Cartilage* 2004; 12(3):177-190
2. Harris ED Jr (2001) The bone and joint decade: a catalyst for progress. *Arthritis Rheum* 44(9):1969-1970
3. Lawrence JS, Bremner JM, Bier F. Osteo-arthritis. Prevalence in the population and relationship between symptoms and x-ray changes. *Ann.Rheum.Dis.* 1966;25(1):1-24.
4. Felson DT, Chaisson CE, Hill CL, Totterman SM, Gale ME, Skinner KM et al. The association of bone marrow lesions with pain in knee osteoarthritis. *Ann.Intern.Med.* 2001;134(7):541-549.
5. Bellamy N, Buchanan WW, Goldsmith CH, Campbell J, Stitt LW. Validation study of WOMAC: a health status instrument for measuring clinically important patient relevant outcomes to antirheumatic drug therapy in patients with osteoarthritis of the hip or knee. *J Rheumatol* 1988; 15(12):1833-1840.
6. Felson DT, McLaughlin S, Goggins J, LaValley MP, Gale ME, Totterman S et al. Bone marrow edema and its relation to progression of knee osteoarthritis. *Ann Intern Med* 2003; 139(5 Pt 1):330-336.
7. Cicuttini F, Wluka A, Hankin J, Wang Y. Longitudinal study of the relationship between knee angle and tibiofemoral cartilage volume in subjects with knee osteoarthritis. *Rheumatology (Oxford)* 2004; 43(3):321-324.

8. Link TM, Steinbach LS, Ghosh S, Ries M, Lu Y, Lane N et al. Osteoarthritis: MR imaging findings in different stages of disease and correlation with clinical findings. *Radiology* 2003; 226(2):373-381.
9. Phan CM, Link TM, Blumenkrantz G, Dunn TC, Ries MD, Steinbach LS et al. MR imaging findings in the follow-up of patients with different stages of knee osteoarthritis and the correlation with clinical symptoms. *Eur Radiol* 2005;1-11.
10. Hill CL, Gale DG, Chaisson CE, Skinner K, Kazis L, Gale ME et al. Knee effusions, popliteal cysts, and synovial thickening: association with knee pain in osteoarthritis. *J.Rheumatol.* 2001;28(6):1330-7.
11. Riyazi N, Meulenbelt I, Kroon HM, Runday KH, Hellio le Graverand MP, Rosendaal FR et al. Evidence for familial aggregation of hand, hip, and spine but not knee osteoarthritis in siblings with multiple joint involvement: the GARP study. *Ann Rheum Dis* 2005; 64(3):438-443.

Samenvatting

Hoofdstuk 1 geeft een algemene introductie op dit proefschrift. Het belangrijkste doel van het promotieonderzoek is het ontwikkelen en optimaliseren van een scoreformulier en MR imaging technieken om data van patiënten met OA te verzamelen, en deze data vervolgens te associëren met klinische klachten van de patiënten. Het uiteindelijk doel is om OA voorspellende afwijkingen te kunnen identificeren.

In Hoofdstuk 2 wordt aangegeven hoe een scoreformulier ontwikkeld werd om aan artrose gerelateerde veranderingen in de knie, geobserveerd met MRI, te kunnen kwantificeren. Ook werd de "inter-" en "intra-observer" reproduceerbaarheid van het scoreformulier vastgesteld. Het scoreformulier werd met name ontworpen om in een onderzoeksomgeving medische onderzoeken te kunnen monitoren. Twee onafhankelijke waarnemers bekeken 25 aaneengesloten MRI onderzoeken van de knie van patiënten met artrose. De MRI's werden beoordeeld op de aanwezigheid van kraakbeendefecten, osteophyten, cysteuze afwijkingen, beenmergoedeem, afwijkingen aan de meniscus, vocht in het gewricht, synovitis en Bakerse cysten. Alle afwijkingen werden vastgelegd op een van tevoren vastgestelde semi-kwantitatieve schaal. Kappa's, gewogen kappa's en intraclass correlation coefficienten (ICC's) werden uitgerekend om de "inter-" en "intra observer" reproduceerbaarheid te kwantificeren. Deze reproduceerbaarheid was goed (ICC van 0.77). Uit het onderzoek werd geconcludeerd dat het uitgebreide scoreformulier voor het scoren van aan artrose gerelateerde veranderingen een goede "inter-" en "intra-observer" reproduceerbaarheid heeft en dus gebruikt kan worden voor gestandaardiseerd beoordelen van aan artrose gerelateerde veranderingen. Dit om medische therapie in onderzoeksverband te kunnen monitoren.

In Hoofdstuk 3 wordt een "water selective balanced steady-state free precession (WS-bSSFP)" sequentie vergeleken met conventionele MRI sequenties met betrekking tot het afbeelden van kraakbeen in knieën van patiënten met artrose. "Flip angles" van sagitale en transversale WS-bSSFP sequenties werden bij drie vrijwilligers geoptimaliseerd. Vervolgens werden in 10 knieën van patiënten met gegeneraliseerde artrose sagitale en transversale WS-bSSFP opnamen alsook conventionele opnamen vervaardigd. Contrastuis verhoudingen tussen kraakbeenen het omliggende weefsel werden bepaald om de sequenties onderling te kunnen vergelijken. Met behulp van toegespitste software en anatomische plakken van de tibia werd de nauwkeurigheid met betrekking tot het meten van kraakbeenvolumes bepaald. De contrastuis verhouding tussen kraakbeen en het omliggende weefsel, gemeten met de WS-bSSFP sequentie was maximaal in het geval van een "flip angle" van 20-25 graden. Tevens werd geconcludeerd dat WS-bSSFP sequenties superieur zijn ten opzichte van conventionele sequenties met betrekking tot het afbeelden van kraakbeen in de knie van patiënten met artrose.

In Hoofdstuk 4 worden “three-dimensional spoiled gradient recalled echo (3D-SPGR)” en “3D steady-state free precession (SSFP)” sequenties op 1.5T en 3.0T MRI scanners met elkaar vergeleken met betrekking tot het optimaal afbeelden van kraakbeen. Kraakbeen signaalruis verhouding, contrastruis verhouding en kraakbeen diktemetingen op 1.5T en 3.0T MRI scanners werden gebruikt om 3D-SPGR en twee SSFP sequenties met elkaar te vergelijken. Beide knieën van 5 vrijwilligers werden gescand met een “transmit-receive quadrature extremity coil” op een 1.5T en een 3.0T MRI scanner. Elk onderzoek bestond uit een 3D SPGR, een 3D-SSFP en een Dixon 3D-SSFP sequentie in de sagitale richting. Kraakbeen signaalruisverhouding, contrastruisverhoudingen kraakbeendiktemeting werden gebruikt om de verschillende sequenties kwantitatief te vergelijken. Kraakbeen signaalruis verhouding op 3.0T nam toe met een factor 1.83 (spreiding: 1.40-2.09) voor de 3D-SPGR sequentie. De signaalruis verhouding van FS-SSFP sequenties nam toe met een factor 2.13 (spreiding: 1.81-2.39) en met een factor 2.39 (spreiding: 2.09-2.83) voor de Dixon SSFP sequentie. De contrastruis verhouding tussen kraakbeen en het omringende weefsel nam bij de 3.0T MRI scanner toe ten opzichte van de 1.5T scanner met een factor 2.12 (spreiding: 1.75-2.47) voor de 3D-SPGR sequentie, met een factor 2.11 (spreiding: 1.58-2.80) voor de FS-SSFP sequentie en met een factor 2.39 (spreiding: 2.09-2.83) voor de Dixon SSFP sequentie. De gemiddelde kraakbeendikte op het gewicht dragende gedeelte van het kraakbeen verschilde niet tussen de verschillende sequenties of bij de verschillende veldsterktes ($P > 0.05$). De gemiddelde kraakbeendikte van alle knieën was 2.28 mm. Geconcludeerd werd dat wat betreft het afbeelden van kraakbeen in de knie op een 3.0T MRI scanner een toename van signaalruis alsook contrastruis verhoudingen optrad in vergelijking met een 1.5T scanner, met name voor wat betreft de SSFP sequenties. Tevens werd geconcludeerd dat er geen verschil gemeten werd tussen de verschillende sequenties of verschillende veldsterktes voor wat betreft de gemiddelde kraakbeendikte.

In Hoofdstuk 5 worden twee verschillende 3.0T MRI scanners van verschillende fabrikanten vergeleken met betrekking tot de gemiddelde kraakbeendikte en het kraakbeenvolume bij gezonde vrijwilligers. Tien knieën van vijf gezonde vrijwilligers werden gescand op een 3.0T General Electric (GE) en een 3.0T Philips scanner met een “fast three-dimensional fat-suppressed spoiled gradient (SPGR)” sequentie. De acquisitie parameters werden van tevoren geoptimaliseerd en werden zo gelijk als mogelijk gehouden op beide scanners. De gemiddelde kraakbeendikte en het gemiddelde kraakbeenvolume van de gewichtdragende delen van het kraakbeen op de femur condylen werden gebruikt als kwalitatieve maat ter vergelijking. Een “univariate repeated-measures analysis of variance” (ANOVA) test werd gebruikt om het effect van positie, condyle en type scanner op de metingen aan te tonen. De gemiddelde kraakbeendikte alsook het gemiddelde kraakbeenvolume verschilde niet tussen de twee verschillende 3.0T MRI scanners. Er werd geen significant effect van positie of femurcondyle op de metingen gevonden. Geconcludeerd werd dat de gemiddelde kraakbeendikte of het

gemiddelde kraakbeenvolume, gemeten met MRI scanners van twee verschillende fabrikanten, vergelijkbaar zijn.

In Hoofdstuk 6 wordt de prevalentie en locatie van centrale osteophyten, bij patiënten die verwezen zijn voor een MRI van de knie bepaald, alsook de relatie van deze centrale osteophyten met andere op MRI gedetecteerde pathologische veranderingen in het kniegewricht. Tweehonderd opeenvolgende patiënten, die verwezen werden voor een MRI van de knie werden bekeken op de aanwezigheid van centrale osteophyten, kraakbeendefecten, marginale osteophyten, meniscusafwijkingen en gescheurde voorste kruisbanden. Een 1.5T scanner werd gebruikt voor dit onderzoek. Twee ervaren musculoskeletale radiologen evalueerden de MRI onderzoeken in consensus. Zeven patiënten werden uitgesloten, waardoor er nog 193 overbleven in de studiegroep. De prevalentie van centrale osteophyten in de knie was 15% (35 centrale osteophyten in 29 patiënten). Patiënten met centrale osteophyten waren ouder (gemiddeld 52 jaar ten opzichte van 38 jaar), zwaarder (gemiddeld 92 kg versus 78 kg), hadden meer kraakbeen defecten (gemiddeld 4.3 versus 1.3) en hadden meer marginale osteophyten (gemiddeld 3.9 versus 1.1) dan patiënten zonder centrale osteophyten. Het was meer waarschijnlijk dat patiënten met centrale osteophyten een meniscusscheur hadden. Dit gold niet voor het optreden van een voorste kruisbandletsel. Alle centrale osteophyten hadden een geassocieerd "full thickness" of "near-full thickness" kraakbeendefect op dezelfde locatie (in 32 van de 35 centrale osteophyten). Geconcludeerd werd dat centrale osteophyten vrij veel voorkomen bij patiënten die een MRI scan van de knie krijgen. Tevens werd geconcludeerd dat wanneer een centrale osteophyt in de knie aanwezig is, er een grote kans op een geassocieerd "full thickness" of "near-full thickness" kraakbeen defect bestaat.

In Hoofdstuk 7 wordt de relatie tussen aan artrose gerelateerde afwijkingen van het patellofemorale of tibiofemorale compartiment van de knie geïnventariseerd. In 105 broer/zus paren (210 patiënten) met artrose in meerdere gewrichten werd een MRI van de knie gemaakt. Om in de studie opgenomen te worden moest de knie een Kellgren and Lawrence score van 2 of 3 hebben. MRI opnamen werden geanalyseerd met betrekking tot de aanwezigheid van kraakbeendefecten, beenmergoedeem en meniscusafwijkingen. De relatie tussen de mediale en laterale patellofemorale en tibiofemorale compartimenten werd geanalyseerd. De hoeveelheid kraakbeendefecten aan ofwel het laterale ofwel het mediale patellofemorale compartiment correleerde met kraakbeendefecten aan de ipsilaterale kant van het tibiofemorale compartiment (Odds ratio (OR) 55, confidence interval (CI), 7.8-382). De hoeveelheid kraakbeendefecten in het patellofemorale compartiment correleerde positief met scheuren in de ipsilaterale meniscus (OR 3.7, CI 1.0-14) en ipsilaterale patellofemoraal beenmergoedeem (OR 17, CI 3.8-72). Kraakbeendefecten in het tibiofemorale compartiment correleerde positief met scheuren in de ipsilaterale meniscus (OR 9.8, CI 2.5-

38) en ipsilateraal tibiofemoraal beenmergoedeem (OR 120, CI 6.5-2221). Geconcludeerd werd, dat aan artrose geassocieerde defecten de neiging hebben ipsilateraal voor te komen in het patellofemorale en tibiofemorale compartiment van de knie bij patiënten met milde artrose.

In Hoofdstuk 8 wordt de associatie tussen klinische bevindingen en afwijkingen op MRI van de knie bij patiënten met artrose beschreven. In 205 (20% man, leeftijd tussen 43 en 77 jaar, gemiddelde leeftijd 60 jaar) van de in totaal 210 patiënten, die waren gediagnosticeerd met symptomatische artrose in verschillende gewrichten, werden MRI's vervaardigd. Alle patiënten kregen vragen te beantwoorden met betrekking tot pijn en stijfheid in de knie. Een grote hoeveelheid effusie in het kniegewricht was geassocieerd met pijn (Odds Ratio (OR): 9.99; Confidence Interval (CI): 1.28-149) en stijfheid (OR: 4.67; CI: 1.26-26.1). De aanwezigheid van een osteophyt in het patellofemorale compartiment was geassocieerd met pijn (OR: 2.25; CI: 1.06-4.77). Alle andere met MRI afgebeelde parameters zoals focale of diffuse kraakbeendefecten, cystes, beenmergoedeem, subluxatie van de meniscus, meniscusscheuren of Bakerse cystes werden niet geassocieerd met klinische symptomen. Geconcludeerd werd dat slechts een klein aantal afwijkingen, gedetecteerd met een MRI van de knie, correleerde met klachten van patiënten met artrose.

In Hoofdstuk 9 worden veranderingen in beenmergoedeem in een periode van twee jaar, bij patiënten met artrose beschreven. Tevens worden deze veranderingen gecorreleerd aan klinische klachten van de patiënt. Een MRI van de knie werd verricht bij 182 (20% man, leeftijd tussen 43-76 jaar, gemiddeld 59 jaar) patiënten, die waren gediagnosticeerd met familiale, symptomatisch artrose in meerdere gewrichten. MRI's werden vervaardigd bij de start van de studie en na twee jaar. De MRI's werden beoordeeld door 2 ervaren radiologen met een gevalideerd scoreformulier, beschreven in Hoofdstuk 2. De patiënten werden tevens gevraagd een WOMAC formulier in te vullen. OR met 99% confidence intervals en linear mixed models met fixed effects werden gebruikt om veranderingen in beenmergoedeem te correleren met klinische bevindingen. 132 patiënten (75%) had beenmergoedeem gedurende de twee jaar. In totaal werden 327 beenmergoedeem laesies geconstateerd. Bij 90 patiënten (66%) veranderde de beenmergoedeem laesie in volume. 147 beenmergoedeem laesies veranderde in volume (45%): 69 nieuwe laesies (21%), 32 (10%) van de laesies verdween, 26 (8%) laesies namen toe in volume, 20 (6%) laesies namen af in volume. In totaal werden 222 cysteuze laesies gescoord in 182 patiënten (55%). Zeventig (32%) cysteuze laesies in 56 patiënten (30%) veranderde in volume. Als een cysteuze laesie in volume toe- of afnam, veranderde het geassocieerde beenmergoedeem in dezelfde richting (toe- of afname). Er werd geen associatie tussen een verandering in beenmergoedeem volume gedurende 2 jaar en WOMAC scores gevonden. Geconcludeerd werd, dat beenmergoedeem fluctueerde in volume over een periode van 2 jaar bij de meerderheid van patiënten met artrose. Tevens werd geconcludeerd dat

beenmergoedeem gedetecteerd met behulp van MRI geen voorspellende waarde heeft met betrekking tot WOMAC scores na een periode van 2 jaar.

Algemene conclusie

Dit proefschrift beschrijft ten eerste hoe aan artrose gerelateerde afwijkingen optimaal, met behulp van MRI, geregistreerd kunnen worden. Een in dit proefschrift hiervoor ontwikkeld hulpmiddel is het "Knee Osteoarthritis Score System (KOSS)". Dit is een score formulier waarop structuren in de knie met behulp van MRI gescoord worden. Juist die structuren worden geregistreerd welke mogelijk bij artrose afwijkend kunnen zijn. Behoudens een ander hiervoor ontwikkeld score formulier genaamd de "Whole Organ Magnetic Resonance Imaging score (WORMS)" zijn er geen andere formulieren in de literatuur beschreven met dezelfde functie (1).

In dit proefschrift worden tevens enkele "state of the art" MRI sequenties beschreven en met elkaar vergeleken. Het gaat hierbij om MRI sequenties die geoptimaliseerd zijn voor het afbeelden van kraakbeen in de knie. Globaal genomen kunnen deze sequenties in twee verschillende groepen worden ingedeeld. Te weten conventionele "Spoiled Gradient (SPGR)" en relatief nieuwere "Steady State Free Precession (SSFP)" sequenties. Gezien het feit dat 3.0T scanners steeds frequenter in de klinische setting voorkomen, zijn in dit proefschrift bovengenoemde sequenties bestudeerd op zowel 1.5T en op 3.0T scanners. De conclusie die de auteur op basis van dit proefschrift trekt met betrekking tot het gebruik van verschillende kraakbeen specifieke sequenties is enige terughoudend met het gebruik van SSFP type sequenties op 3.0T scanners voor het beoordelen van kraakbeen. Mogelijk dat op de 3.0T scanners de conservatieve SPGR sequenties hiervoor beter zijn. Echter op 1.5T scanners hebben SSFP type sequenties wél enige voordelen boven de SPGR sequenties met betrekking tot het beoordelen van kraakbeen.

Artrose is momenteel een van de belangrijkste invaliderende aandoeningen in de steeds ouder wordende Westerse populatie (2). Klinische symptomen van de patiënt alsook röntgenfoto's van de knie worden in de kliniek nog steeds gebruikt om de verandering van de ziekte te monitoren. De correlatie tussen pijn en artrose op röntgenfoto's is echter slecht (3). Omdat er veel discussie bestaat over de relatie tussen afwijkingen in de knie en kniepijn zijn er internationaal meerdere studies opgezet om dit met behulp van MRI te onderzoeken. De vraag is dan ook of MRI ons meer kan vertellen over de relatie tussen de aan artrose gerelateerde afwijkingen in de knie en de klachten van de patiënt?

Volgens dit proefschrift is "Nee" het korte antwoord op deze vraag. Een groot gedeelte van de resultaten welke in dit proefschrift worden beschreven komen

uit een longitudinale studie genaamd de “Genetica, Artrose & Progressie” (GARP) studie. In de GARP studie worden voor artrose specifieke afwijkingen in de knie gecorreleerd aan de klinische klachten van de patiënten. Geconcludeerd wordt dat de meeste op MRI gevonden afwijkingen niet correleren met de klachten die de patiënten hebben, enkele kleine uitzonderingen daargelaten.

Deze bevinding staat in contrast met een groot aantal andere publicaties in de literatuur over dit onderwerp (4). Met name de in dit proefschrift beschreven bevinding dat beenmergoedeem niet correleert met de klachten van de patiënt is een belangrijke contrasterende bevinding. Ook de bevinding dat veranderingen in beenmergoedeem geen voorspellende waarde hebben voor de ernst van de klachten van de patiënt na twee jaar gemeten met behulp van de “Western Ontario and McMaster Universities Osteoarthritis (WOMAC) score” is controversieel (5). Dit wil zeggen dat wanneer beenmergoedeem in patiënten toeneemt er geen hogere WOMAC scores worden gevonden na 2 jaar. Zelfs wanneer het beenmergoedeem volledig verdwijnt worden geen lagere WOMAC scores gevonden. Dit terwijl in een studie van Felson et al. Beenmergoedeem geassocieerd is met progressie van artrose gemeten met röntgenfoto's van de knie en met pijn in de knie (4;6-10). Aan de andere kant is dit verschil ook niet geheel verrassend. Phan et al. suggereert dat de verschillen in pijn sensatie tussen de verschillende patiënten en de complexiteit van de pijn sensatie alleen al deze verschillen kunnen verklaren. Het feit dat in de GARP studie en in de studie van Felson verschillende resultaten gevonden zijn kan ook verklaart worden doordat er verschillende patiënten populaties gescand zijn. In de populatie van Felson (4) zitten wellicht patiënten met een ernstigere vorm van knieartrose omdat in die populatie alleen patiënten voorkomen die artrose van de knie hebben, terwijl in de GARP populatie (11) patiënten zitten die artrose in meerdere gewrichten hebben, en dus niet noodzakelijkerwijs de knie. Een aanzienlijk deel van de GARP populatie had geen artrose van de knie, en daardoor waren de gemiddelde WOMAC scores wellicht lager. Hoe dan ook blijft de associatie tussen kniepijn en afwijking gevonden in de knie op MRI controversieel.

De bevinding dat beenmergoedeem in 66% van de patiënten fluctueert geeft aan dat beenmergoedeem een dynamisch proces is in artrose. Beenmergoedeem is geen constante afwijking zoals bijvoorbeeld kraakbeen verlies. Het is dus belangrijk om te realiseren dat de gevonden afwijkingen in het beenmerg een enkele tijdsopname is en geen constante. Deze fluctuaties van beenmergoedeem zijn eerder beschreven (9). Ook is het interessant om te zien dat 10% van de beenmergoedeem laesies volledig verdwijnen. Dit is met name interessant omdat beenmergoedeem vaak als een inclusie criteria of surrogaat eindpunt in studies is.

De bevindingen in dit proefschrift pleiten dan ook voor terughoudendheid met het uitgangspunt dat beenmergoedeem een maat voor de ernst van artrose zou zijn. Toekomstige klinische trials zouden met deze bevinding rekening moeten houden. Aangezien onderzoek naar artrose van groot belang is, pleit

dit proefschrift voor verder onderzoek naar representatieve, kwantificeerbare parameters, waarmee de progressie van de ziekte te objectiveren valt.

Referenties

1. Peterfy CG, Guermazi A, Zaim S, Tirman PF, Miaux Y, White D et al. Whole-Organ Magnetic Resonance Imaging Score (WORMS) of the knee in osteoarthritis. *Osteoarthritis Cartilage* 2004; 12(3):177-190
2. Harris ED Jr (2001) The bone and joint decade: a catalyst for progress. *Arthritis Rheum* 44(9):1969–1970
3. Lawrence JS, Bremner JM, Bier F. Osteo-arthrosis. Prevalence in the population and relationship between symptoms and x-ray changes. *Ann.Rheum.Dis.* 1966;25(1):1-24.
4. Felson DT, Chaisson CE, Hill CL, Totterman SM, Gale ME, Skinner KM et al. The association of bone marrow lesions with pain in knee osteoarthritis. *Ann.Intern.Med.* 2001;134(7):541-549.
5. Bellamy N, Buchanan WW, Goldsmith CH, Campbell J, Stitt LW. Validation study of WOMAC: a health status instrument for measuring clinically important patient relevant outcomes to antirheumatic drug therapy in patients with osteoarthritis of the hip or knee. *J Rheumatol* 1988; 15(12):1833-1840.
6. Felson DT, McLaughlin S, Goggins J, LaValley MP, Gale ME, Totterman S et al. Bone marrow edema and its relation to progression of knee osteoarthritis. *Ann Intern Med* 2003; 139 (5 Pt 1):330-336.
7. Cicuttini F, Wluka A, Hankin J, Wang Y. Longitudinal study of the relationship between knee angle and tibiofemoral cartilage volume in subjects with knee osteoarthritis. *Rheumatology (Oxford)* 2004; 43(3):321-324.
8. Link TM, Steinbach LS, Ghosh S, Ries M, Lu Y, Lane N et al. Osteoarthritis: MR imaging findings in different stages of disease and correlation with clinical findings. *Radiology* 2003; 226(2):373-381.
9. Phan CM, Link TM, Blumenkrantz G, Dunn TC, Ries MD, Steinbach LS et al. MR imaging findings in the follow-up of patients with different stages of knee osteoarthritis and the correlation with clinical symptoms. *Eur Radiol* 2005;1-11.
10. Hill CL, Gale DG, Chaisson CE, Skinner K, Kazis L, Gale ME et al. Knee effusions, popliteal cysts, and synovial thickening: association with knee pain in osteoarthritis. *J.Rheumatol.* 2001;28(6):1330-7.
11. Riyazi N, Meulenbelt I, Kroon HM, Runday KH, Hellio le Graverand MP, Rosendaal FR et al. Evidence for familial aggregation of hand, hip, and spine but not knee osteoarthritis in siblings with multiple joint involvement: the GARP study. *Ann Rheum Dis* 2005; 64(3):438-443.

Curriculum vitae

De auteur van dit proefschrift werd geboren op 31 augustus 1976 te Eindhoven. Aan het Chr. Lyceum Dr. Visser 't Hooft te Leiden behaalde hij in 1994 het VWO diploma. In datzelfde jaar ving hij aan met de studie Geneeskunde aan de faculteit der geneeskunde van de Universiteit Leiden. Hij werkte daarnaast als student-assistent bij de vakgroep Fysiologie en bij computer ondersteund onderwijs. Als afstudeerproject verrichtte hij onderzoek naar acute lymfatische leukemie op de afdeling Kindergeneeskunde van het Leids Universitair Medische Centrum. Een extra afstudeerproject verrichtte hij gedurende een half jaar naar het voorkomen van centrale osteophyten in de knie met behulp van magnetic resonance imaging aan Yale University Medical School, Department of Radiology, New Haven, USA, onder leiding van prof. dr. T.R. McCauley. In 2002 behaalde hij zijn arts-examen. In datzelfde jaar startte hij met promotie onderzoek op de afdeling Radiologie van het Leids Universitair Medisch Centrum. Het onderzoek richtte zich op artrose van de knie met in het bijzonder het afbeelden van kraakbeen met behulp van magnetic resonance imaging onder leiding van prof. dr. J.L. Bloem. Begin 2004 vertrok hij voor een half jaar naar Stanford University Medical School, Department of Radiology, Palo Alto, USA, waar hij onderzoek verrichtte naar het optimaal afbeelden van kraakbeen onder leiding van prof. dr. G.E. Gold. Op 1 mei 2005 startte hij met de opleiding Radiologie aan het Leids Universitair Medisch Centrum.